Final Report

FEHMARNBELT FIXED LINK HYDROGRAPHIC SERVICES (FEHY)

Marine Soil - Baseline

Sea Bed Morphology of the Fehmarnbelt Area

E1TR0056 - Volume I

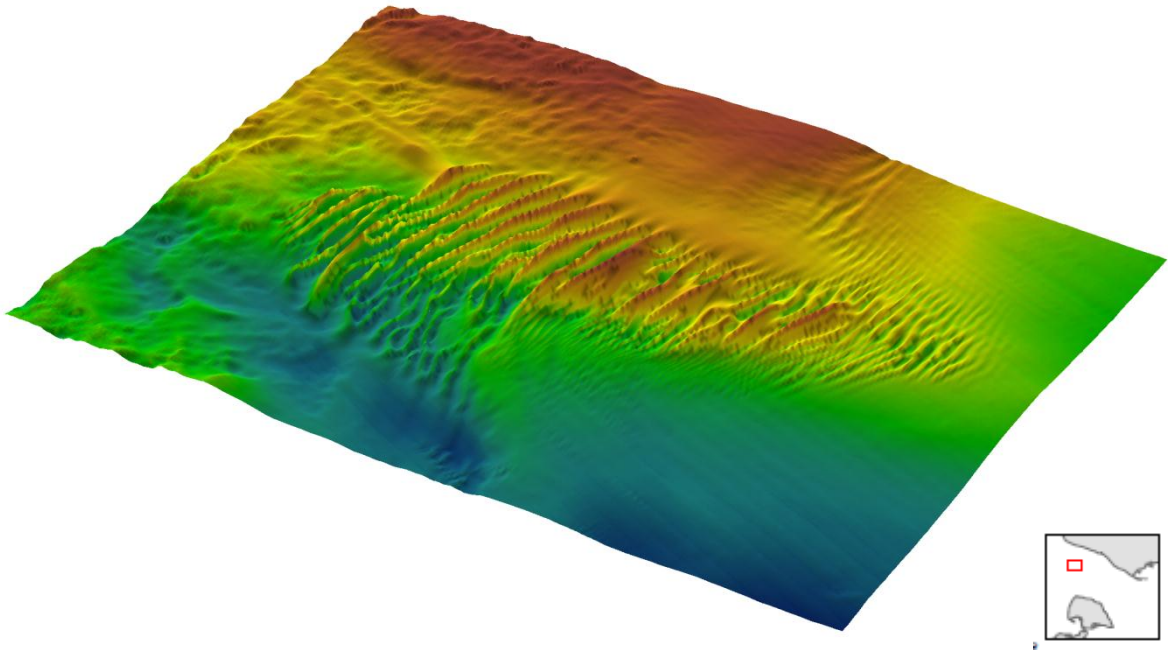

Prepared for: Femern A/S

By: DHI/IOW Consortium

in association with LICengineering, Bolding & Burchard and Risø DTU

Responsible editor:
FEHY consortium / co DHI
Agern Allé 5
DK-2970 Hørsholm
Denmark

FEHY Project Director: Ian Sehested Hansen, DHI
www.dhigroup.com

Please cite as:
FEHY (2013). Fehmarnbelt Fixed Link EIA.
Marine Soil - Baseline.
Seabed Morphology of the Fehmarnbelt Area.
Report No. E1TR0056 – Volume I

Report: 119 pages
One appendix (ISBN 978-87-92416-70-4)

May 2013

ISBN 978-87-92416-32-2

Maps:
Unless otherwise stated:
DDO Orthofoto: DDO®, copyright COWI
Geodatastyrelsen (formerly Kort- og Matrikelstyrelsen), Kort10 and 25 Matrikelkort
GEUS (De Nationale Geologiske Undersøgelser for Danmark og Grønland)
HELCOM (Helsinki Commission – Baltic Marine Environment Protection Commission)
Landesamt für Vermessung und Geoinformation Schleswig-Holstein (formerly Landes-vermessungsamt Schleswig-Holstein) GeoBasis-DE/LVermGeo SH
Model software geographic plots: Also data from Farvandsvæsenet and Bundesamt für Seeschifffahrt und Hydrographie

Photos:
Photos taken by consortium members unless otherwise stated

Co-financed by the European Union
Trans-European Transport Network (TEN-T)

CONTENTS

Lists of figures and tables are included as the final pages

APPENDIX

(UNDER SEPARATE COVER)

A MAPS OF BED FORMS AND THEIR CHARACTERISTICS

Note to the reader:
In this report the time for start of construction is artificially set to 1 October 2014 for the tunnel and 1 January 2015 for the bridge alternative. In the Danish EIA (VVM) and the German EIA (UVS/LBP) absolute year references are not used. Instead the time references are relative to start of construction works. In the VVM the same time reference is used for tunnel and bridge, i.e. year 0 corresponds to 2014/start of tunnel construction; year 1 corresponds to 2015/start of bridge construction etc. In the UVS/LBP individual time references are used for tunnel and bridge, i.e. for tunnel construction year 1 is equivalent to 2014 (construction starts 1 October in year 1) and for bridge construction year 1 is equivalent to 2015 (construction starts 1st January).

1 *EXTENDED SUMMARY*

This report covers the baseline mapping of the sediment transport conditions and the dynamic large-scale bed forms offshore of the 6 m depth contour in the Fehmarnbelt. Mapping and assessment of hard substrate on the sea bed such as reefs are treated as a part of the marine biology in (FEMA 2013).

The report includes the following main parts:

- Results from simulations of the mobility of non-cohesive sediments
- Mapping and classification of the bed forms in the Fehmarnbelt
- Analysis of the interaction between the bed forms and the flow field in the Fehmarnbelt
- Overview of present pressures on the bed forms
- Importance of the bed forms

A summary of the findings are presented in this chapter.

1.1 Mobility of Sediment

Annual sediment transport capacities were calculated in the alignment area for the planned fixed link. The annual gross and net sediment transport capacities and sediment transport in each of the main directions of the flow - eastwards and westwards have been calculated. All results are given in annual sediment transport volumes per m along the alignment between the Danish and the German coasts.

The sediment transport rates were based on simulations of the 2005 hydrodynamic conditions. The year 2005 is a representative year for the typical hydrodynamic conditions in the Fehmarnbelt.

The hydrodynamic simulations of the 2005 conditions were carried out with a model, which is identical to the one used for the hydrographic studies, but further refined to obtain correct near-bed current speeds in the Fehmarnbelt. Measurements from measuring stations in the Fehmarnbelt from 2009 were applied for the calibration of the near bed conditions of the model.

The comprehensive sets of sea bed samples were analysed and applied in the sediment transport model. Note: the transport capacities correspond to 100% availability of loose sediments on the sea bed. In areas with only partial coverage actual transport rates are less than the capacity.

The net annual non-cohesive sediment transport capacities are shown in Figure 1.1 for water depths >4 m. "Lower limit" and "higher limit" of the transport capacities refer to results obtained for coarser and finer representative grain sizes respectively found along the alignment.

At the Danish coast a net littoral drift of 10,000-20,000 m^3/year eastwards is estimated, while the net transport is estimated at 0-2,000 m^3/year towards the northwest at the German coast east of Puttgarden Harbour. Note: littoral drift is the sediment transport within the surf zone, which in this case is limited to water depths

less than 3 - 4 m. The sediment transport capacities across the alignment are summarized in Table 1.1.

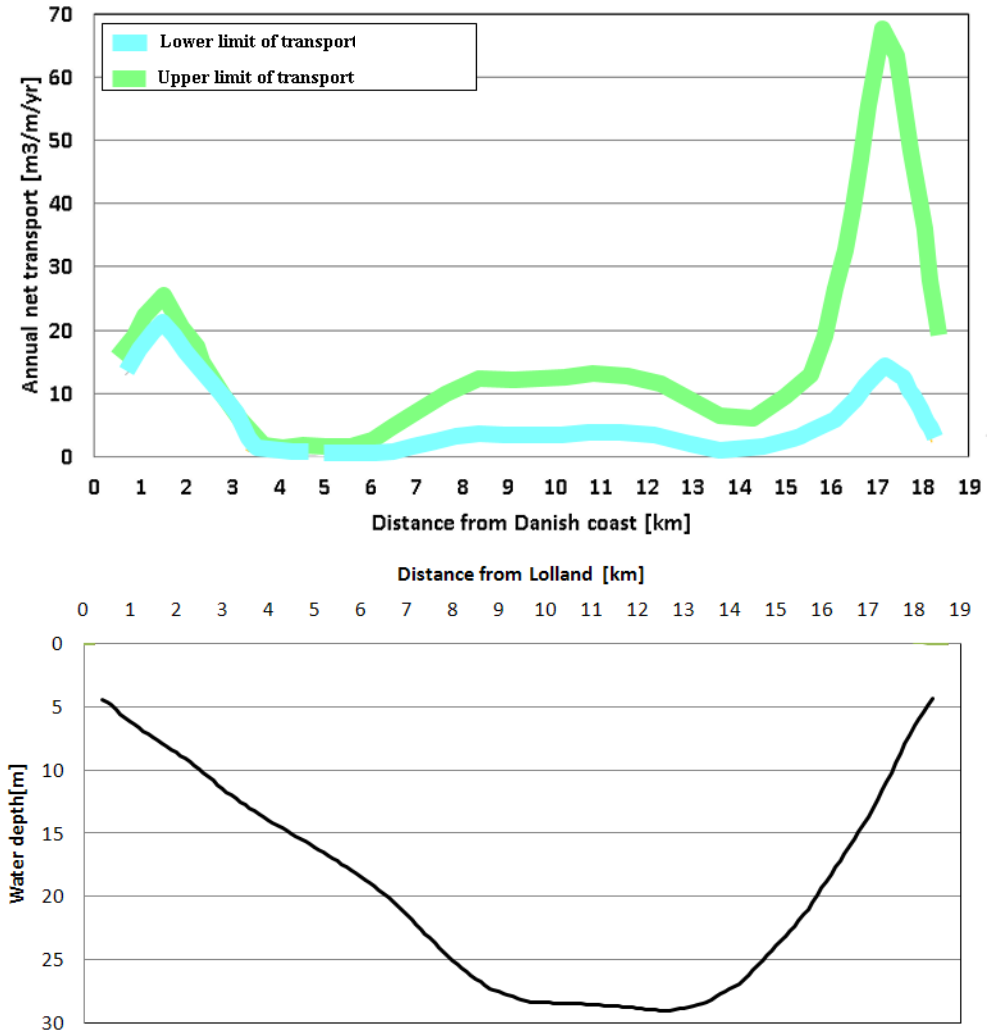

Figure 1.1 *Annual net sediment transport rates (2005) across the Fehmarnbelt in the alignment area (upper figure) for water depths >4 m. The depths in the cross section are shown in the lower figure. The net sediment transport is directed towards the Baltic Sea*

Table 1.1 *Estimated annual sediment transport rates across the alignment, water depth > 4m*

	Water depth [m]	**Length [m]**	**Annual transport capacity of non-cohesive sediment across the alignment [m^3/m/year]**			
Stretch			**Gross**	**Net**	**Eastwards**	**Westwards**
Danish side	4-12	2,500	15-45	5-25	10-35	5-15
Central area	>12 (DK) >20 (G)	12,500	5-25	1-15	3-20	2-12
German side	4-20	2,500	7-95	3-70	5-85	2-15

1.2 Mapping and Classification of Bed Forms

Large-scale bed forms of different types are found at a number of locations spread over the sea bed of the Fehmarnbelt. These bed forms vary from isolated lunate features in the central part of the Belt to more regular sand waves on the shoulders of the Belt.

The bed forms were studied extensively. The primary purposes for the interest in the bed forms in relation to the EIA for the Fehmarnbelt are:

- Parts of the bed forms are within environmentally protected Natura2000 areas
- The bed forms impose resistance on the flow field. In case the bed forms are affected by the link, this could have an effect on the flow through the Belt. The effects of the spatially varying resistance due to the bed forms have therefore been quantified

The mapping of the bed forms was based on a detailed multi beam echo sounding of the bathymetry in the Fehmarnbelt. Sea bed slope and difference maps were created and based on these striking maps of the bed form characteristics, different types and areas of bed forms were identified.

Two main types of bed forms were found on the sea bed of the Fehmarnbelt: sand waves and lunate bed forms. Sand waves are large-scale flow-transverse ridges of sand, i.e. the crests of the sand waves are flow transverse, but may also be inclined at an angle to the main flow direction where there is a gradient in the flow. Lunate bed forms are 3D in their nature and have lunate shape with the "arms" pointing in the direction of the Baltic Sea. They consist of loose sediment (fine sand) on an otherwise more or less immobile bed. The two main types cover most sea bed features but other less characteristic forms exist which have a considerable size and clearly indicate that the flow over loose sediments on the sea bed is strong enough to cause movement of sand grains and formation of rhythmic features. Such bed forms are identified as "other active bed forms".

The bed forms are described by their height, length and local maximum steepness. Their primary migration direction was evaluated from their shape and for the bed forms in the alignment area their migration rate was furthermore estimated based on the simulated sediment transport rates. The characteristics of the bed forms in the Fehmarnbelt are summarised in Figure 1.2.

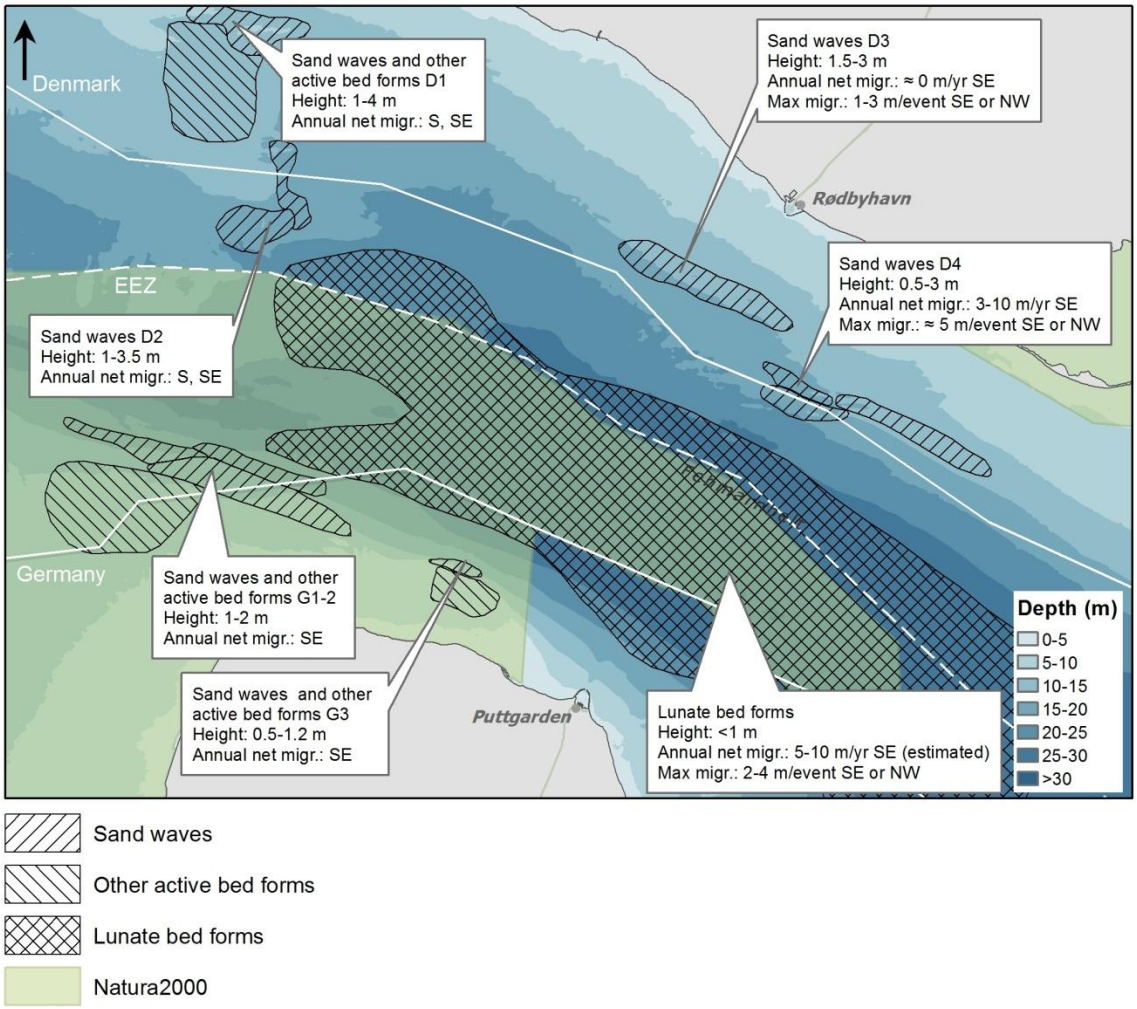

Figure 1.2 *Main bed form areas in the Fehmarnbelt and their main characteristics. The maximum migration rates are related to events occurring 2-5 times a year and lasting approximately 2 days (note: D1-D4 and G1-G3 refer to sub areas used for the detailed classification. Maps from the sub areas are included in Appendix A).*

1.3 Interaction between Bed Forms to the Flow Field

The bed forms in the Fehmarnbelt interact with the flow: the flow generates sediment transport, which for certain flow conditions lead to the formation of bed forms and the bed forms constitute flow roughness elements or flow resistance.

The influence of spatially varying flow resistance due to the bed forms was analysed by comparing the hypothetical situation of no bed forms in the Fehmarnbelt with the situation where the bed roughness is increased in the bed form areas of the Fehmarnbelt. The analysis was based on flow simulations of both situations. The flow resistance from each of the individual areas of bed forms was calculated by detailed CFD-modelling. Only sand waves and areas of 'other active bed forms' were found to give a significant contribution to the flow resistance.

The analysis led to the conclusions that the discharge through the Fehmarnbelt was reduced by up to 0.04% when the bed forms are included in the simulations compared to the hypothetical situation without the bed forms. The influence of the bed forms was found to be smaller for outflow situations from the Baltic Sea than for inflow situations.

The spatially varying resistance due to sand waves was found to slightly redistribute the flow in the Fehmarnbelt. During inflow situations the flow is diverted slightly towards the Danish coast due to the sand waves near the German coast. A smaller diversion of the flow towards the German coast is found during outflow due to the sand waves in the alignment area near the Danish coast and further west from there.

Note: in this analysis the effect of bed forms has been included as an *additional* roughness. This is the reason why the simulations lead to a slight change in the overall net (out-) flow from the Baltic Sea through the Fehmarnbelt and the Øresund. In case simulations had shown significant redistribution of flow due to spatial variations in roughness a more advanced comparison of results from modelling with and without spatial variations but with the same overall resistance would have been relevant.

In conclusion, only a very small impact of the bed forms on the flow field in the Fehmarnbelt was found. The influence is mostly due to the sand waves near the German coast about 20 km from the alignment area.

1.4 Present Pressures

Sand mining and disposal of dredged material are the only present pressures on the sea bed forms. Mining of sea bed material takes place in two of the sand wave fields on the Danish side with permission from the Ministry of Environment, Agency for Spatial and Environmental Planning (in Danish: Naturstyrelsen). Disposal of material dredged in Rødby and Gedser Harbours takes place in an area WSW of Rødbyhavn. This site is located at the boundary of one of the sand wave fields on the Danish side. The two sand mining areas and the disposal site are shown in Figure 1.3.

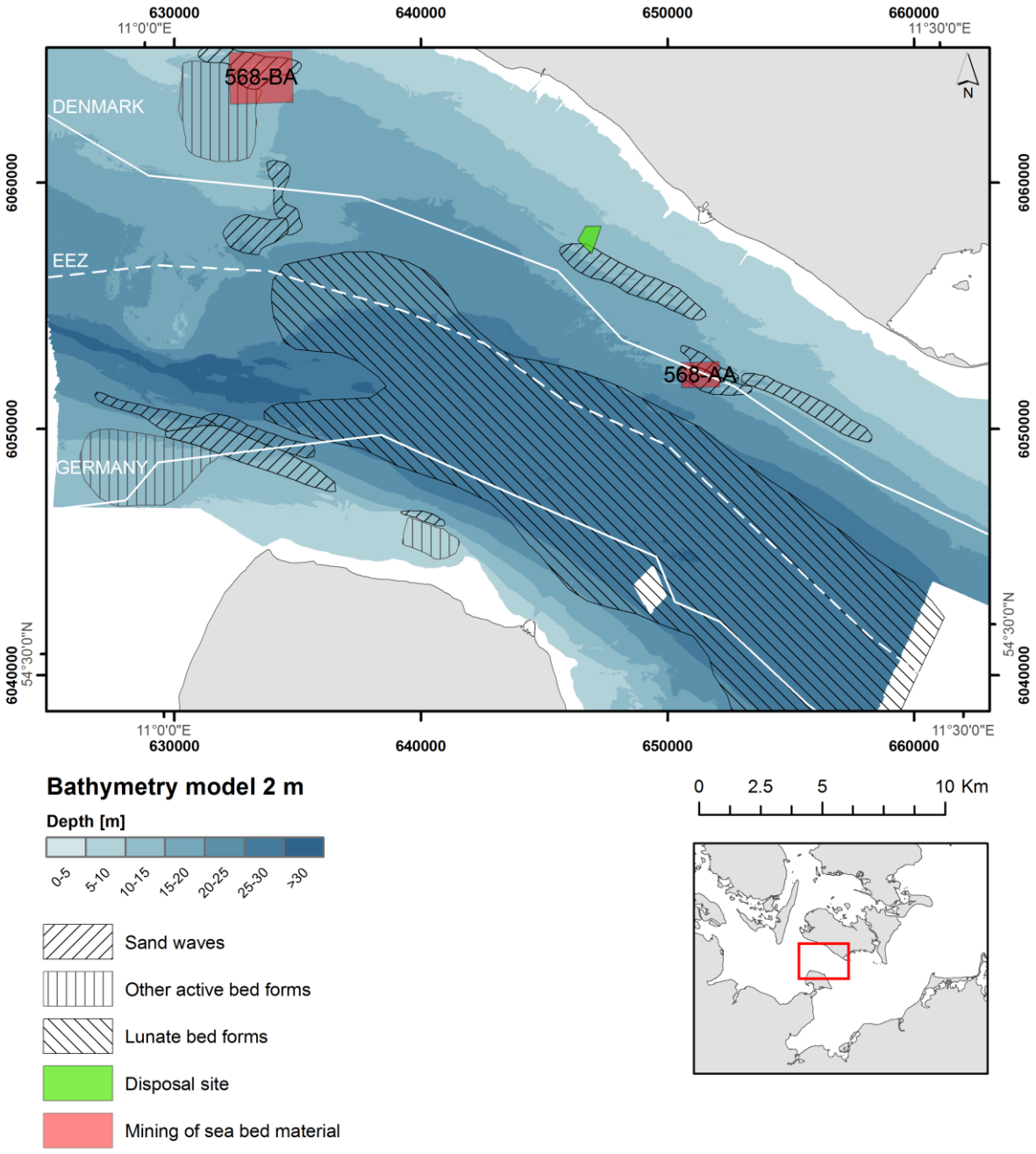

Figure 1.3 Areas with permission for mining of sea bed material and disposal site. Information from Ministry of Environment, Agency for Spatial and Environmental Planning

The analysis of sand waves in the two sand mining areas shows that the bed forms recover from the extraction, but the recovery time is long (>10 years) when substantial amounts of material have been extracted. The disposal site shows up on the multi beam survey as an elevation locally of the sea bed but no disturbance of the nearby sand waves has been registered.

1.5 Importance of the Bed Forms

The importance of the sea bed forms has been assessed based on the conservation objectives of the Natura 2000 areas occurring within the area of investigation and for the hydrodynamic conditions in the Fehmarnbelt area.

Some areas within the Fehmarnbelt area have been protected with "large-scale, morphological active bed forms" as conservation objectives under Natura 2000. These areas are accordingly used in the assignment of importance levels for sea bed morphology. The bed form classification map combined with the Natura 2000 areas are shown in Figure 1.4.

The bed forms act as roughness elements on the flow. The fact, that they are not evenly distributed in the Fehmarnbelt lead to a spatial variation in the flow resistance. The importance of the bed forms on the overall hydrodynamics is concluded to be negligible.

The importance levels and descriptions are summarised in Table 1.2. The mapping of bed forms has been utilised to determine the importance map for sub factor Marine Soil, which is shown in Figure 1.5.

Table 1.2 Importance levels for the Marine Soil component: Sea bed morphology

Importance level	Description
Very high	Sand wave areas within Natura 2000 areas, where these are part of the conservation objectives
High	Other sea bed areas with prominent large-scale, morphologically active bed forms (sand waves/lunate bed forms/other prominent bed forms) not included under the 'Very high' category
Medium	All other sea bed areas, which are not heavily influenced by anthropogenic activities as mentioned under the "Minor" category
Minor	Areas under heavy anthropogenic influence, including dredged navigation channels, disposal sites, areas with sand and gravel mining and harbours

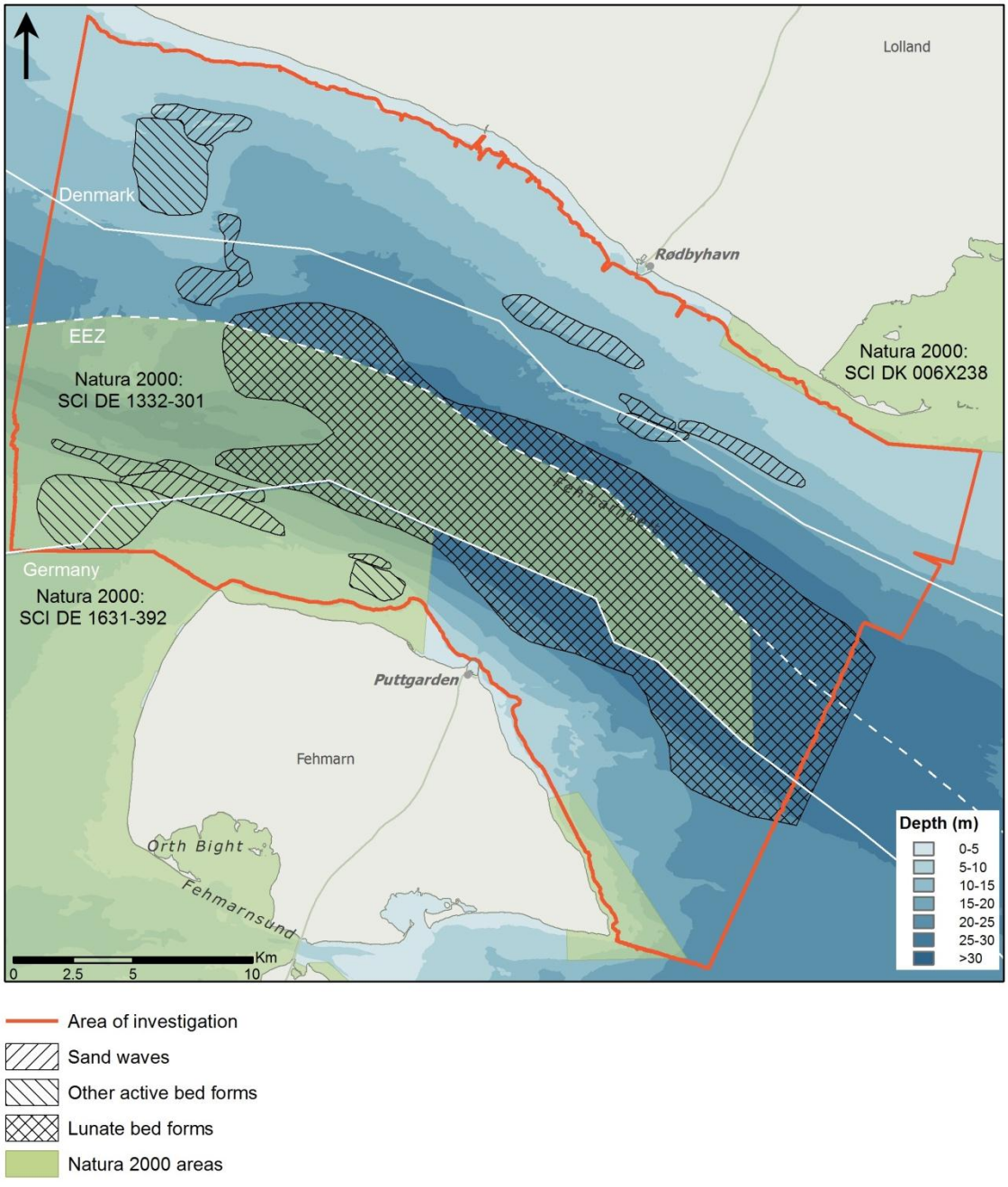

Figure 1.4 The bed form classification map combined with the Natura2000 area. Marine parts of the Natura 2000 areas are shown

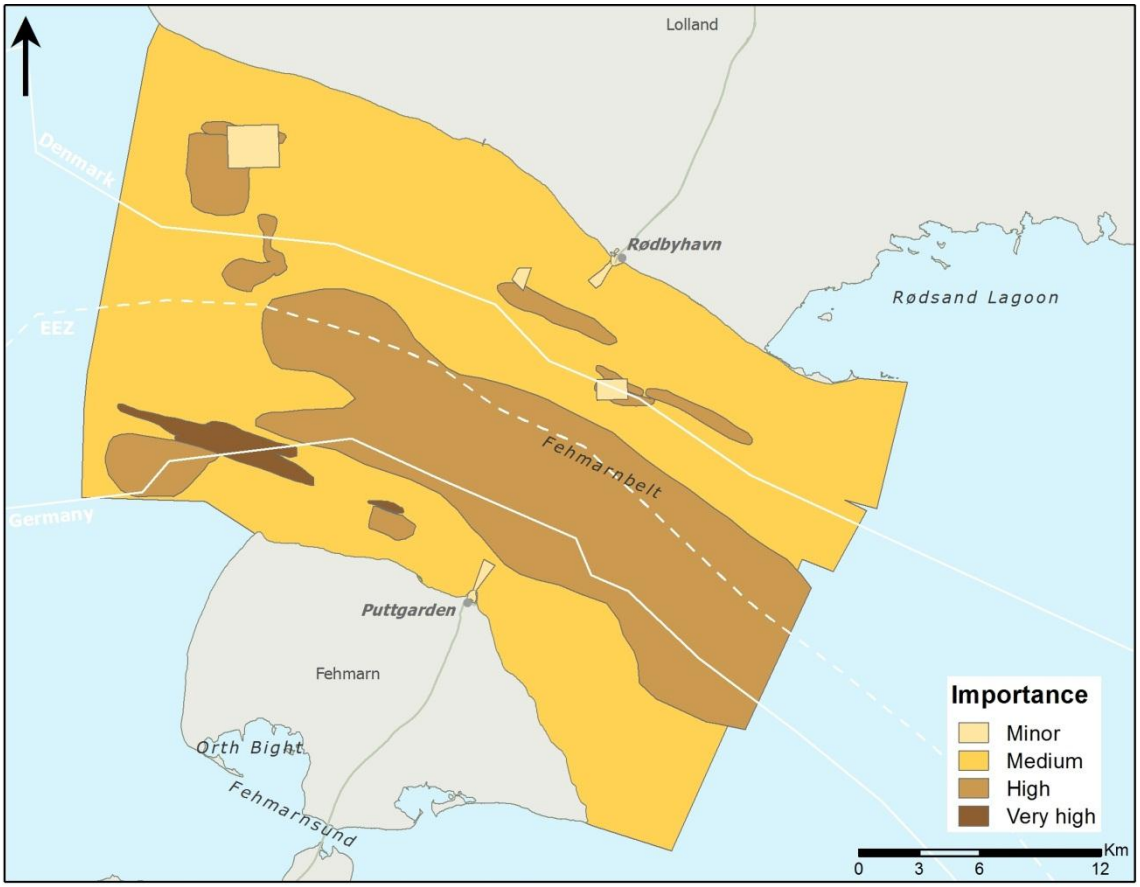

Figure 1.5 Importance map for sub-factor Marine Soil component Sea Bed forms

2 *INTRODUCTION*

Sea bed sediments and sea bed morphology concern the state of the sea bed including the mobility of the sea bed materials and the varying bed forms at the sea bed of the Fehmarnbelt. The state of the sea bed is of importance for flora and fauna on the sea bed.

An infrastructure project like the Fehmarnbelt project will unavoidably have some impact on the sea bed morphology due to the construction of large structures on the sea bed and dredging of sea bed material in relation to the construction. Analysis of the baseline conditions of the sea bed is used as a reference for the assessment of potential impacts on the sea bed sediments and sea bed morphology of the fixed link.

The present report includes the following:

- Analysis of sediment mobility
- Mapping and analysis of bed forms
- Analysis of the interaction between the flow and the bed forms

This report deals with the dynamic morphological elements of the sea bed. The sea bed forms are the result of interaction between loose sediments on the sea bed and the flow above the sea bed. Other morphological elements, such as reefs, are usually areas under erosion where coarser materials such as stones and other hard substrates occupy larger parts of the sea bed. Such reefs may constitute important habitats for benthic flora and fauna. Reefs are therefore considered a biotope in relation to the EIA for the Fehmarnbelt Fixed Link and mapping and assessment of reefs are hence not treated along with the dynamic sea bed morphology in this report, but as a part of the marine biology in (FEMA 2013).

Morphological features and landscape related to the coastal processes in the nearshore zone (water depths less than 6 m), such as for instance sand bars in the coastal profile as well as the special morphological features such as Grüner Brink on Fehmarn and the Hyllekrog/Rødsand formations on the Danish side, are treated in the report related to coastal morphology (FEHY 2013a).

The present hydrographic conditions (bathymetry, currents and waves) and sea bed sediments are pre-requisites for the above listed analysis. Brief summaries of available data and relevant references are therefore presented in Chapter 3, Data Basis and Methods, together with the methods applied for undertaking of the analysis. Chapter 4 includes descriptions of the Fehmarnbelt area with respect to relevant conditions.

The analysis of bed forms includes considerations of migration speeds of the bed forms. The migration speeds depends on the sediment mobility which is therefore included in the present report in Chapter 5.

The description and classification of bed forms are presented in Chapter 6. The interaction between bed forms and overall flow is discussed in Chapter7.

The present pressures on the sea bed and bed forms and assessment of the importance of the bed forms are presented in Chapter 8 and 9, respectively.

3 DATA BASIS AND METHODS

3.1 Hydrography

3.1.1 Data basis

Analyses of the hydrographic conditions are carried out based on the following sources of information.

Currents

- Measurements of current speed and directions from two fixed stations deployed in March 2009 in the Fehmarnbelt
- Modelled current speeds and directions for the Fehmarnbelt. The model setup is described in Section 3.1.2
- Modelled current speeds and directions for the Fehmarnbelt for the year 2005

Waves

- Measurements of wave heights, periods and directions from the two fixed stations deployed in March 2009 in the Fehmarnbelt
- Modelled wave conditions for the Fehmarnbelt for the year 2005

The modelled waves applied for assessment of sediment mobility are modelled with the spectral wind wave model MIKE FM SW. The model and the model set-up are presented in FEHY(2013a); however, the results presented in this report are obtained using wind fields from WATCH (version R13) from DMI.

Additional sources to information on hydrographic data are presented in FEHY (2013b).

Field measurements of current conditions and waves have been carried out at two stations in the central part of the Fehmarnbelt, see Figure 3.1 and Table 3.1.

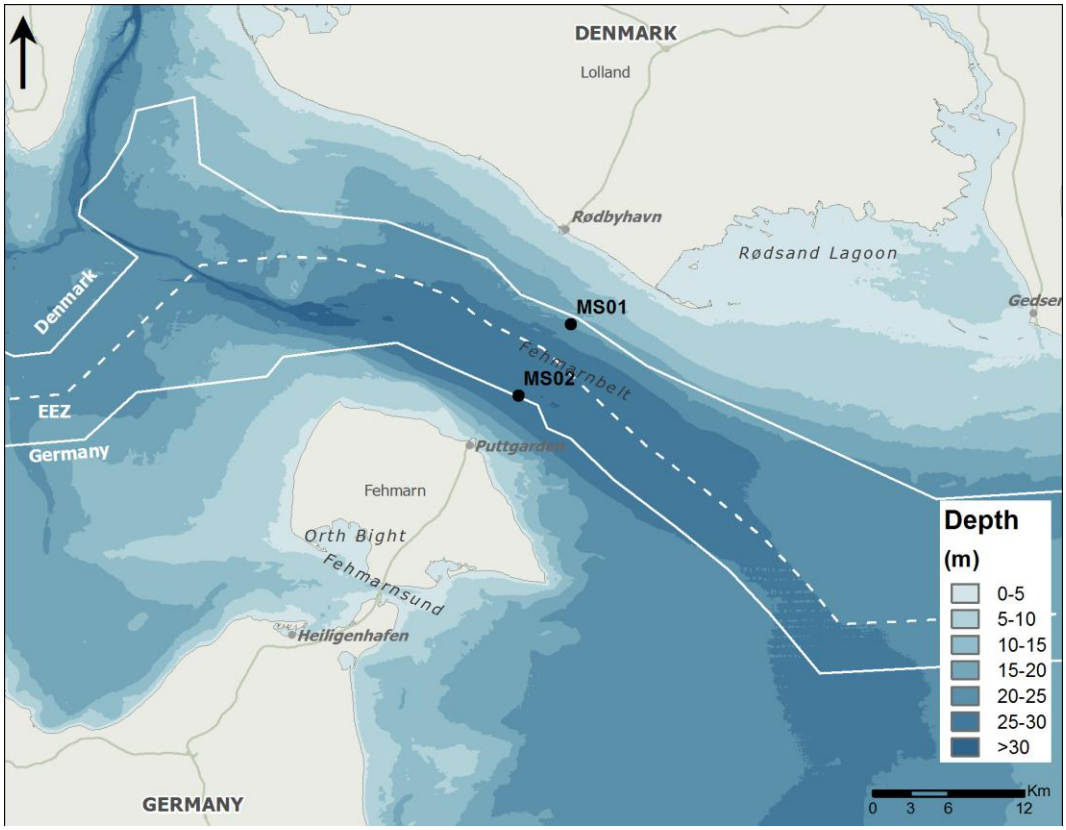

Figure 3.1 Locations of main stations in the Fehmarnbelt, where measurements of currents and waves have been carried out since March 2009 at the two Main Stations MS01 and MS02

Table 3.1 Main measurement stations in the Fehmarnbelt

Main station	Water depth [m]	Location	Measuring period
MS01	20	11.3553 degr. E; 54.5859 degr. N	March 2009 – End 2011
MS02	29	11.288 degr. E; 54.536 degr, N	March 2009 – End 2011

3.1.2 Methods

Detailed hydrodynamic modelling is carried out for Femern A/S with three different modelling systems, see (FEHY 2013b). DHI's MIKE model is one of these modelling systems. The model set-up for the so-called "local hydrodynamic model area" has been fine-tuned to obtain the best possible results with regard to the near flow field for the assessment of sediment mobility. This model set-up is briefly described below.

MIKE3 FM-HD is a 3D flow model applicable for analysis of free-surface flow hydrodynamics in coastal areas and seas that are stratified. MIKE3 calculates the evolution in water levels, currents, salinity, and water temperature, operating on a flexible mesh with triangular elements. The elements can be concentrated in areas where high resolution is most important. A general description of MIKE3 FM-HD is found at

www.mikebydhi.com/~/media/Microsite_MIKEbyDHI/Publications/PDF/MIKE213_FM HD_Short_Description.ashx.

The applied model setup is in general the same as the local hydrodynamic model applied for the general analysis of flow in the Fehmarnbelt, see FEHY(2013b) with some modifications. The fine-tuning of the general model is described briefly below. The model setup for the model applied for the assessment of sediment mobility is summarised in Table 3.2. For further information about the various model parameters see the above link and with regard to boundary conditions also (Blayo and Debreu 2005).

The present model applies 30 Sigma-layers across the water depth – in the following this model is called the "Sigma-Model". This is different from the general model which uses a combination of Sigma- and z-layers, in the following denoted the "Sigma-Z-Model". By experience it is known that when modelling stratified waters with MIKE3 FM HD, the latter is a better choice with regard to getting the stratification correctly. However, flow speeds especially near the bed may suffer in accuracy when applying z-layers near the bed. These are more correctly modelled with Sigma-layers.

The Sigma-Model applied in the present work therefore obtains the temperature and salinity fields from the Sigma-Z-Model in order to keep the stratification correct.

The bed roughness applied in the Sigma-Model has been calibrated to obtain the best comparison between modelled and measured near-bed flow at the fixed stations. The following calibration parameters have included: bed roughness, horizontal and vertical resolution, vertical distribution of layers, parameter settings for the horizontal and vertical eddy viscosity and dispersion coefficients. Among the calibration parameters, the bed roughness was found to have the largest influence on the near-bed flow.

The main focus has been on the higher current speeds since no or low mobility of the sediment is expected during the average flow conditions. The critical current speed for mobilising sediment is in the order of approximately 0.3 m/s at 2 m above the sea bed at a water depth of 20 m (grain size 0.1 mm).

A global bed roughness height in the Sigma-Model was calibrated to $k_{a,g}$=0.05 mm. During the calibration of the Sigma-Model the following bed roughnesses were tested: 0.05 m, 0.025 m, 0.005 m and 0.05 mm. The model was calibrated in the period July-August 2009 since these were the data available at the time of calibration. The best match for the peak currents during that time was obtained with the very small roughness of $k_{a,g}$=0.05 mm. Theoretically the roughness is in the order of about 2.5 times the grain size for a flat bed (the Nikuradse bed roughness) and higher if the sea bed has small bed forms or vegetation. In the Fehmarnbelt, the grain diameter is above 0.1-0.2 mm and a physical bed roughness above 0.5 mm is realistic. However, the smaller roughness in the numerical model is found to give the best match to the near-bed current field.

Results from a run with a roughness of $k_{a,g}$=0.025 m are shown in the following for comparison with the run with the roughness of $k_{a,g}$=0.05 mm. A bed roughness of $k_{a,g}$=0.025 m is in the order magnitude that is typically found for a ripple-covered bed (small bed forms with height up to 0.10 m), and is in that regard anticipated as an upper level for the bed roughness in areas with an otherwise flat bed (without large-scale bed forms and vegetation).

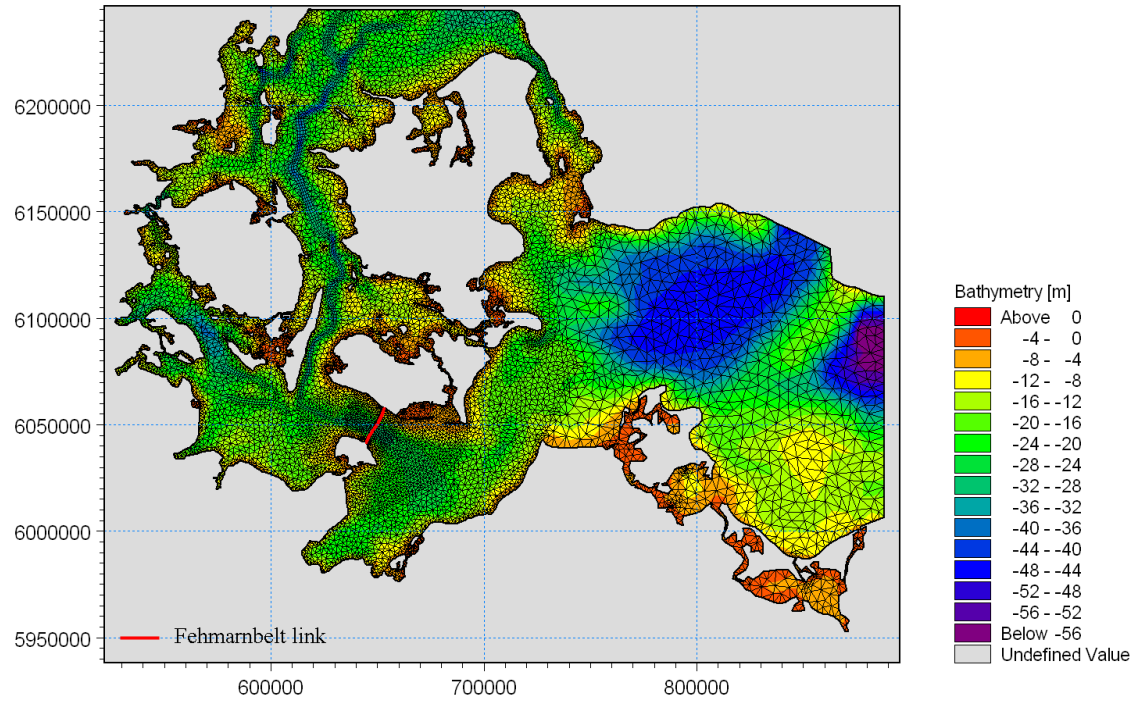

Figure 3.2 Model area, mesh and bathymetry for the flow model

Table 3.2 Model setup for the Sigma-Model MIKE3 FM-HD

Model parameter/setting	**Parameter specification**
Simulation model	MIKE 3 flow model FM, non hydrostatic
Vertical spacing, no. of layers	30 sigma
Mesh resolution	Baltic Sea: ~ 4000-5000 m Kattegat and Belt Sea: ~2000-2500 m Fehmarnbelt: ~1000 m
Turbulence model – vertical	k-ε
Turbulence model – horizontal	Smagorinsky *)
Boundary Kattegat	Flather boundary condition *)
Boundary Baltic Sea (Poland-Bornholm)	Flather boundary condition
Boundary Baltic Sea (Bornholm-Sweden)	Flather boundary condition
Bed roughness	0.05 mm, 0.025m
Smagorinsky factor	0.5
Salt and temperature	3D field, varying in time. From DHI's local model for Zero Solution Analysis
Heat exchange • Air Temperature • Humidity • Clearness	 2D map, time varying Constant 82.5 % 2D map, time varying
Precipitation	2D map, time varying
Wind	2D map, time varying
Wind friction factor	Linear (7-25 m/s) 0.001255 – 0.002425

*) See FEHY (2013b) for reference

Figure 3.3 and Figure 3.4 show near-bed current speeds at the two main measurement stations, MS01 and MS02, located centrally in the Fehmarnbelt near the proposed alignments for the tunnel as well as the bridge solution. Zooms of periods in September and October, where the highest near-bed current speeds occur are shown in Figure 3.5 and Figure 3.6.

At MS01 located at 20 m water depth, current speeds up to 0.40 m/s are measured 3 m above the sea bed during the summer period, while during the autumn measured current speeds occasionally reached values above 0.55 m/s.

At MS02 located at 29 m water depth, near-bed current speeds are generally lower than at MS02. During the summer peak current speeds reached up to about 0.30 m/s at a height 3 m above the sea bed, while current speeds during the autumn reached values about 0.50 m/s.

Measured as well as modelled current speeds and directions are shown in Figure 3.3 and Figure 3.4. The comparison has been found satisfactory. During the calibration and validation of the sigma model the primary focus has been on getting the peak current speeds as correct as possible in the numerical model, since sediment mobility is the main aim with this model set-up and the surface sediments are only expected to be mobile during these peak flow events. The peak current speeds are seen to be modelled better with the low bed roughness, $k_{a,g}$=0.05 mm, than with the larger bed roughness of $k_{a,g}$=0.025 m. During a major event in the beginning of October the model overpredicts the current speeds at MS01 as well as at MS02, and at MS02 also at an event later in October. In general, though, the overall comparison is good.

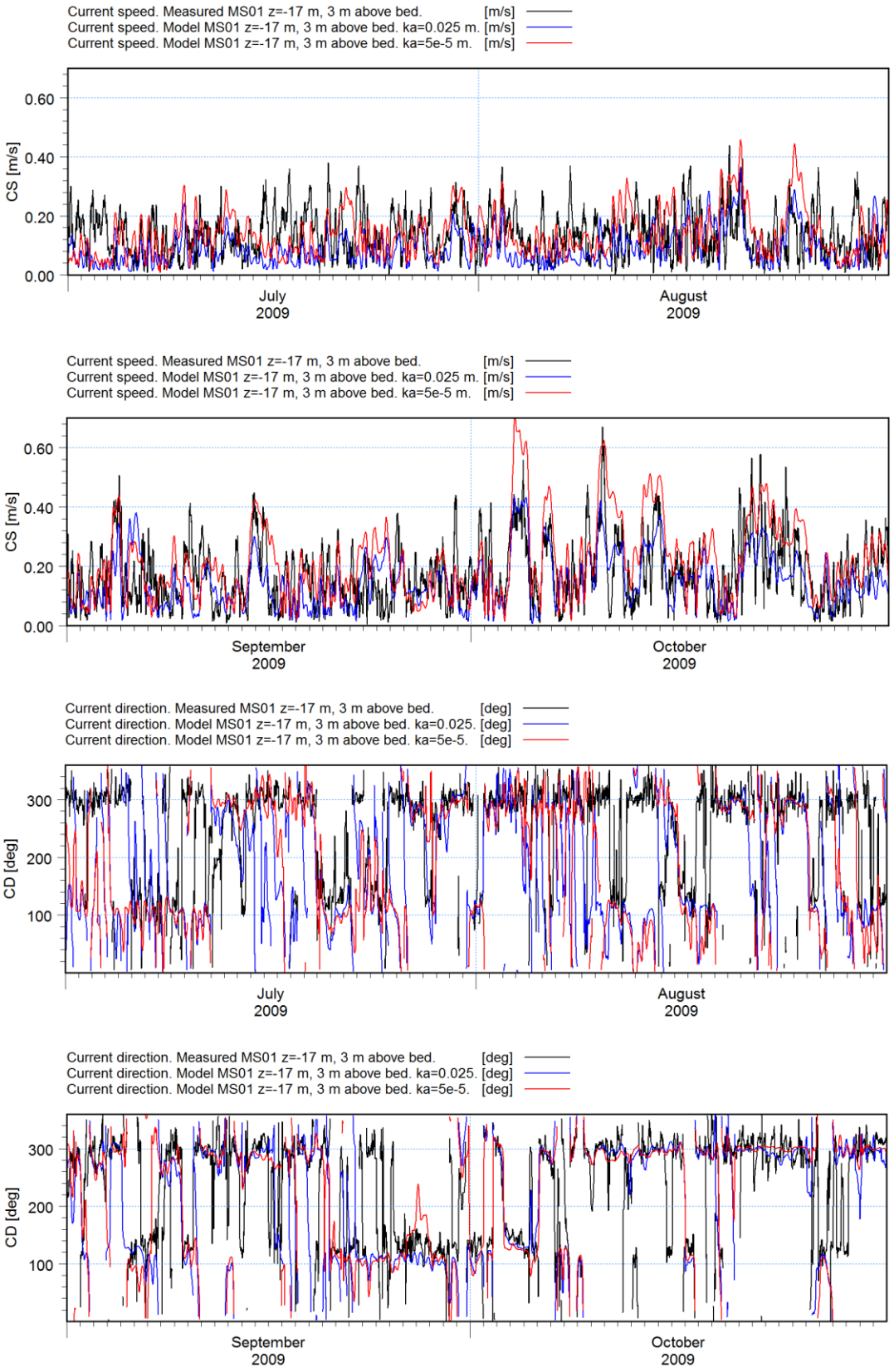

Figure 3.3 Comparison of modelled and measured near-bed current speeds and directions at fixed measurement station MS01. Sigma-Model. Bed roughness, $k_{a,g}$=0.05 mm and $k_{a,g}$=0.025m

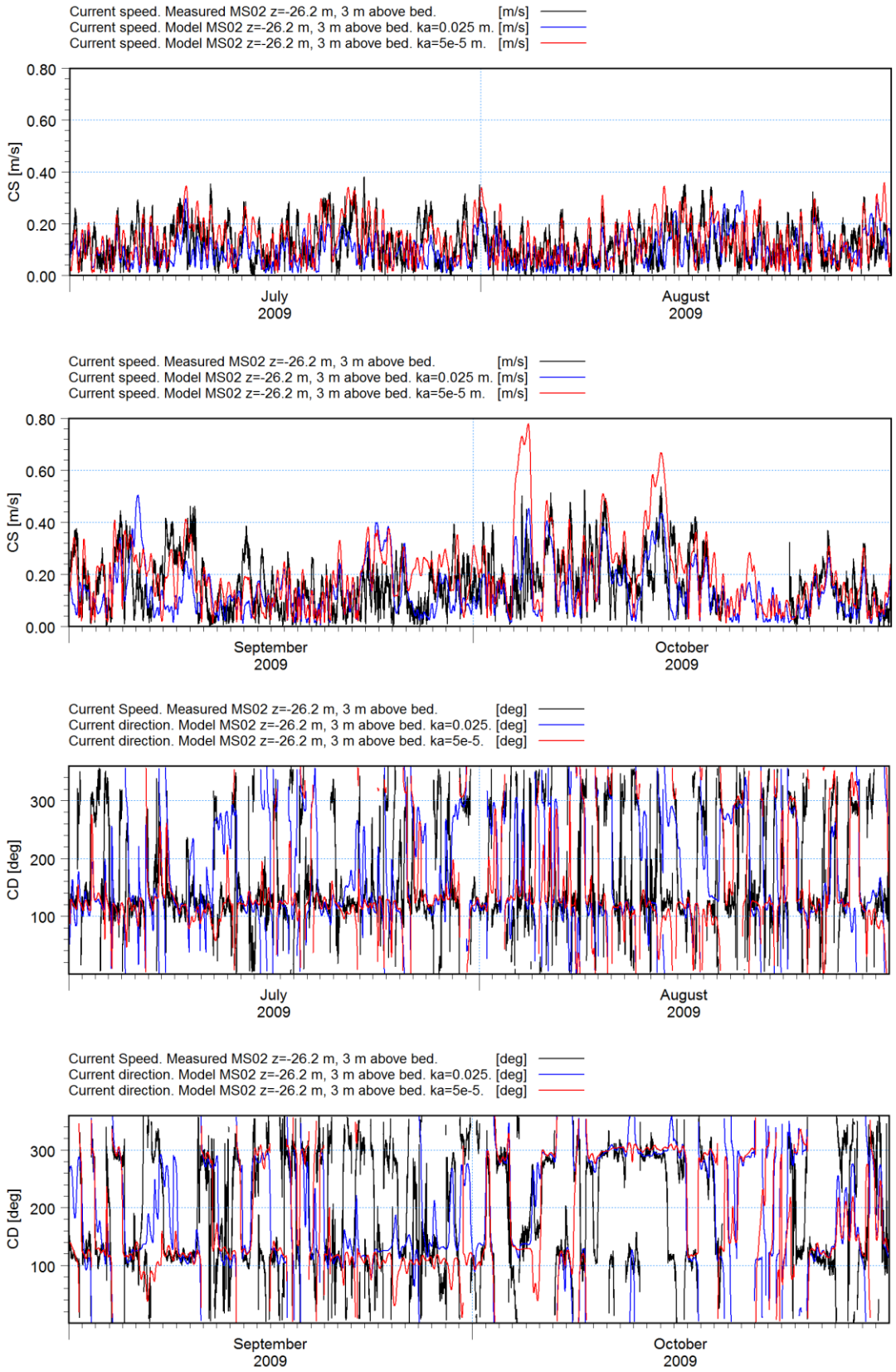

Figure 3.4 Comparison of modelled and measured near-bed current speeds and directions at fixed measurement station MS02. Sigma-Model. Bed roughness, $k_{a,g}$=0.05 mm and $k_{a,g}$=0.025m

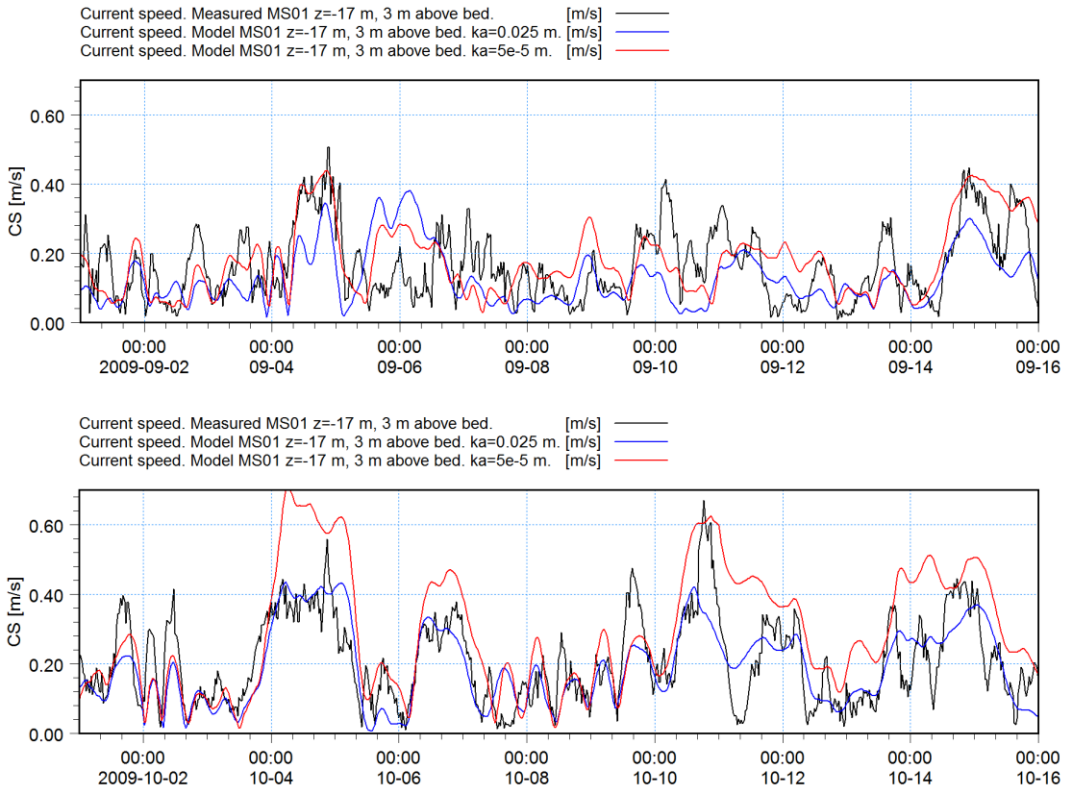

Figure 3.5 Comparison of modelled and measured near-bed current speeds at MS01 – zoom of selected periods in September and October

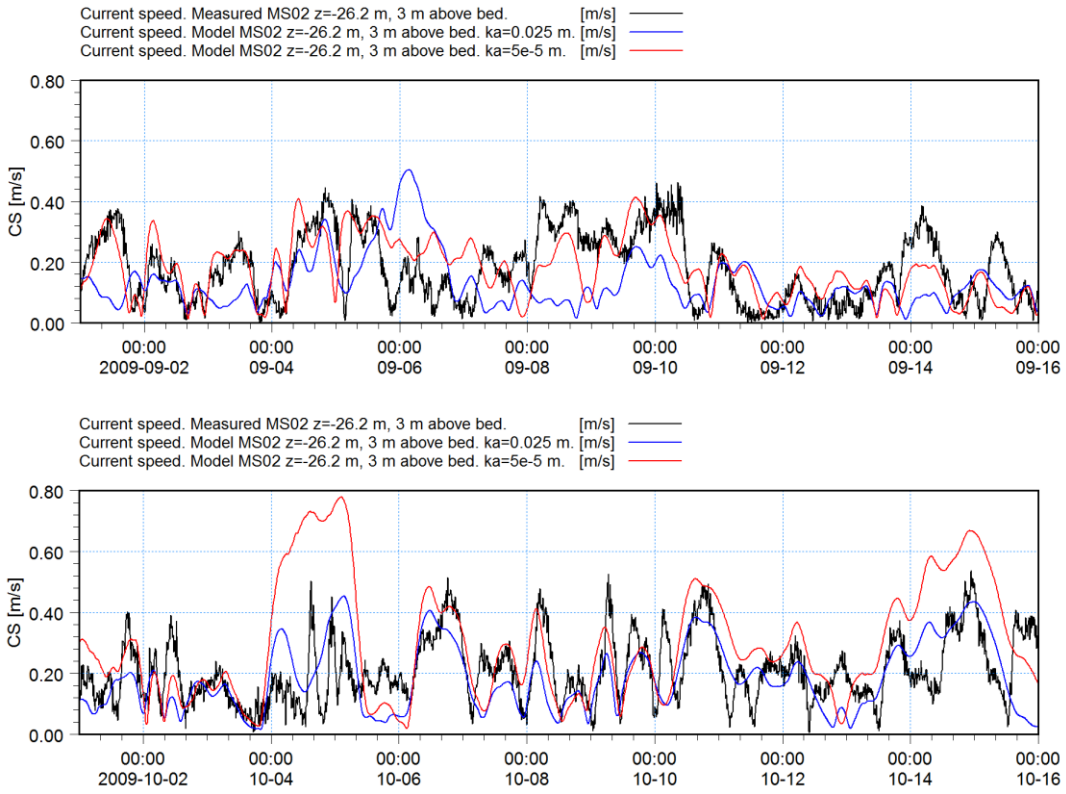

Figure 3.6 Comparison of modelled and measured near-bed current speeds at MS02 – zoom of selected periods in September and October

The distribution between in- and outflow near the bed in the Fehmarnbelt (inflow defined towards the Baltic Sea) determines the net sediment transport direction. The distribution between the flow directions is illustrated in Figure 3.7, where all current directions between 40-220 degr. N are regarded as 'inflow' (positive current speeds) and current directions between 220-40 degr. N are regarded as 'outflow'. Model results for the calibrated roughness of $k_{a,g}$=0.05 mm as well as the larger roughness of $k_{a,g}$=0.025m are compared to the measured near-bed speeds for both of the main stations, MS01 and MS02. During the model period Aug.-Oct. 2009, outflow near the bed at MS01 seemed to occur slightly more often than inflow, especially during events with higher current speed. The flow model with $k_{a,g}$=0.05 mm predicts outflow situations with current speeds between 0.3 and 0.6 m/s during a larger part of the time than measured at this station, but underpredicts the near-bed current speeds slightly for the event at Oct. 11 (ref. Figure 3.5) where the velocity exceeds 0.6 m/s. For inflow situations (current flow towards the Baltic Sea), the moderate inflow velocities (0.3-0.5 m/s) occur less frequent in the model during the period Aug.-Oct. 2009; however, the model predicts higher frequencies of high inflow velocities (above 0.5 m/s) than measured at MS01. This overprediction of high-speed inflow is related to the storm event in the beginning of Oct. 2009 (ref. Figure 3.5). The flow model with the higher roughness of $k_{a,g}$=0.025 m, in general underpredicts the current speeds and in particular the flow situations with a strong outflow. The flow model with the low roughness ($k_{a,g}$=0.05 mm) is therefore considered to give a better representation of the near-bed flow at measurement station MS01.

At MS02, inflow clearly occurs more frequently than at MS01 as seen in Figure 3.7. This is expected since the station is located at deeper waters, where the higher density water flows towards to the Baltic Sea. The flow model with higher roughness $k_{a,g}$=0.025 m predicts the frequencies of the outflow velocities below 0.45 m/s well, but completely lacks the higher outflow velocities. The flow model with the lower roughness of $k_{a,g}$=0.05 mm on the other hand overpredicts the frequencies of the high outflow velocities (>0.4 m/s). Similarly, the same model overpredicts frequencies of high inflow velocities (>0.5 m/s), while the frequencies of the moderate inflow velocities (0.3-0.5 m/s) are predicted fairly well. In general, the model with the low roughness ($k_{a,g}$=0.05 mm) is hence also considered the best model to predict the near-bed flow at measurement station MS02. The events giving an overprediction of frequencies of high-speed currents can be tracked to the same two events in October 2009, which are discussed above in relation to the comparison between model and measurements at stations MS01 and MS02.

Figure 3.8 shows a similar comparison between the distribution between the near-bed in- and outflow for the two stations MS01 and MS02 for the selected model ($k_{a,g}$=0.05 mm) for a slightly longer model period, Apr.-Oct. 2009. The inclusion of the extra months, Apr.-July 2009 available for comparison between model and measurements, does not change the overall picture of the comparison model vs. measurements, mainly because this period does not supply any significant high-velocity events.

The main purpose of the flow model is to provide input to the sediment transport modelling. Sediment transport capacity at a given time is as a rule of thumb proportional to the cube of the near-bed current speed ($Q_s \sim u^3$). An analysis on the consequences of the differences in the modelled and measured current speeds for the sediment transport rates has been carried out. It was found that the transport rates for the simulation period Apr.-Oct. 2009 applying the modelled current speeds will be about a factor of 1.5-2 too large at station MS02 and about a factor 2-3 too large at station MS01. At MS01 the overprediction of the transport rates is found to be about the same in both directions. The net transport will hence be overpredicted

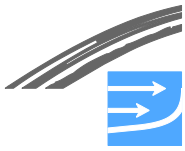

by about the same factor (1.6-1.7). At MS02, the westward transport is overpredicted slightly more (factor of 2.7) than the eastward (factor of 2.1) when applying the model results instead of the measured results. The net transport rates at MS02 (directed eastwards) will therefore be overpredicted with a smaller factor than the gross transport rates in the analysis period. In conclusion, gross as well as net transport rates are estimated to be overpredicted with a factor of about 1.5-3. These factors are within the order of uncertainty in sediment transport calculations.

It is noted that errors and inaccuracies in the hydrodynamic model may be not only due to inaccuracies in the model but may be due to errors in the driving forces.

The possible overpredictions of the sediment transport capacities are seen to be primarily connected to the sediment transport capacity occurring at current speeds above 0.5 m/s, i.e. the individual events where the flow model overpredicted the current speeds. It should be stressed that the comparison between modelled and measured current speeds and evaluated influence of the sediment transport rates is based on a short period of just seven months from Apr. to Oct. 2009, which does not include a full autumn/winter period. This causes such individual events of relatively few hours to show up very clearly in the frequency-calculations, as they are represented with relatively high frequencies in the comparison. Furthermore, events with high near-bed current speeds occur primarily in just one of the seven months, Oct. 2009. A longer period of comparison (preferably including more autumn/winter months where high-velocity events are expected) would provide more confidence in the numerical flow model, but this was not available at the time this work was carried out.

The full year of 2005 is modelled for sediment transport modelling purposes. Figure 3.9 shows how near-bed flow in 2005 seems to be directed towards the Baltic during a larger part of the time than in 2009. This seems to be the case at main station MS01 as well as at MS02. The comparison is based on the period April-Oct. which has been modelled for 2005 as well as 2009. For this period, the flow model does not predict any events with current speeds above 0.5 m/s at either of the stations MS01 and MS02. In conclusion, the flow model seems to predict the near-bed currents relatively well:

- On certain events in 2009 the near-bed current speeds are overpredicted by the model, but there is no general trend of overprediction of the peak current speeds

- During the period of comparison of modelled versus measured currents in 2009, the predicted near-bed current speeds would lead to an overprediction of the sediment transport rates in the eastern as well as the western direction. The overprediction of transport rates was mainly related to the few individual events where the flow model overpredicted the current speeds

- Based on the above analyses of the current speeds for the period Apr.-Nov. 2009 it was found that the sediment transport rates were overpredicted, but it cannot be concluded that the model in general overpredicts the near-bed current speeds and the sediment transport rates

The uncertainty with regard to the accuracy of the results is discussed where relevant in the report.

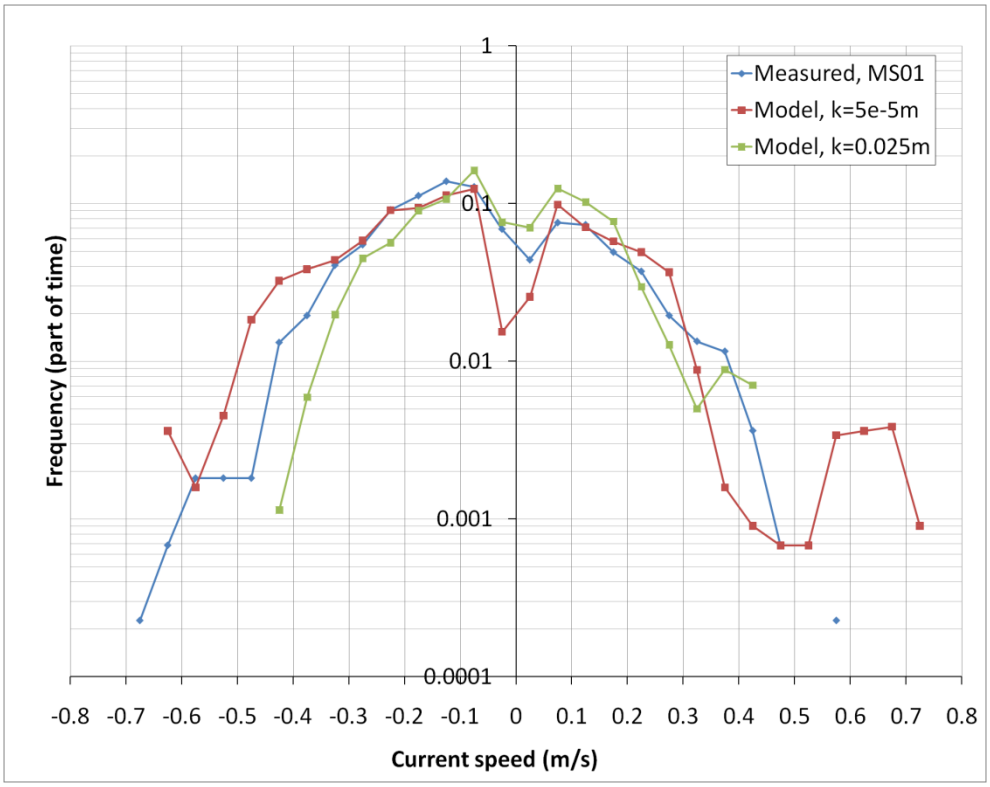

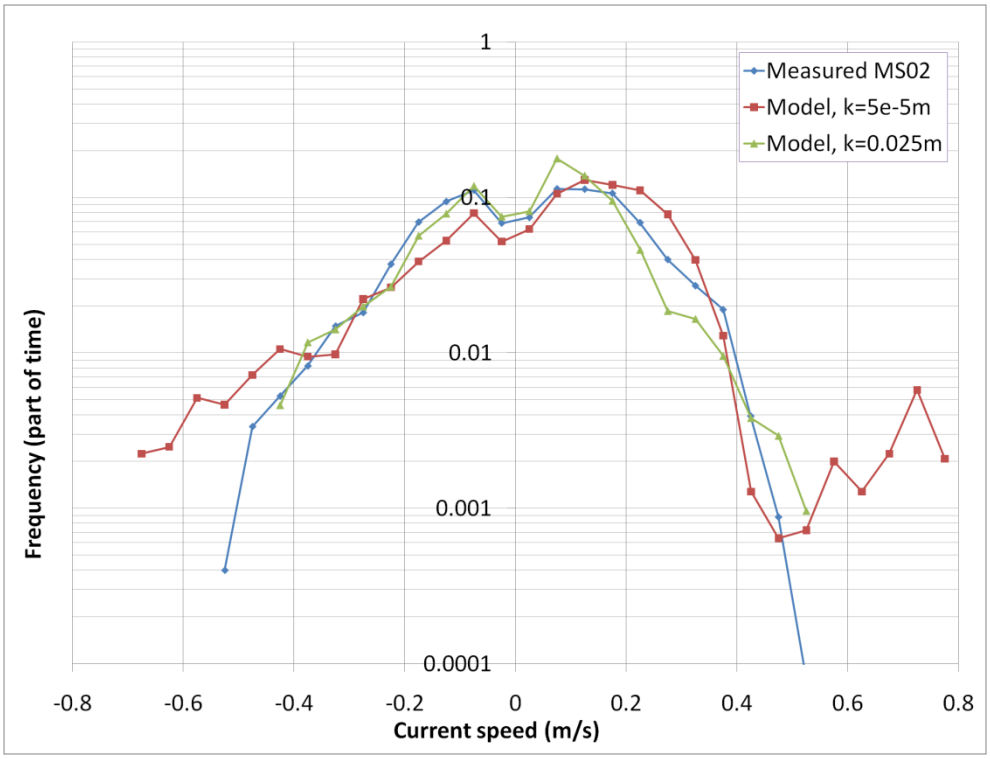

Figure 3.7 Distribution of time on near-bed current speeds at main stations MS01 (above) and MS02 (below) during in- and outflow situations (inflow: positive current speeds; outflow: negative current speeds). Comparison of modelled versus ADCP-measurements. 3 m above the sea bed. Bed roughness in Sigma-Model $k_{a,g}$=0.05 mm and $k_{a,g}$=0.025 m . Period: 1 Aug – 1 Nov 2009

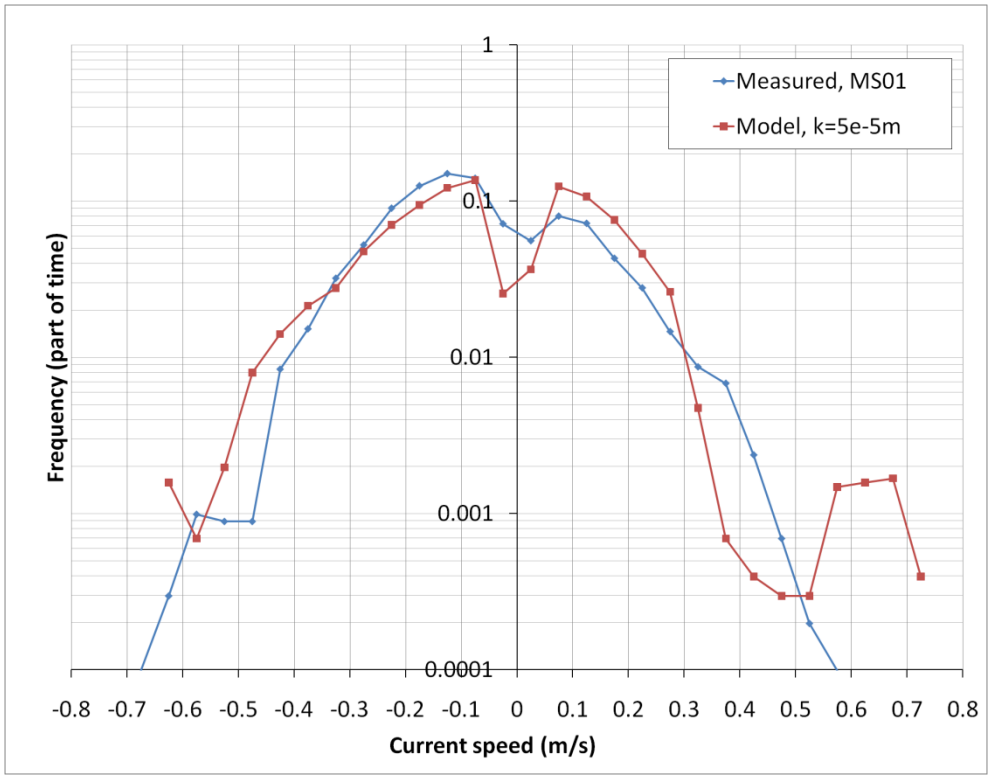

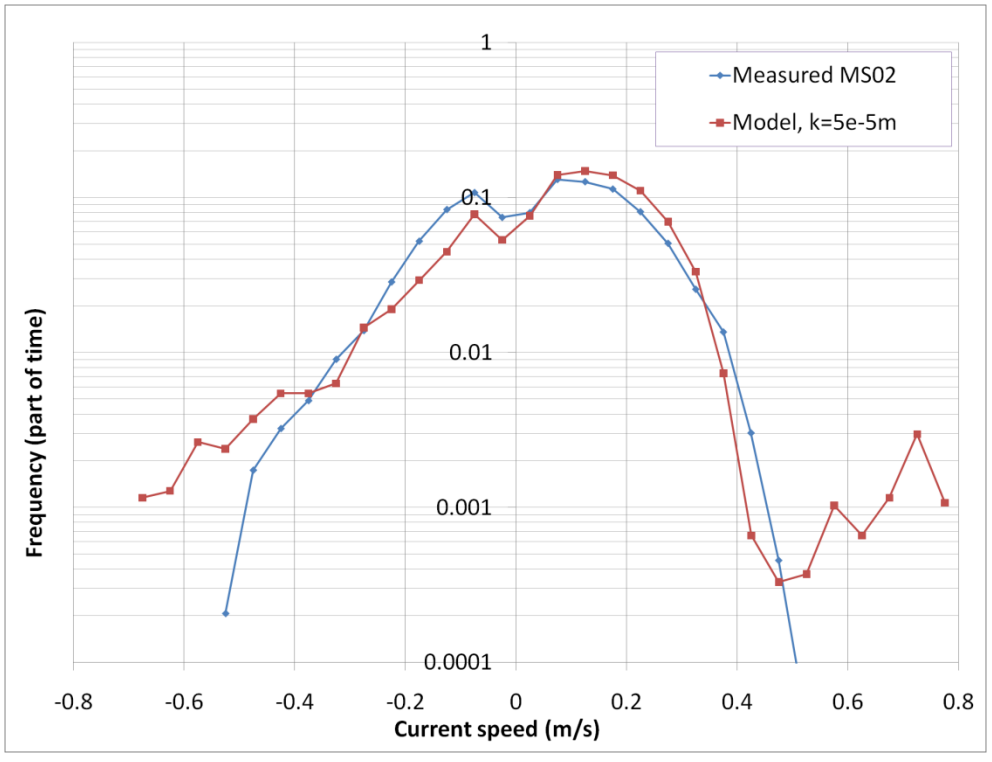

Figure 3.8 *Distribution of time on near-bed current speeds at main stations MS01 (above) and MS02 (below) during in- and outflow situations (inflow: positive current speeds; outflow: negative current speeds). Comparison of modelled versus ADCP-measurements. 3 m above the sea bed. Bed roughness in Sigma-Model $k_{a,g}$=0.05 mm . Period: 1 April – 1 Nov 2009*

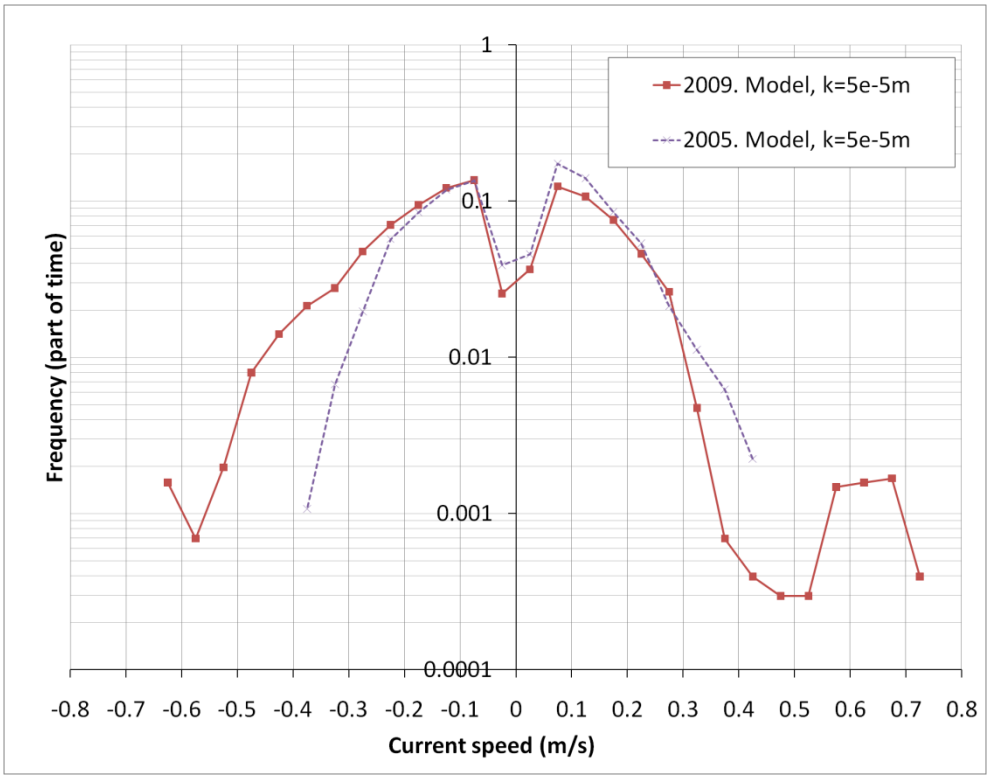

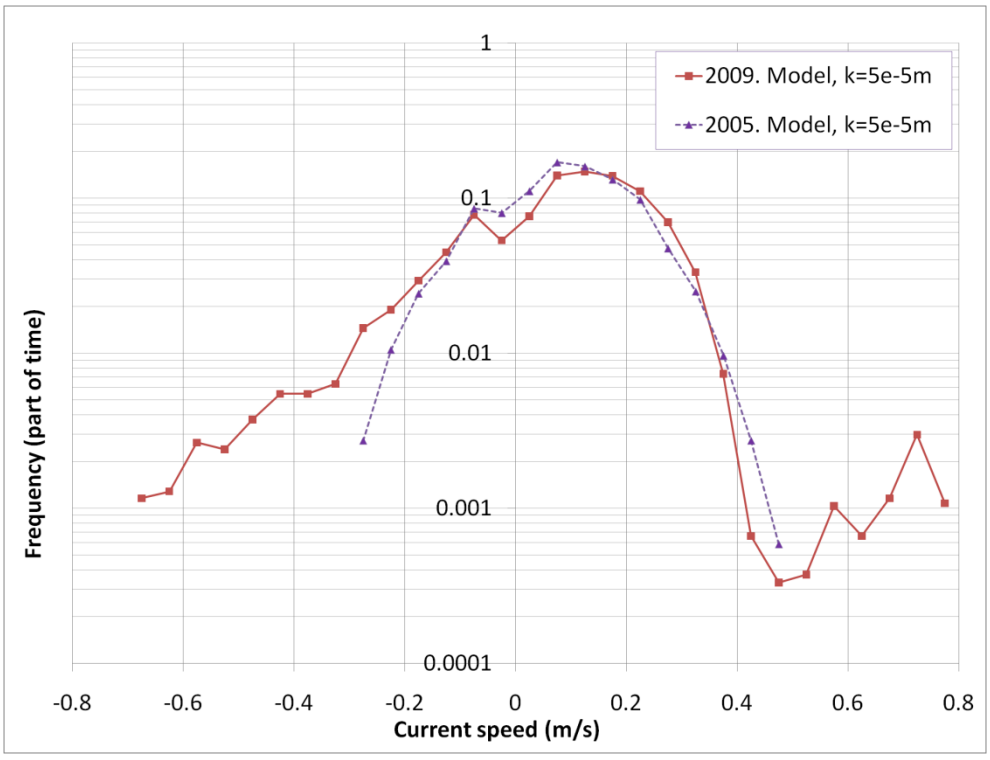

Figure 3.9 Distribution of time on near-bed current speeds at main stations MS01 (above) and MS02 (below) during in- and outflow situations in 2005 and 2009 (inflow: positive current speeds; outflow: negative current speeds). Bed roughness in Sigma-Model $k_{a,g}$=0.05 mm. 3 m above the sea bed. Period: 1 April – 1 Nov.

3.2 Sea Bed Sediments and Sediment Mobility

3.2.1 Data Basis

The surface sea bed material are described based on

- Substrate mapping
- Grab samples

The substrate mapping was carried out by Centre for Environment, Fisheries and Aquacultural Science (CEFAS) of the wider Fehmarnbelt area encompassing parts of Kiel and Mecklenburg Bays. The interpretation is based on different data sources. In the Fehmarnbelt area including the Lagoon of Rødsand and the coastline around Fehmarn, a high resolution was achieved through the use of aerial photography (in shallow waters) and multibeam data (in deeper waters), classified with Definiens image analysis software and ground-truthed with grain-size data from the baseline sampling (see below).

The sea bed sediment is mapped by analysing several hundred grab samples covering all depths in the Fehmarnbelt. In all, 8 sets of grab samples are included in the analysis:

- DHI spring 2009. Danish side at 3, 6 and 9 m depth
- DHI autumn 2009. Danish side at 3, 6 and 9 m depth
- Marilim spring 2009. German side at 3, 6 and 9 m depth
- Marilim autumn 2009. German side at 3, 6 and 9 m depth
- IOW spring 2009. Deep water 10-35 m depth (both sides)
- IOW autumn 2009. Deep water 10-35 m depth (both sides)
- GEUS summer 2009. 0, 1, 2, 3, 4, 5 and 6 m on both sides
- Rambøll winter 2009. All depths
- DHI 1998. Danish and German side. 0-8 m depth

The analysis of the grab samples is based on determination of the median grain size d_{50} and the geometric standard deviation σ_g as well as grain size distribution curves. d_{50} is the grain size for which 50% of the grains have a smaller diameter and 50% have a larger diameter. The homogeneity of the surface sediments is described by $\sigma_g = \sqrt{d_{84}/d_{16}}$.

Figure 3.10 shows a substrate map of the Fehmarnbelt. According to this it is seen that the bed on the Danish side (>-15 m) consists of sand and coarser sediments. The bed on the German side (>-15 m) also mainly consists of sand in the area west of Puttgarden and mainly of coarser sediment south-east of Puttgarden. In general, the sediment is finer on the German side than on the Danish side. At depths less than 20 m the bed consists of sandy mud or thin sandy mud.

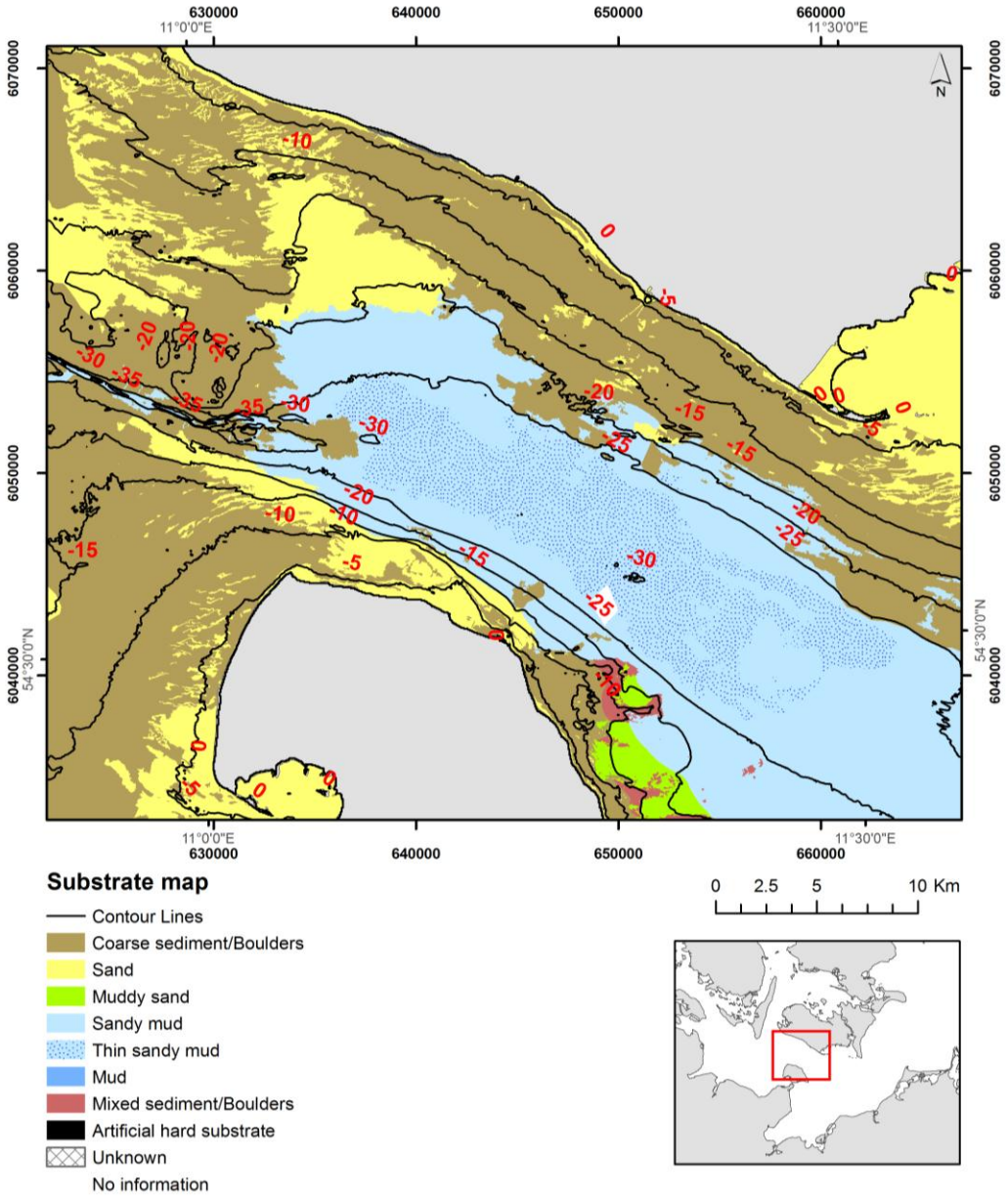

Figure 3.10 Substrate map (CEFAS) based on backscatter analysis from multibeam echo sounder (FEMA 2013)

Sediment properties like the median grain diameter and gradation are of major importance for understanding the dynamic behaviour of the bed. The analysis of the many grab samples shows a large variability of the sediment sizes across the Fehmarnbelt, but the findings agree in general well with the analysis based on the multibeam echo sounder described above.

Focusing on the area near the alignment, where the majority of the samples were collected, mapping of the median grain sizes, d_{50}, shows in general a very patchy picture on the Danish side. East of Rødbyhavn, the samples vary from very fine sand to very coarse sand (d50=0.15-4mm), see Figure 3.12, while west of the harbour the samples of fine sand are found. This indicates that the feed of finer sediments from the west is being accumulated on the west side of the harbour, while the fine sediments from the coastal stretch east of the harbour have been (and still

are) being eroded. At some sample locations (black markers), sampling was not found possible due to hard bottom indicating scarcity in fine material.

The majority of the samples offshore the Danish coast at water depth 5-15 m are medium to coarse sand (d50=0.25-1mm), but samples with finer or coarser sediments are also seen, see Figure 3.12.

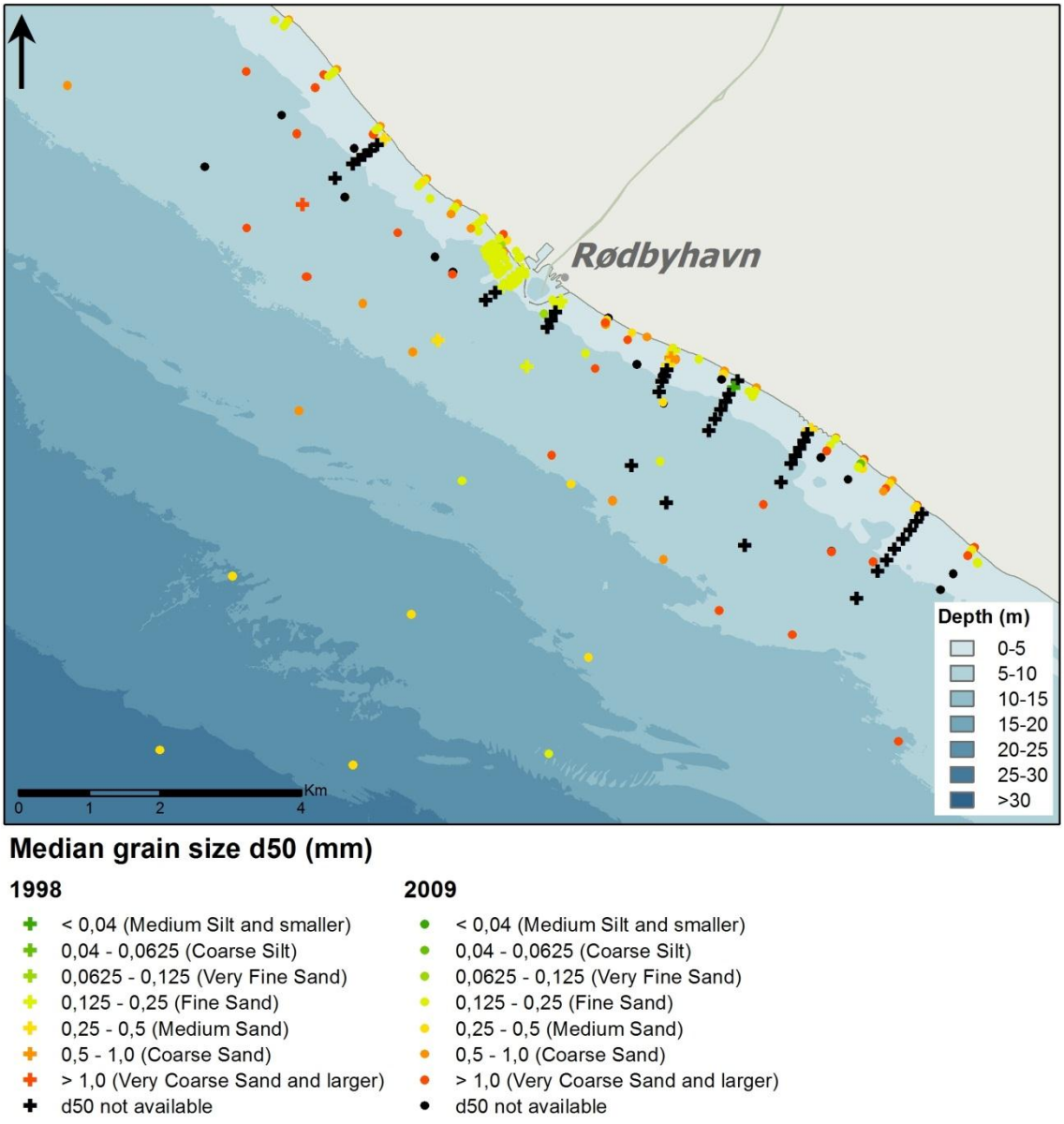

Figure 3.11 Median grain diameter d_{50} along the coast of Lolland (near Rødbyhavn)

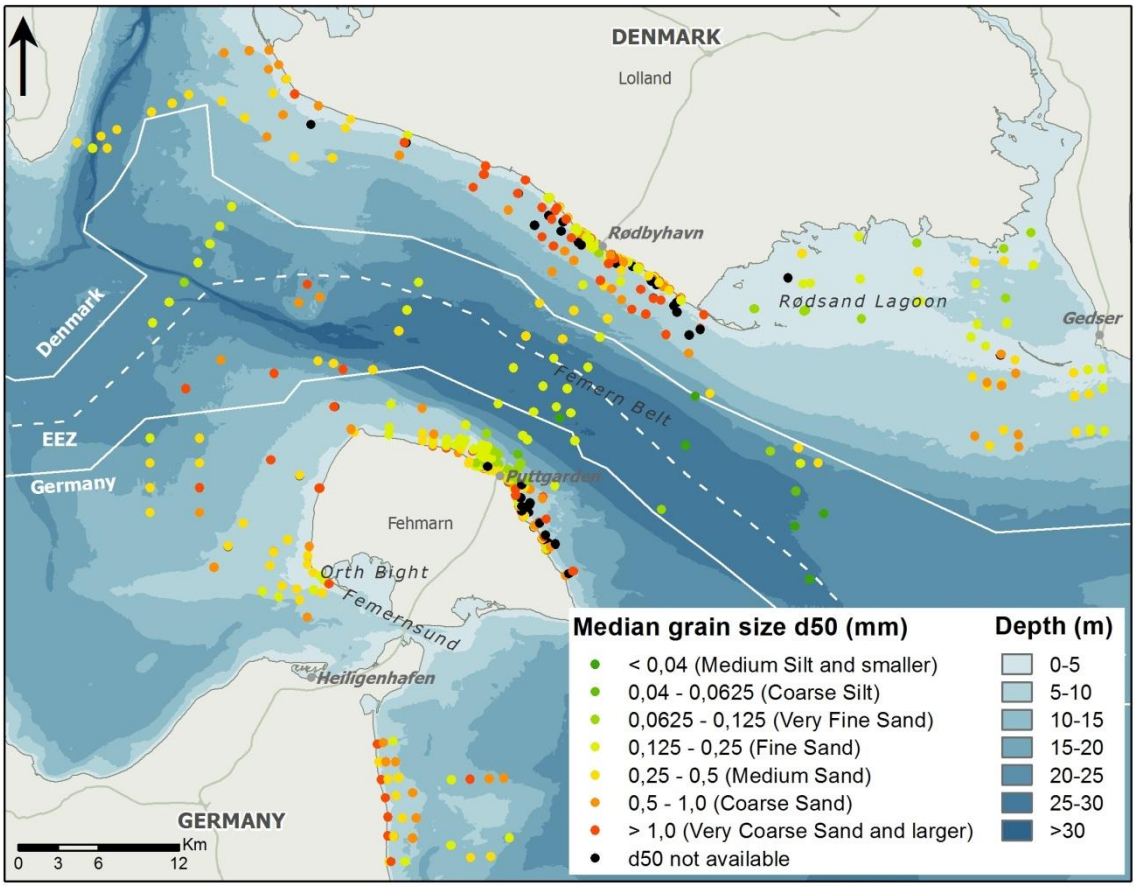

Figure 3.12 Median grain diameter d_{50} in the Fehmarnbelt

The sediment is in general poorly sorted with a geometric standard deviation ($\sigma=\sqrt{(d_{84}/d_{16})}$) of 1.5 or higher, see examples of grain size curves in Figure 3.14. Further offshore from the Danish coast (15-25 m water depths), sediment samples with median grain size of 0.15-0.25 mm are found. In the deeper areas (offshore at about 20 m water depth on the Danish side and offshore at about 15 m water depth on the German side), samples with fine sand with median grain sizes in the range of 0.1-0.15 mm were found. Many of the deep water samples are very poorly sorted, mainly because these contain very fine particles (mud), see grain size curves in Figure 3.15. This is in line with Figure 3.10, where the sea bed is described as consisting of sandy mud/thin sandy mud in these areas.

Offshore the German coast, the sediment is in general finer than offshore the Danish side, see grain size curves in Figure 3.16. Areas with very fine sand and fine sand are found at water depths of 5-15 m, while the coastal stretch immediately east of the harbour consists of medium sand, see Figure 3.13.

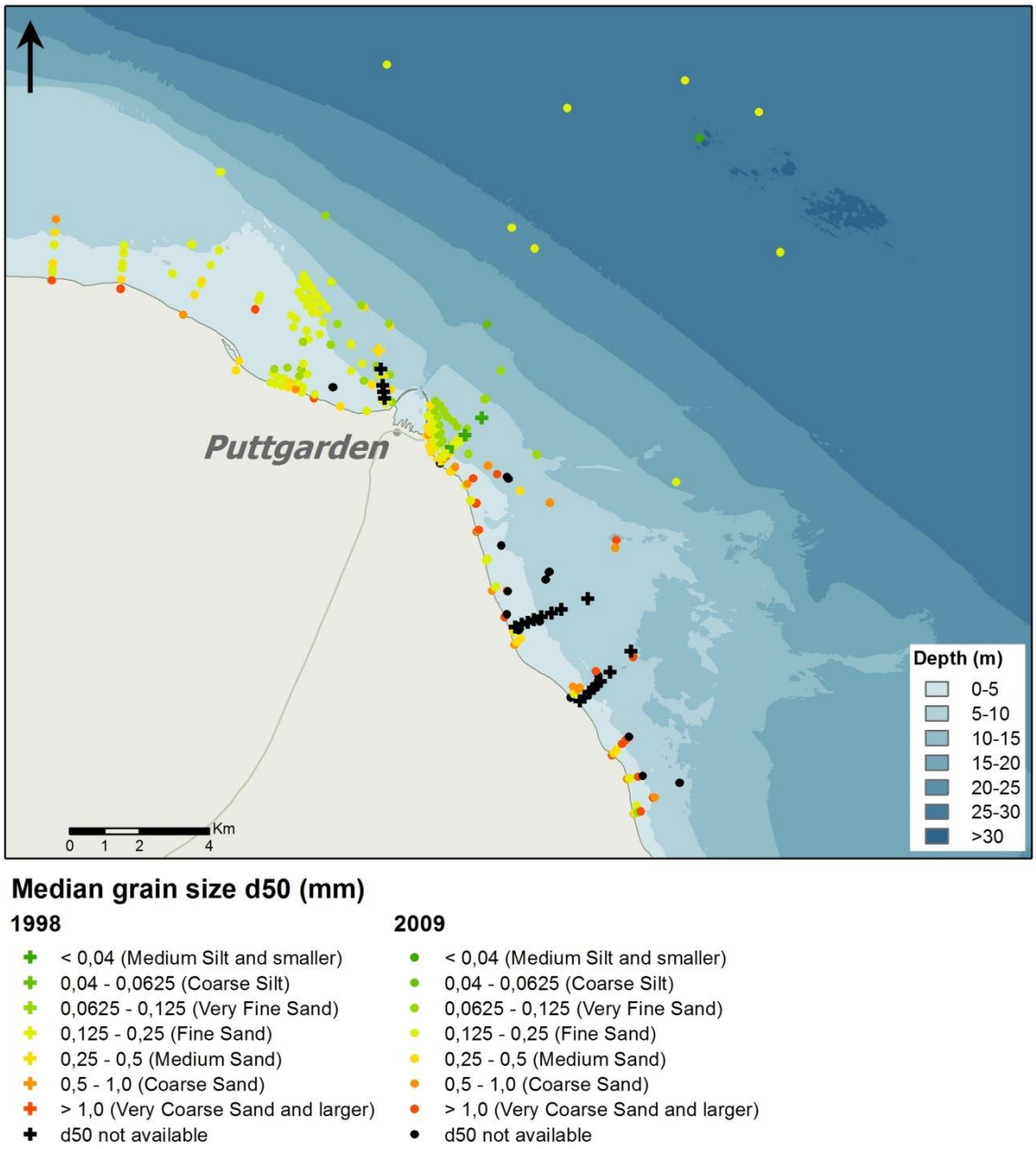

Figure 3.13 Median grain diameter d_{50} along the coast of Fehmarn (near Puttgarden Harbour)

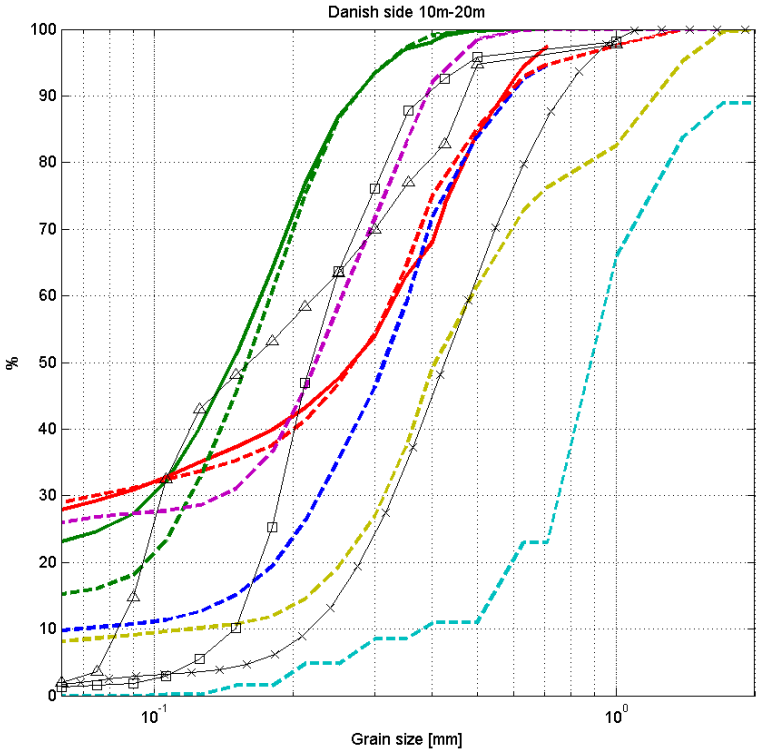

Figure 3.14 Grain size distribution curves. Danish side at 10-20 m depth. Sea bed samples within approximately +/- 2.5 km from alignment

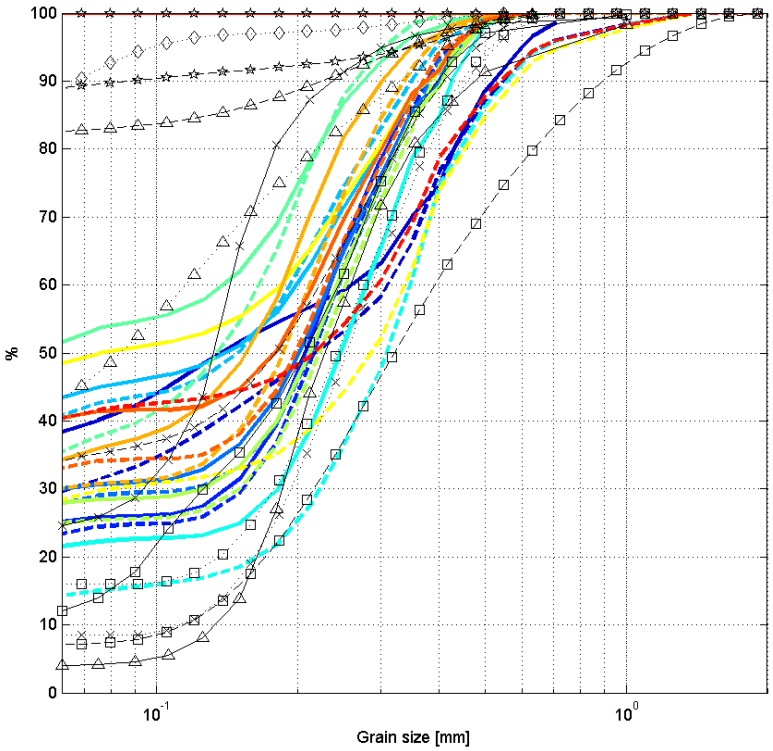

Figure 3.15 Grain size distribution curves. Water depths greater than 20 m. Sea bed samples within approximately +/- 2.5 km from alignment

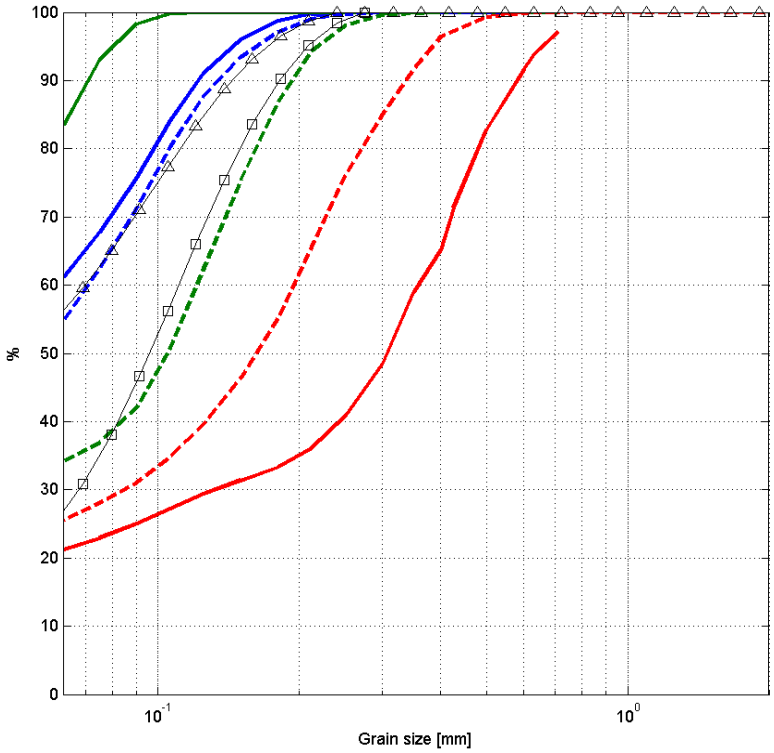

Figure 3.16 Grain size distribution curves. German side at 10-20 m depth. Sea bed samples within approximately +/- 2.5 km from alignment

3.2.2 Methods

The sediment transport in the Fehmarnbelt is modelled with DHI's MIKE3-ST (sediment transport). MIKE3-ST calculates the sediment transport based on a quasi-3D approach, see (Fredsøe et al. 1985, Deigaard et al, 1986).

Outside the wave breaking zone the waves primarily act as an extra force in mobilising the sediment. Inshore of the wave breaking zone, the waves also act to drive a coastal current. Calculations of the long shore littoral drift driven by the coastal current are carried out using LITDRIFT in DHI's LITPACK modelling system. The LITDRIFT module is used to determine the annual littoral drift at a given section of the coast near the land fall areas. It simulates the cross-shore distribution of wave height, set-up and set-down, long-shore current and sediment transport for an arbitrary coastal profile.

The basis for the calculations of the sediment transport rates comprises the gathered information on the sea bed material and the simulations of the near-bed current fields and wave fields for the entire 2005 as described in Section 3.1.2.

All sediment transport rates are inclusive of pore volumes (40%) unless they are otherwise stated specifically in the text as solid volumes.

Model setup for MIKE3-ST - water depths greater than 4 m

Sediment transport at water depths greater than 4 m are modelled with MIKE3-ST for the entire year 2005. MIKE3-ST calculates the sediment transport rates in each computational cell (see computational grid in Figure 3.2) for every time step during 2005.

Besides the current and wave fields, the properties for the sea bed material are the most important parameters governing the sediment transport rates.

The sediment properties in the modelling area are selected such that they represent the surface sea bed material in the alignment area, see Section 3.2.1.

The median grain diameter, d_{50}, and the geometric standard deviation, σ, for samples collected within a zone of approximately 5 km across the Belt in the alignment area are shown in Figure 3.17. The figure illustrates how the sediment properties vary with the water depths on the Danish and German side of the Fehmarnbelt, respectively. Sediment transport simulations are carried out for a lower and an upper limit of d_{50} for ranges of water depth across the belt. These limits are indicated with blue and green lines in Figure 3.17. The limits range between 0.1 and 0.5 mm and are kept slightly in the lower range of grain sizes found in the bed sample analysis.

A geometric standard deviation, σ, of 1.5 is selected in all runs. This is lower than the standard deviation found in the sea bed samples, but reflects (in combination with the selected grain sizes) the range of grain sizes that are expected to be mobile in the Fehmarnbelt.

The bed roughness in the sediment transport calculations, k_N, is 2.5 times the median grain size, d_{50}. This bed roughness is used for calculating the skin friction, which is the forcing between the flow and the individual grains in the sea bed material that acts to mobilise the grains. The "roughness" in the overall hydrodynamic model is a calibration parameter. It is different to the physical skin roughness in the transport model and found by calibration.

Remaining model parameters for MIKE3-ST are summarised in Table 3.3.

Table 3.3 Model parameters for MIKE3-ST

Parameter:	**Parameter setting:**
Sediment description:	Median grain diameter, d_{50} = varying with water depth, see Figure 3.17 Geometrical standard deviation for the grain size diameter, σ = 1.5 Porosity of sediment = 0.4
Bed roughness in sediment transport calculations:	Bed roughness: Nikuradse roughness, $k_N = 2.5*d_{50}$
Critical Shields parameter:	$\theta_c = 0.045$
Sediment transport formulation:	Zyserman-Fredsøe (1994)
Water temperature:	10 degr.
Wave climate:	Time series of 2005 wave modelling data
Current conditions:	Time series of 2005 flow field (3D)

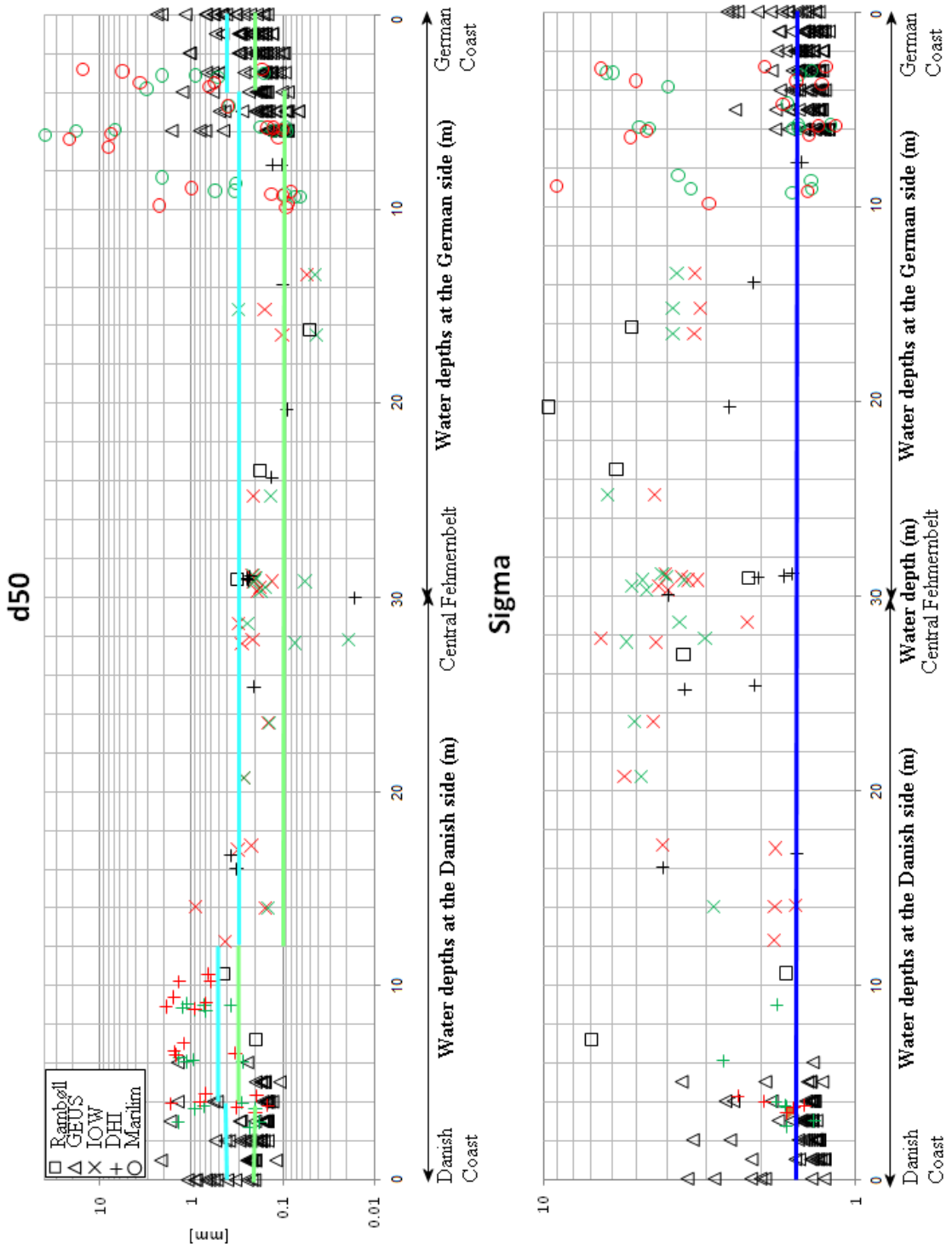

Figure 3.17 Correlation between depth and mean grain diameter/geometric standard deviation in the Fehmarnbelt. Green markers indicate samples taken in spring and red in autumn. The lines show selected grain size diameter in sediment transport modelling: lower limit d_{50} - light green; upper limit d_{50} - light blue; and geometric standard deviation (indigo blue)

Model setup for LITDRIFT - water depths below 4 m

The long shore littoral drift caused by the wave driven currents occurs on both sides of the Fehmarnbelt inshore at water depths less than 4-5 m. LITDRIFT has been calibrated on both coasts. The calibration and the detailed results are presented in FEHY 2013a. The model parameters are summarised in Table 3.4.

Results from littoral drift calculations east of Rødby and east of Puttgarden are used to assess the sediment transport in the near-shore zone.

Figure 3.18 and Figure 3.19 show the bathymetries east of the two harbours and locations of profiles used in (FEHY 2013a). In this report results from profile "D12" and "G9" are reported. The profiles are shown in Figure 3.18 and Figure 3.19, respectively.

The profile used in the LITDRIFT calculations is extracted perpendicular to the near-shore contour lines. The time series for the waves entering the sediment transport calculations are extracted at a water depth of 4 m.

Wave roses for the Danish as well as the German side are shown in Figure 3.20. The wave data are extracted from the wave model documented in (FEHY 2013a).

Table 3.4 Model parameters for LITDRIFT

Parameter:	Parameter setting:
Grid spacing:	1 m
Sediment description:	Graded sediment, 10 fractions d_{50} =0.2- 0.3 mm, σ = 1.3-1.7 (from mapping) porosity = 0.4
Critical Shields parameter:	θ_c = 0.045
Water temperature:	10 °C
Wave climate:	Wave statistics at 4 m from 1989-2010
Bed roughness:	20 d_{50}

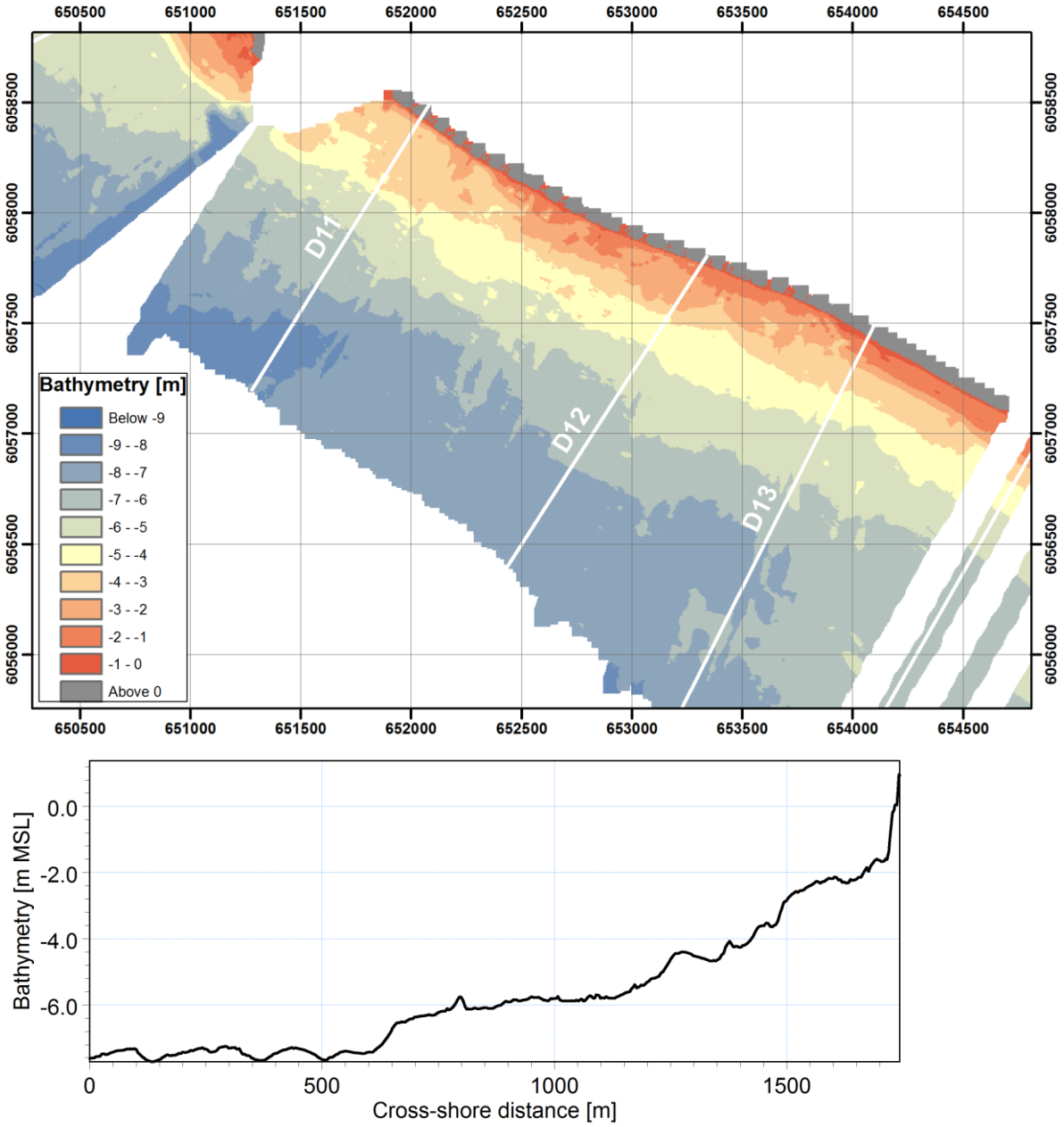

Figure 3.18 Danish near-shore bathymetry and profiles used in LITDRIFT. Lower figure shows a zoom of the coastal profile D12 in the littoral zone.

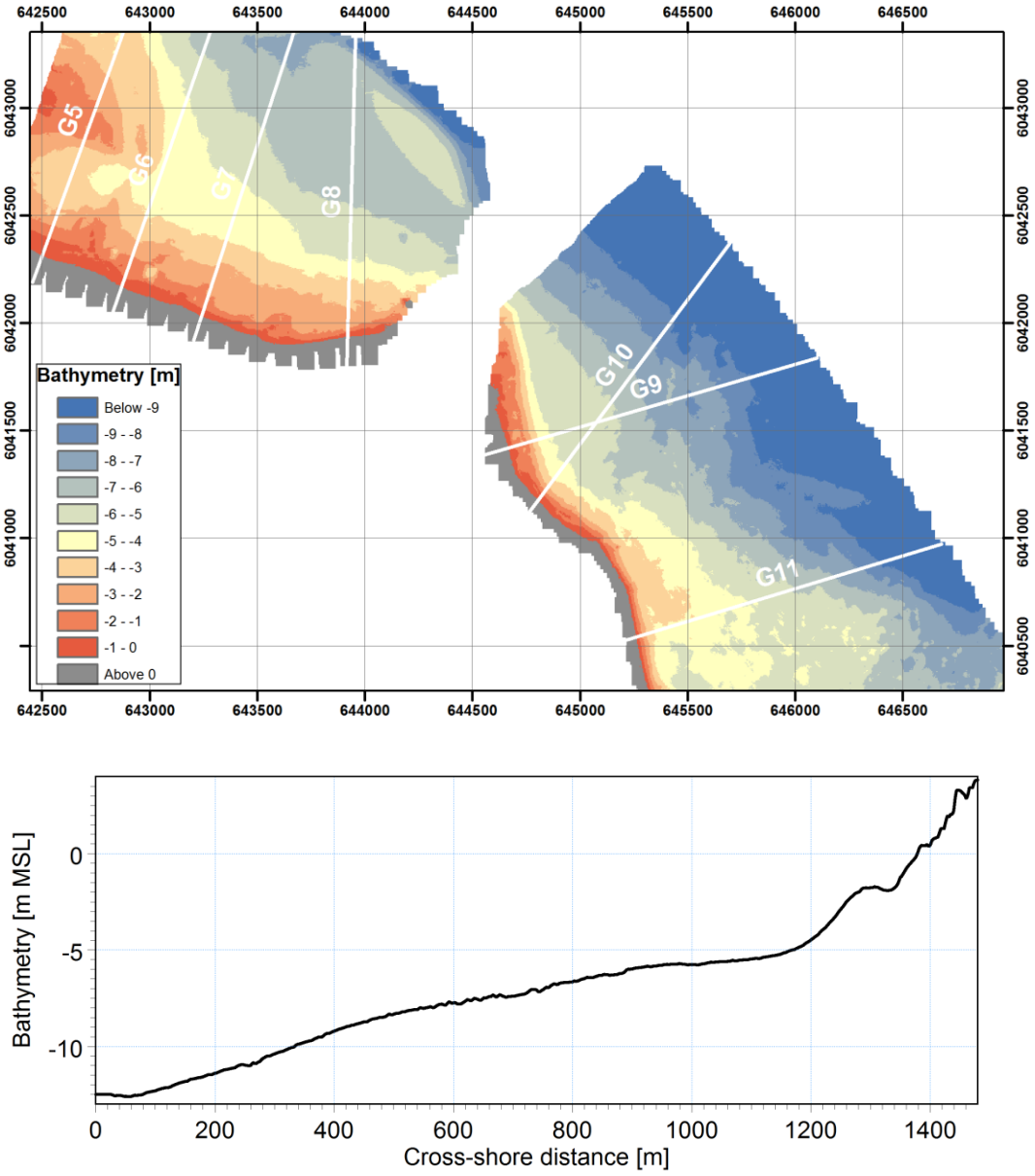

Figure 3.19 German near-shore bathymetry and profile used in LITDRIFT. Lower figure shows a zoom of the coastal profile G9 in the littoral zone

East of Rødby

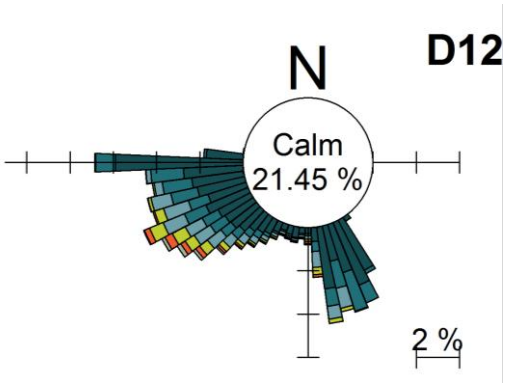

East of Puttgarden

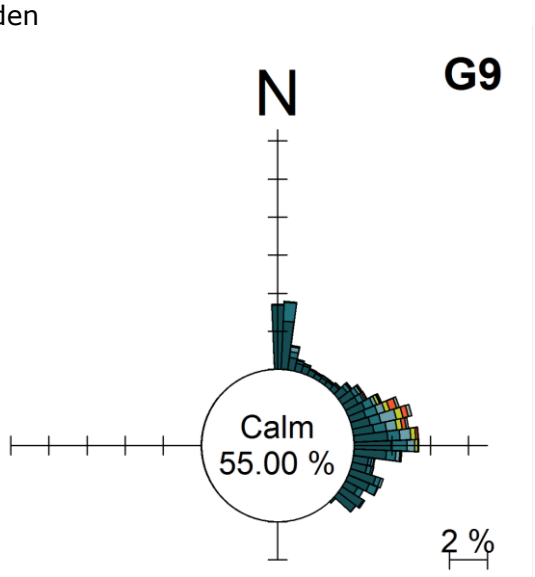

Figure 3.20 Wave roses for the Danish side (4 m water depth, upper figure) and the German side (4 m water depth, lower figure). Wave statistics for the period1989-2010 from.(FEHY 2013a)

3.3 Sea Bed Morphology and Bed Forms

3.3.1 Data Basis

The sea bed morphology is based on a detailed mapping of the bathymetry performed in 2009 by Rambøll/Marin Mätteknik for the Fehmarnbelt using multibeam echo sounder. The multibeam measurements are carried out for water depths greater than approximately 6 m. The resolution of the provided sea bed measurements is 2 m. The measurement accuracy in the water depths from the multibeam dataset is varying slightly from area to area, but is in the order of about +/-0.2 m. The extend of the data set is shown in Figure 3.21.

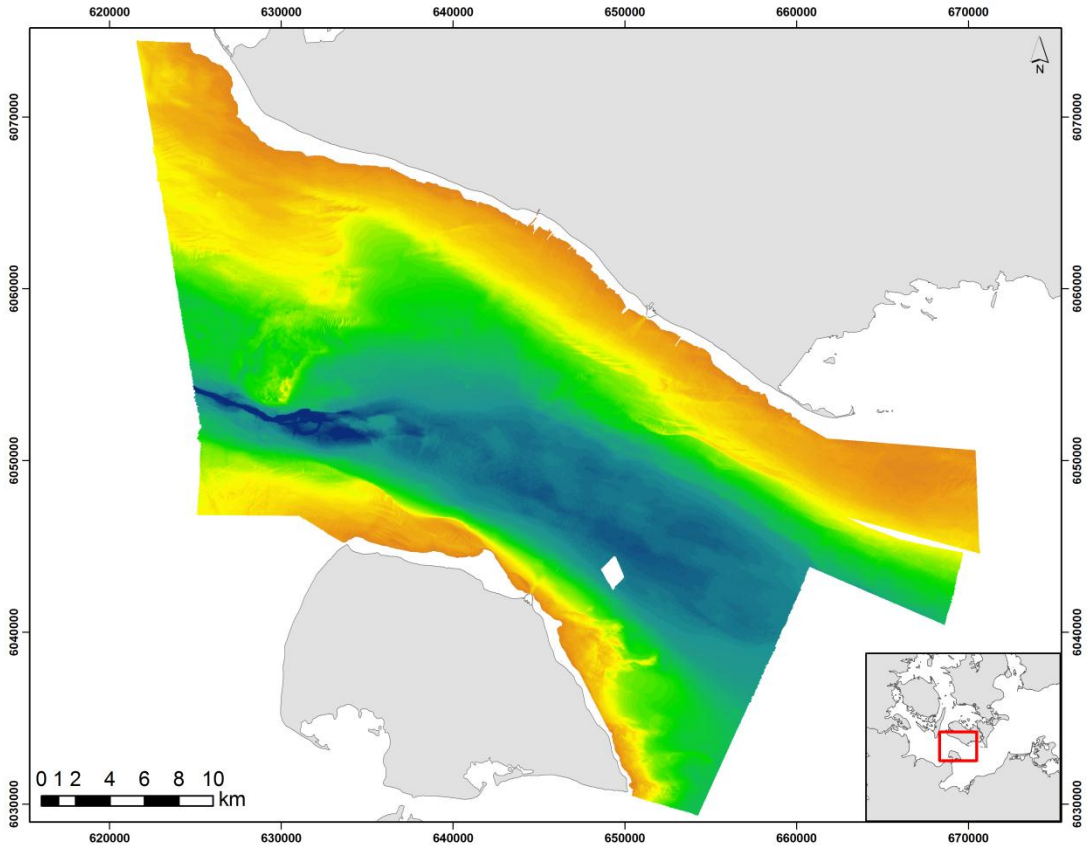

Figure 3.21 Illustration of the multi beam data set from 2009.

3.3.2 *Methods - Classification*

Areas with significant bed forms in the Belt are identified by a "bed slope" and a "difference" analysis. The slope analysis is based on calculations of the maximum slope between a given 2x2 m cell and its neighbouring cells. This analysis results in a map showing the slopes of the sea bed in degrees in the Fehmarnbelt. The difference analyses are made by calculating the average bathymetry within a radius of 200 m of each cell and subtract it from the actual bathymetry. This results in a map showing the striking undulations of the sea bed.

Based on the slope and difference maps it is possible to identify different areas with large concentration of bed forms. These areas are investigated further and detailed maps for these areas are shown in Chapter 6 and in Appendix A, which comprises zooms of individual areas with bed forms.

The bed forms are described by a number of characteristic parameters such as the height, length and local maximum steepness. The height of the bed forms is defined as the total height from the local maximum bed level (denoted top of the bed form) to the following local minimum bed level (denoted the trough of the bed form) and the length of the bed forms is described as the distance from a local minimum to the following local minimum (trough to trough).

The migration rates of the sand waves in the areas closest to the alignment are estimated based on the sediment transport rates evaluated in Chapter 6.

The migration rate of sand waves can in the case where the sediment is primarily being transported near the bed (bed load) be estimated as the relation between the sediment transport and the sand wave height, see (Fredsøe 1982) and Figure 3.22:

$$Migration\ rate\ (m/year) = \frac{sediment\ transport\ rate\ (m^3/m\ /year)}{sand\ wave\ height\ (m)}$$

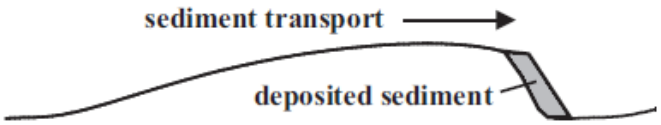

Figure 3.22 Conceptual drawing of sand wave migration

3.3.3 *Methods - Interaction between Bed Forms and Overall Flow*

The interaction between the bed forms and the flow is analysed by comparing the flow fields calculated by the numerical three-dimensional flow model, MIKE3, for the situation with a flat seabed without sand waves and for the situation with sand waves in the areas where they have been identified in the Fehmarnbelt.

The flow model applied is the model setup described in Section 3.1.2, which covers the southern part of Kattegat, the Belt Sea and the south-eastern part of the Baltic Sea. The time period of the analysis covers three months from 1st of August 2009 to 1st of November 2009.

The flow resistance from the sea bed can be divided in two contributions:

A: Skin friction

B: Form drag

The skin friction, A, is caused by the friction between the sea bed material and the water. The skin friction hence represents the local bed shear stresses along the dune, which are present as the near-bed flow is retarded close to the bed. The form drag, B, is due to pressure differences on the upstream and downstream sides of the dune, which result in a net-force.

In Figure 3.23 the upper panel shows a steep dune where the downstream slope of the dune is so steep that the near-bed flow is not able to follow the dune shape. Downstream of the crest the flow detaches near the bed, and the so-called flow separation occurs where a recirculation zone is present downstream of the crest. This causes a pressure variation along the dune which corresponds to the form drag. The lower panel shows a flat dune, where no separation occurs so the form drag becomes much smaller. In this case the flow resistance is mainly due to skin friction.

Due to computational time the bathymetry in the hydrodynamic model does not resolve the individual sand waves. Also this type of model does not resolve the near-bed physics accurately enough to determine the drag contribution from the bed forms. The additional flow resistance due to the presence of bed forms is therefore

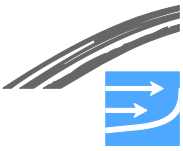

"parameterized" by an increased skin friction in areas where bed forms have been identified. The parameterization is based on detailed calculations of the local pressure variation with a separate CFD model, Dune, see (Niemann 2003) and (Tjerry and Fredsøe 2005).

The analysis hence includes the following tasks:

Task 1: Detailed calculations of the additional flow resistance along individual dunes with the model Dune. Calculations of skin friction and form drag from the sand waves are calculated for all transects shown in Section 6.3 through the individual sand wave fields.

Task 2: Parameterization of flow resistance. The increase in flow resistance due to sand waves is parameterized such that the additional flow resistance from the sea bed forms is included in the areas where the sand waves have been identified.

Task 3: Simulation of flow fields in MIKE3 with and without the additional flow resistance from the sand waves included.

Task 4: Analysis of flow results and quantification of the interaction between the sand waves and the flow field.

The detailed calculations of the flow field and the pressure variation along the sand waves using the model Dune to obtain the form drag are described below. The calculations enable us to describe the flow resistance for the sand waves in any combination of the flow direction and the directions of sand waves. The parameterization of the drag, which is the input to the hydrodynamic model of the Fehmarnbelt, is also described below.

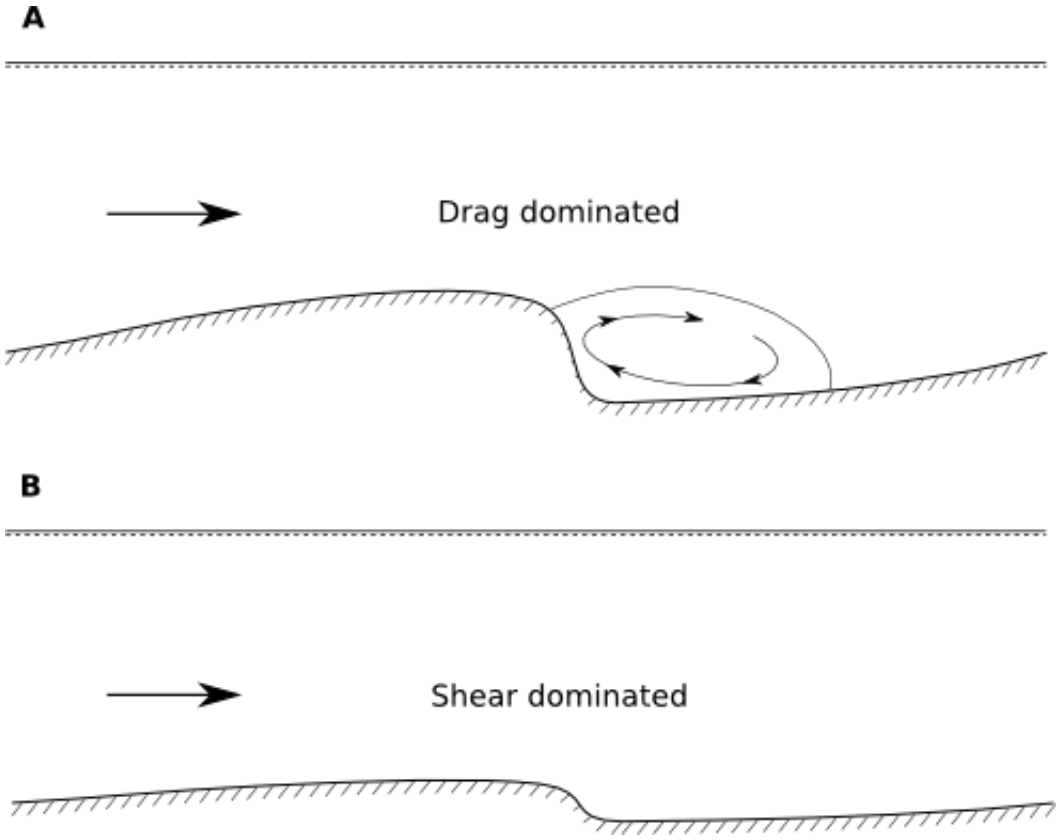

Figure 3.23 Two types of dunes with different steepness. A: The flow resistance is dominated by form drag. B: The flow resistance is dominated by shear/skin friction

Task 1: Method for detailed calculations of flow resistance along individual sand waves

The pressure and bed shear stress distributions are the basis for the resistance computation. The total flow resistance per metre length of a sand wave is given as the sum of bed shear stresses and pressure drag averaged over a sand wave field.

$$C_d = C_f + C_p = \frac{2}{\lambda \rho V^2}\int_0^{\lambda} \tau_b dx + \frac{2}{\lambda \rho V^2}\int_0^{\lambda} p\vec{n}\cdot\vec{e}_x dx \qquad (3\text{-}1)$$

where C_d, C_f and C_p are the coefficients due to total flow resistance, skin friction and form drag, respectively. Further λ is the length of the sand wave, V is the depth average velocity, τ_b is the bed shear stress, ρ is the density of water, p is the pressure along the bed, $\vec{n}$ the vector normal to the bed and $\vec{e}_x$ the unit vector in the x-direction.

The CFD model, Dune, fully resolves the near-bed flow in the vertical as well as in the horizontal directions and enables computation of the detailed flow along the individual sand waves and obtain the shear stresses, velocities and pressures in any 2-dimensional non-uniform plane flow (the plane has one horizontal and one vertical coordinate). The assumption in such a model is that the dunes are 2-dimensional, i.e. their crests are parallel in the plane view. This is generally the case in the Fehmarnbelt, where the length of the crest typically is several times the length of the dune. One exception is bed forms in lunate bed forms dune, which

have pronounced 3-dimensional features. This bed form will be treated separately, see below.

In the framework of 2DV computations, it is possible to evaluate C_d in four different flow directions, namely when the current is in either direction perpendicular to the dune crest and in the two directions parallel to the dune crest. In the last case the two coefficients obviously are identical, as it corresponds to the flat bed case. This is illustrated in Figure 3.24A, where an arbitrary orientation of the dune field has been defined as α_d.

A complete description of the angle between the dune field orientation and the near bed current direction is needed in the MIKE3 framework and a reasonable variation must be specified. In the present case this variation has been chosen to follow an elliptic shape, which is further supported by the final results, as the ellipse is almost circular because most of the flow resistance is carried by the bed shear stress while the drag contribution is small.

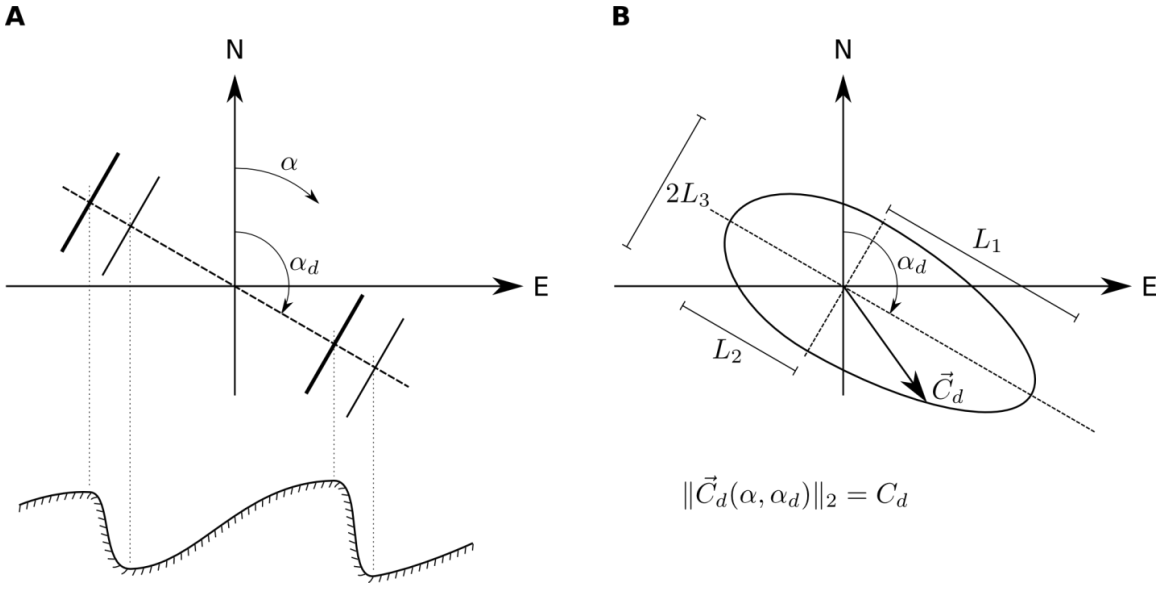

Figure 3.24 A definition sketch of A: the dune orientation relative to true north and B: the elliptic variation of C_d as a function of current and dune field orientations

The elliptic variation, see Figure 3.24B, can be described in the following way:

$$\vec{C}_d = \left(L(\alpha,\alpha_d)\cos(\alpha-\alpha_d), L_3\sin(\alpha-\alpha_d)\right)$$

where

$$L(\alpha,\alpha_d) = \begin{cases} L_1 & \text{for} \quad \alpha_d - \dfrac{\pi}{2} < \alpha \le \alpha_d + \dfrac{\pi}{2} \\ L_2 & \text{for} \quad \alpha_d + \dfrac{\pi}{2} < \alpha \le \alpha_d + \dfrac{3\pi}{2} \end{cases}$$

Based on the above, C_d is given as the length of the elliptic variation, e.g. $\left\|\vec{C}_d(\alpha,\alpha_d)\right\|_2$.

The flow simulations are carried out as steady flow cases for three velocities 0.3 m/s, 0.5 m/s and 0.7 m/s (depth averaged values) to cover the variation in the Fehmarnbelt. The simulations are carried out for the two horizontal flow directions perpendicular to the crest line of the sand wave fields.

The bed roughness for calculation of the skin friction in Dune has been taken as $k_{a,Dune}$ =0.5 mm, 0.00125 m and 0.025 m. The skin friction impacts the near-bed flow field and hence also changes the bed pressure and hence the form drag. The latter value is used to take into account the presence of current ripples on top of the dunes.

The bed shear stresses and the pressure drag for the 3D-shaped lunate bed forms have been analysed using a general 3-dimensional flow solver (OpenFoam®). This model solves the full 3-dimensional flow field and is based on the same general flow equations. Similar boundary conditions as the CFD-model, Dune, used for the 2D-case were applied. This flow model was set up for one representative lunate bed form only. The model was set up for a flow direction of 138 degr. N for which angle, the current is approximately perpendicular to the steepest angle of the bed form and the pressure drag therefore at a maximum.

Task 2 and 3: Parameterization of the flow resistance from the sand waves
In MIKE3 the flow resistance from the sea bed is included by the means of a roughness height assuming a logarithmic velocity profile near the sea bed. This means that the total sea bed resistance (skin friction + form drag) is included as skin friction/bottom shear stress in the model.

The influence of the sand waves is included by increasing the roughness height locally in the areas where the sand waves have been identified:

$$k_{a,tot} = k_{a,g} + \Delta k_a$$

The increase in the roughness height, Δk_a, is calculated such that it corresponds to the extra flow resistance from the form drag as evaluated in the detailed calculations of the flow resistance, see above. In other words the form drag from the sand waves is added to the global skin friction in the identified areas with sand waves.

The increase in the bed roughness in the MIKE3 is dependent on:

- the individual areas of the sand waves (geometrical properties of sand waves)
- the angle between the flow direction and the orientation of the dune field, α-α_d
- the skin friction (in Dune: $k_{a,Dune}$)

The simulations are made with a global roughness of $k_{a,g}$=0.05 mm and $k_{a,g}$=0.025 m, respectively. The form drag contributions evaluated for a bed roughness related to skin friction of $k_{a,Dune}$=0.005 m in Dune (see above) have been applied in the MIKE3 model setup with the smaller global roughness of $k_{a,g}$=0.05 mm, while the form drag contributions evaluated for a bed roughness of $k_{a,Dune}$ =0.025 m in Dune have been applied in the MIKE3 model setup with a global roughness of $k_{a,g}$=0.025 m. See Table 3.5 for an overview of the model simulations. Theoretically, the global roughness in the MIKE3 Sigma-Model and in the Dune-model should be the same (as in the latter case with a bed roughness of 0.025 m). However, a better calibration of the Sigma-Model was obtained with a smaller roughness, $k_{a,g}$, than expected from a theoretical point of view. Dune applies different boundary conditions at the sea bed than the Sigma-Model and hence the theoretical value of the bed roughness, $k_{a,Dune}$, is kept for this model.

The simulations are carried out for the time period 1/7-1/11 2009. The applied flow model is the same as described in Section 3.1.2, except for the applied roughness map.

Table 3.5 Overview of model simulations in relation to flow resistance from sand waves

MIKE3 model runs without influence of sand waves (reference)	**MIKE3 model runs with influence of sand waves**
Global bed roughness: $k_{a,tot}=k_{a,g}=0.05$ mm	Outside sand wave areas: $k_{a,tot}=k_{a,g}=0.05$ mm Within sand wave areas: $k_{a,tot}=k_{a,g}+\Delta k_a(A,\alpha-\alpha_d,k_{a,Dune})$ ($k_{a,Dune}=0.5$mm)
Global bed roughness: $k_{a,tot}=k_{a,g}=0.025$m	Outside sand wave areas: $k_{a,tot}=k_{a,g}=0.025$ Within sand wave areas: $k_{a,tot}=k_{a,g}+\Delta k_a(A,\alpha-\alpha_d,k_{a,Dune})$ ($k_{a,Dune}=0.025$m)

Task 4: Analysis of the interaction between the bed forms for the flow
The influence on the current field in the Fehmarnbelt due to the sand waves is analysed by comparison of the flow simulations with and without the effects of the bed forms included.

Two levels of influence from the bed forms to the flow are evaluated:

- Regional influence: influence to the discharge through the Fehmarnbelt and the Øresund
- Local influence: redistribution of the discharge and vertical flow profile within the Fehmarnbelt

4 THE INVESTIGATION AREA

4.1 Bathymetry of the Fehmarnbelt

The present day bathymetry of the Fehmarnbelt is shown in Figure 4.1. Since the final retreat of glaciers from the South-Western Baltic area, the Fehmarnbelt has been characterised by highly variable sedimentary processes and environments, (Novak and Björck 2002).

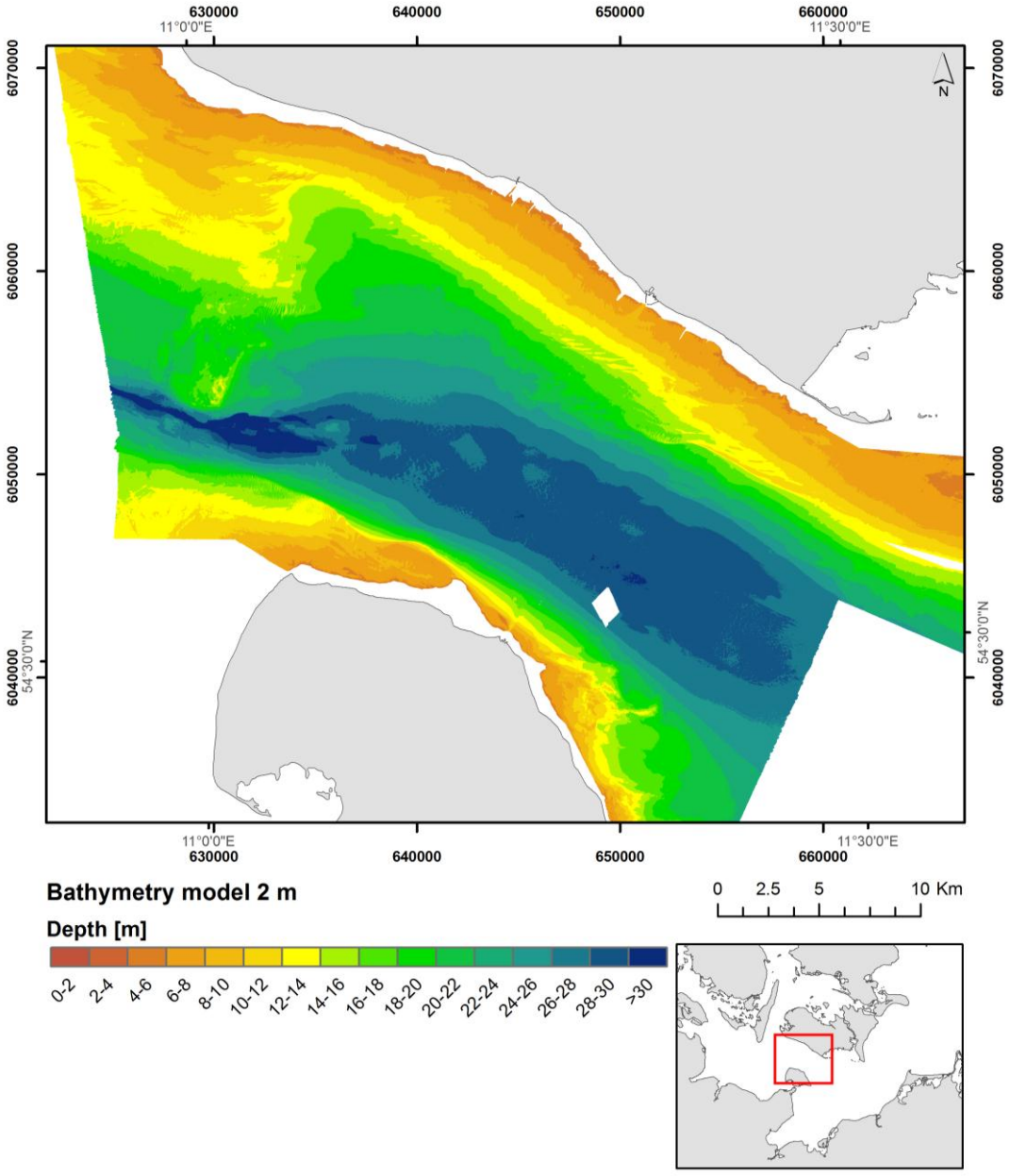

Figure 4.1 Bathymetry of the Fehmarnbelt using multibeam echo sounder, 2009

Isostatic rebound dominated after the ice recession and lakes were formed, kept in place by uplifted threshold areas. Overflow from the lakes to Kattegat through the Great Belt and the Øresund changed position several times over 4000 years causing the Fehmarnbelt to have a highly dynamic history. Among other things the hypothesis of the "Dana River" by (Von Post 1929) can be mentioned, which proposes the drainage of the Ancylus Lake (after Yoldia) through a river in the Great Belt.

Reminiscences of the ancient fluvial system, Figure 4.2, in the Fehmarnbelt due to these occurrences are reported in several reports; for a review see (Novak and Björck 2002). This fluvial system contains features like "oxbow morphology" or "pool like morphology", both originating from a meandering river during the drainage of the Ancylus Lake.

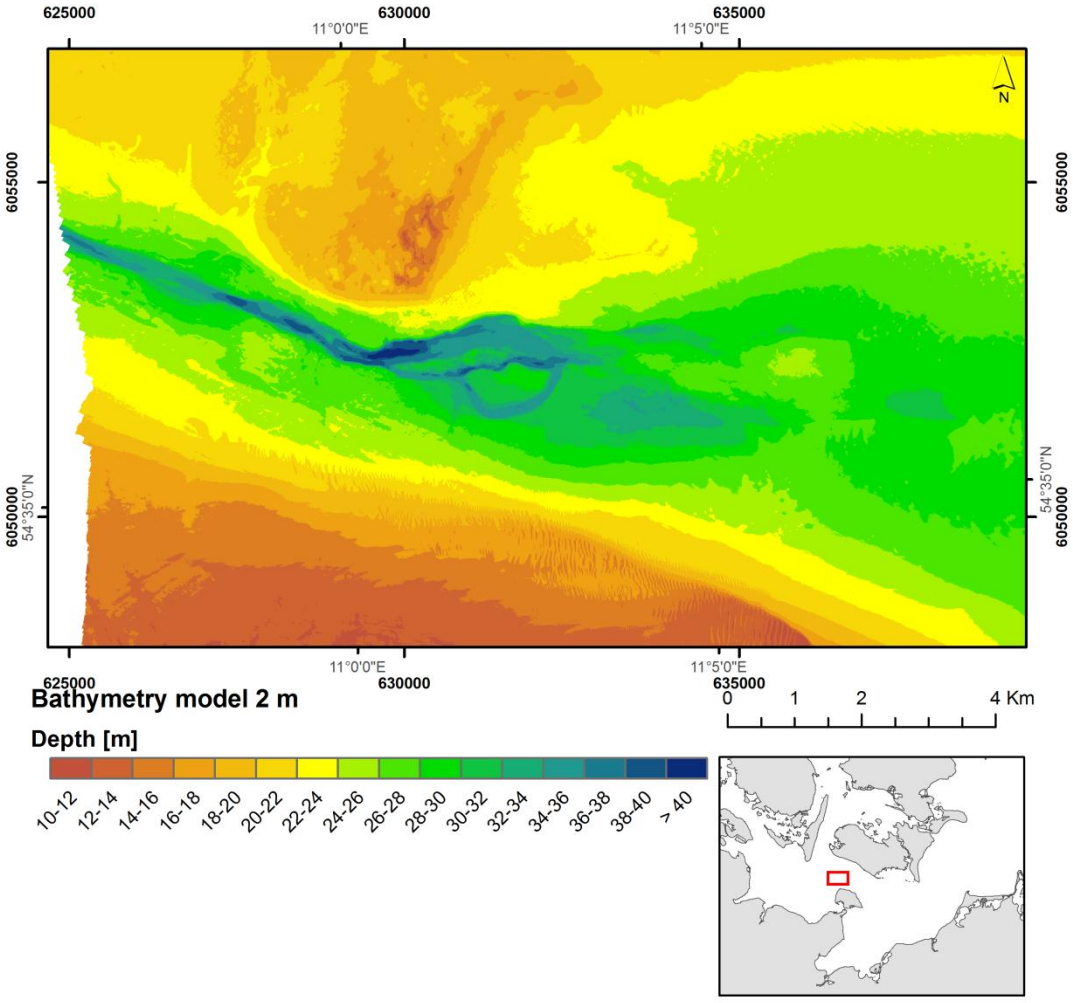

Figure 4.2 Reminiscences of the ancient fluvial system in the Fehmarnbelt. North-West of Fehmarn. Bathymetri measured by multibeam echo sounder, 2009

How dynamic the seabed morphology is today is a bit open and a number of consecutive detailed bathymetry surveys are necessary to identify the dynamic behaviour. The main part of the old fluvial system is located in the deepest part of the belt, and nearly no movement in the bed is expected here.

A much more striking feature which can be observed in the bed is large areas covered by bed forms. They mainly occur as larger undulations of the seabed on the slopes of the bottom, where the water depth typical is in the range 10-20 m, and as smaller undulations in the deeper areas. These are described further in Chapter 6.

4.2 Hydrographic Conditions

Currents

The Fehmarnbelt is part of a shallow transition area between the North Sea and the Baltic Sea, connecting the southern part of the Great Belt and the Kiel Bight with the Mecklenburg Bight.

The general intuitive picture that the currents flowing through the Fehmarnbelt correspond to an estuarine circulation, with out-flowing fresh surface water and inflowing saline water below, applies only for long term averages.

Irregular weather patterns and storms with time scales of a few days are typical for the area and generate in the Baltic Sea a variety of mesoscale currents, such as eddies, coastal jets and associated up- and downwelling patterns with time scales of a few days to weeks. As a small connecting strait between Kattegat and the Baltic Proper, the Fehmarnbelt is affected by local and remote forcing. The local forcing is represented by winds which mix the surface water and drive Ekman transport in the upper layer and opposite Ekman recirculation below the upper layer. The remote forcing is due to the large scale pressure gradients, which are built up by winds forming different wind set-up of the sea levels in the Kattegat and in the Arkona Sea. When the wind changes, the barotropic pressure gradient manifested by a large scale sea level slope, is not balanced and forces strong currents through the narrow straits in the transition zone, and in particular through the Fehmarnbelt. The strongest locally generated flows are the alongshore wind driven currents. Moreover, the currents are forced by water bodies with different salinities at the western and eastern end of the Fehmarnbelt. Furthermore, wave breaking along the coastlines forces longshore currents. However, total fluxes of wave driven currents are insignificant compared to the large scale flow in the Fehmarnbelt.

The flow in the Fehmarnbelt has been modelled in great detail, see 3.1.2 for a description of the model and its calibration. The year 2005 has been identified to be representative for the hydrographic conditions, see (FEHY 2013b).

The current is the dominant mechanism in transporting material along the sea bed in the deeper part of Fehmarnbelt. Waves act to increase the mobility of sediment in shallower areas and very near the coast also to drive a coastal current.

Current roses for currents 2 m above the sea bed at seven locations across the Fehmarnbelt in the alignment area are shown in Figure 4.3 for the entire year of 2005. The seven locations are shown in Figure 4.4.

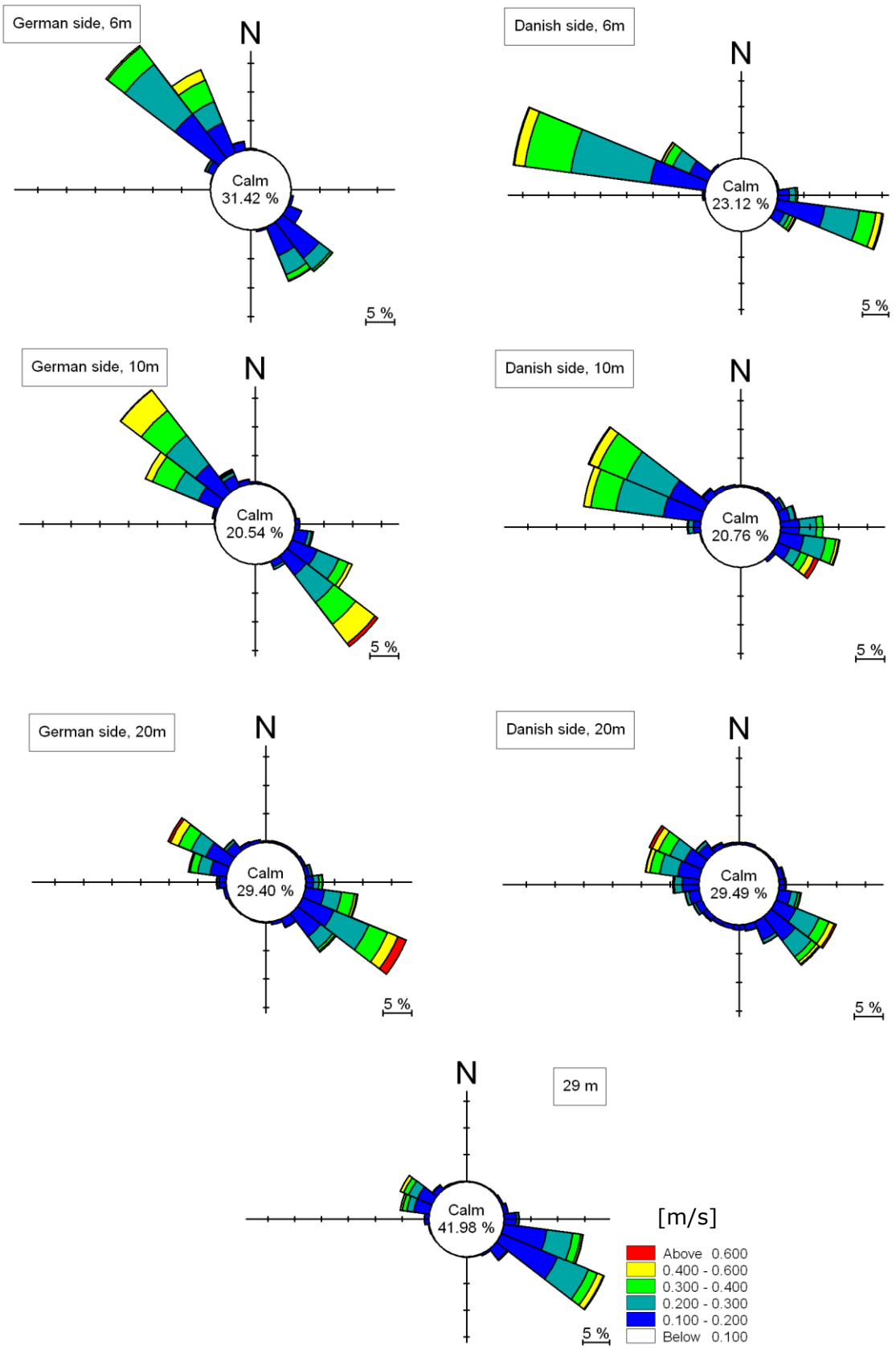

Figure 4.3 Current roses for currents 2 m above the sea bed in the locations shown in Figure 4.4. Results from Sigma-Model for the entire year of 2005

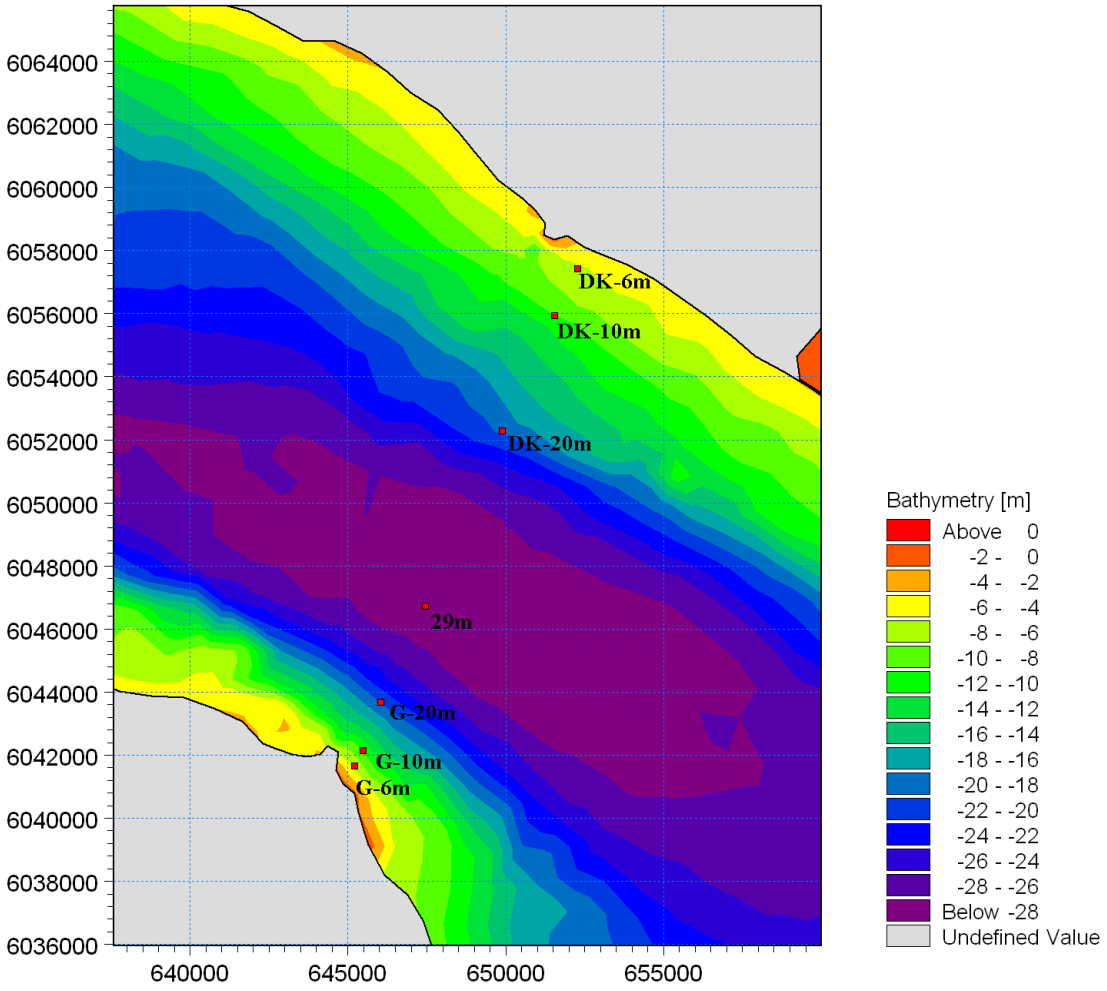

Figure 4.4 Locations where data are extracted for current roses and wave roses

Waves

Waves in the Fehmarnbelt are primarily wind generated and strong correlations were found between wind speed and wave height and between wave period and wave height. The land areas on both sides of the Fehmarnbelt, however, restrict the fetch available for the waves to grow and limit the wave heights for waves from some directional sections depending on the geographical position in the Belt.

Wave roses for seven locations across the Fehmarnbelt in the alignment area are shown in Figure 4.5. The seven locations are shown in Figure 4.4. The waves are in general relatively small with significant wave heights rarely exceeding 1.5 m. The significant wave height is a measure for the average wave height for the highest one third of the waves in an irregular wave field.

The wave heights are seen to be larger near the Danish coast than near the German coast. The dominant wave direction near the Danish coast is from WSW-WNW with a significant fraction of waves occurring also from directions E-SE. Towards the German side, the directions shift to NNW and E, respectively.

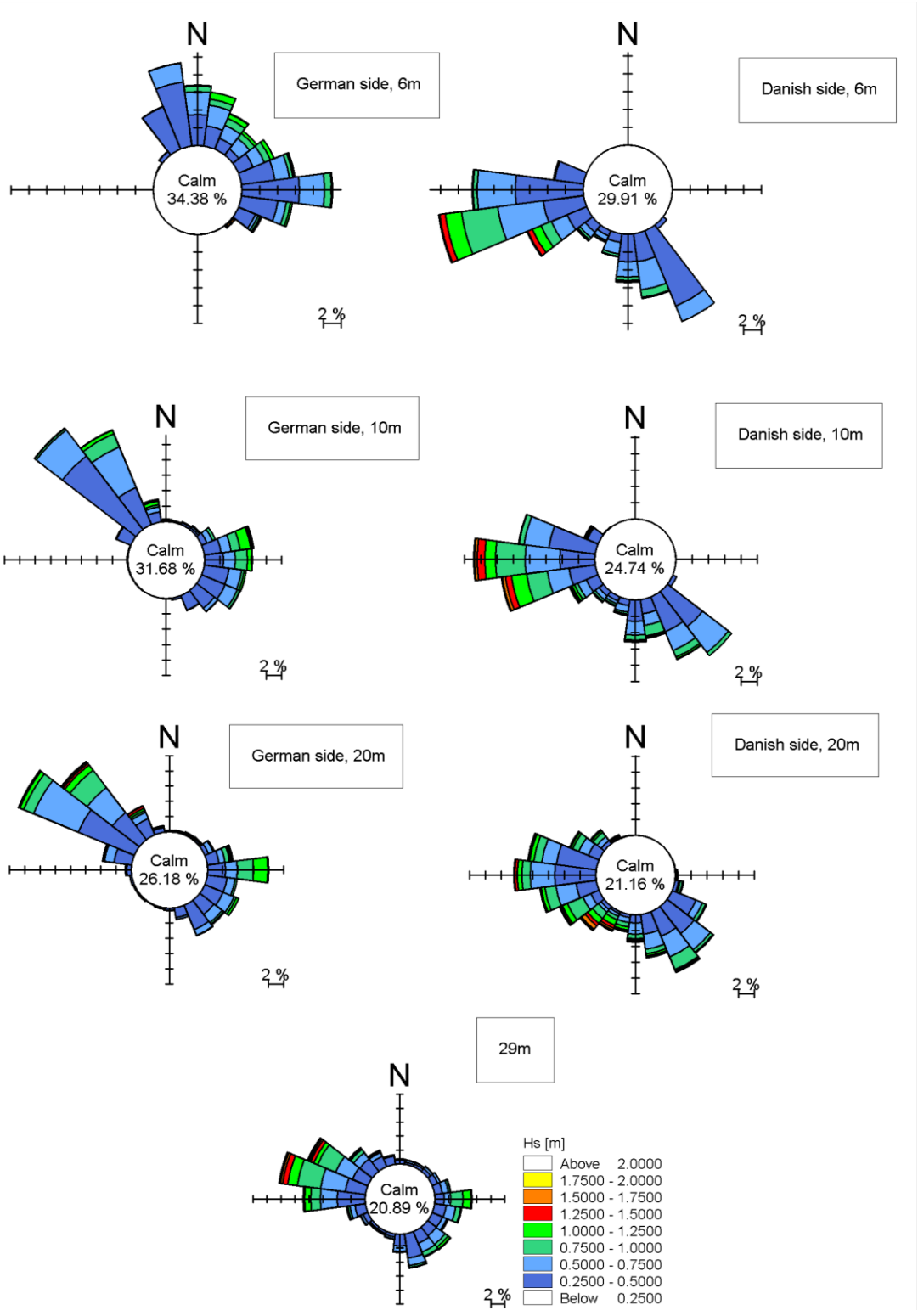

Figure 4.5 Wave roses for seven locations across the Fehmarnbelt. The locations are shown in Figure 4.4

5 SEDIMENT MOBILITY

The current- and wave action mobilise the surface sea bed material. The sediment is transported as bed load, i.e. as grains rolling and jumping very close to the bed, and may during periods with higher current speeds or under the influence of waves be lifted into the water phase and transported as suspended sediments.

The annual sediment transport rates are evaluated with the purpose of supplying information regarding the dynamics of the bed forms. The focus of the sediment transport is restricted to the alignment area.

The content of fine cohesive sediments in the water column is documented in (FEHY 2013c). The natural amounts of fine suspended sediment (wash load) are too small to influence the sea bed morphology in the Fehmarnbelt.

5.1 Sediment Mobility at Water Depths Greater than 4 m

Sediment transport at water depths outside the littoral drift zone is mainly transported by the near-bed currents. The waves act to help mobilise the sediments at water depths, where the wave action is strong enough at the sea bed.

In general, the sediment transport pattern in the Fehmarnbelt follows the pattern of the currents. During large parts of the time, the current speeds in the deeper parts of the Belt, however, are too low to initiate transport. In these areas transport will only occur during peak current speeds. In the areas where waves have an influence in mobilising the bed material, sediment transport will occur also during periods of time with lower current speeds.

Figure 5.1 illustrates an example of a simulated sediment transport field during a strong inflow situation through the Fehmarnbelt. The median grain size is assumed to be 0.3 mm in this simulation and the geometric standard deviation is 1.5. Current speeds 3 m above the sea bed are 0.35-0.4 m/s in the deeper areas and 0.5-0.6 nearer the coasts. Wave heights reach 0.6-1.2 m with the largest waves in the Danish part of the Belt. Transport rates are found to be highest near the German coast at this point in time and reach about 0.00002 m^3/m/s of solid volume which corresponds to nearly 1.5 m^3/m in 12 hours.

A simulated sediment transport field during an outflow situation is shown in Figure 5.2. In this situation current speeds are lower (about 0.20-0.3 m/s in the deeper parts and 0.5 m/s near the coasts), but the waves are higher. The wave heights are 1-1.4 m and highest on the Danish part of the Belt. The sediment transport mainly occurs where the waves have an impact.

Annual transport rates for 2005 are calculated for a cross section in the alignment area. Transport rates are evaluated for a range of the median sediment grain size. The limits for the grain sizes in the simulations vary across the belt as shown in Figure 3.17.

Annual transport rates perpendicular to the cross section shown in Figure 5.1 are given in Figure 5.3. The annual rates are calculated for the eastwards and westwards directions, respectively. Estimated annual sediment transport rates towards the east in the deeper parts of the belt (water depth >12-15 m) are in the range of 5-25 m^3/m/year, while nearer the shorelines, where waves have an impact, transport rates reach up to 35 m^3/m/year on the Danish side and up to 85 m^3/m/year on the German side.

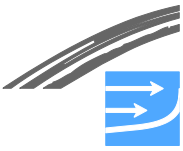

In general, the annual eastward sediment transport rates are larger than the westwards transport rates for this cross section. The calculated westwards transport rates are about half of the eastwards transport rates in the deeper areas and even less near the coast. It may be noted that the east going transport component in the near-shore zone especially on the Danish side is almost identical for the two grain sizes whereas the west going transport is higher for the smaller grain size in this zone. This is due to the complex interaction between waves, currents and skin friction. For larger grain sizes the roughness and bed shear stress are higher than for fine grains and therefore the sediment transport capacity increases with increasing grain size for certain combinations of waves and currents.

This agrees well with the general understanding of the near-bed current direction being primarily directed towards the east. It is in line with the findings in Section 4.2 that the main current direction near the bed is directed towards the east in 2005. The annual net sediment transport rates shown in Figure 5.4 give a net transport directed towards the east across the entire section.

Comparison of near-bed currents modelled for the period April-November for 2005 and 2009, however, showed that the eastwards current speeds were less dominating in 2009. 2009 showed a more even distribution between the main current directions, also during periods with higher current speeds. This indicates that in some years the westward transport rates may be larger than estimated for 2005 and net sediment transport rates may be smaller for these years.

It is noted that the calculated transport rates correspond to the transport capacity for the situation of 100% coverage of the sea bed with loose sediments. This is not the case in all areas and the full transport capacity will not be effectuated.

The validation and analysis of the flow model applied to calculate the sediment transport rates were discussed in Section 3.1. It was found that the model would cause an over-prediction of the transport rates with a factor of about 1.5-3 in the validation period. The validation period was, however, not sufficiently long to make any firm conclusions on the general uncertainty on the sediment transport rates and the estimations in Figure 5.3 and Figure 5.4 are therefore the best possible estimates. A summary of transport rates (net, gross, eastwards and westwards) are provided in Table 5.1.

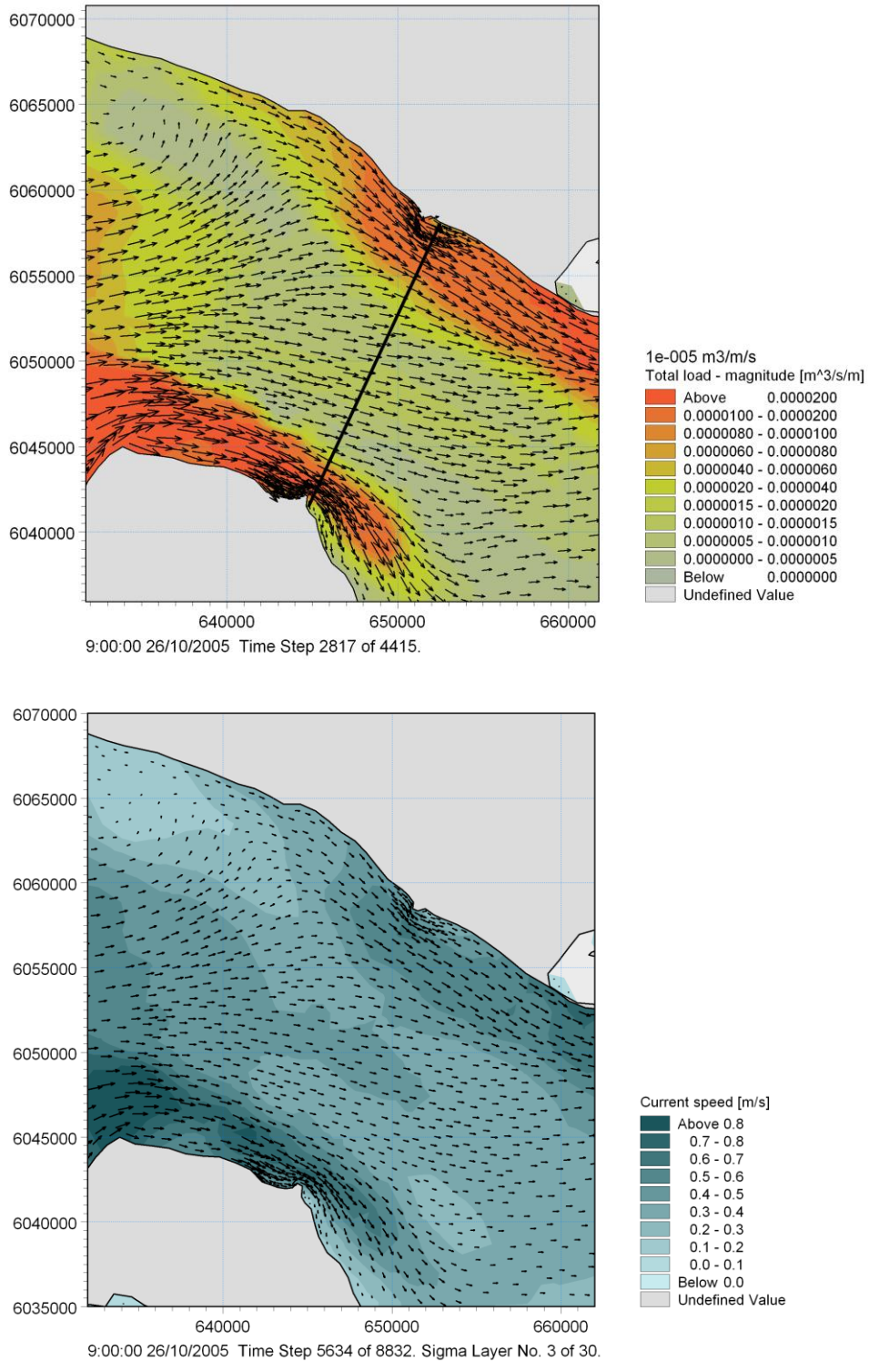

Figure 5.1 Example of modelled 2D sediment transport field (upper figure) during a situation with strong inflow through the Fehmarnbelt and relatively high waves. 26/10-2005 9AM. d50=0.3mm. Solid volumes. Cross section indicates where annual transport rates are evaluated. Modelled current field approximately 3 m above sea bed (lower figure)

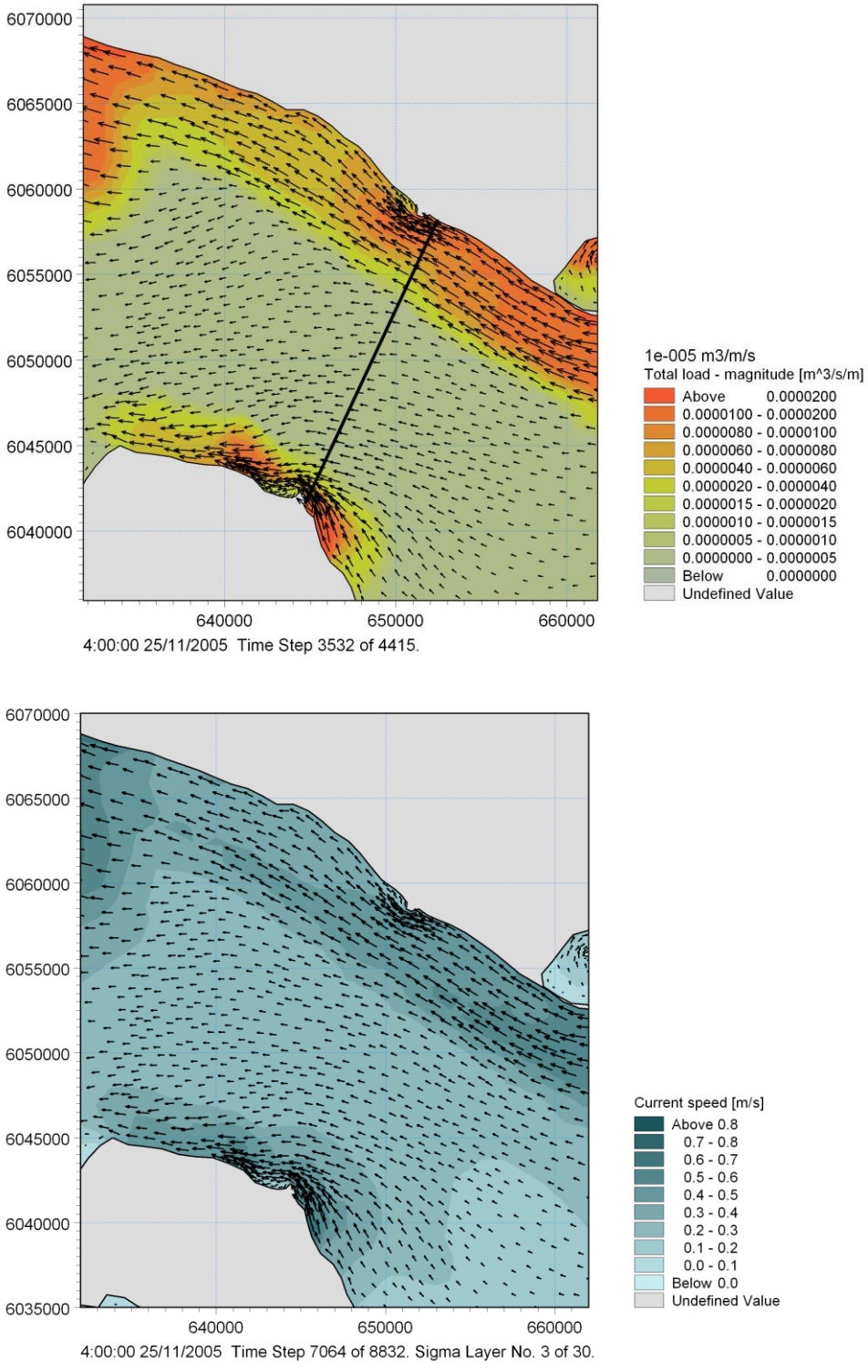

Figure 5.2 *2D field of modelled sediment transport (upper figure) during situation with medium outflow through the Fehmarnbelt and relatively high waves. 25/11-2005 4AM. d50=0.3mm. Solid volumes. Cross section indicates where annual transport rates are evaluated. Modelled current field approximately 3 m above sea bed (lower figure)*

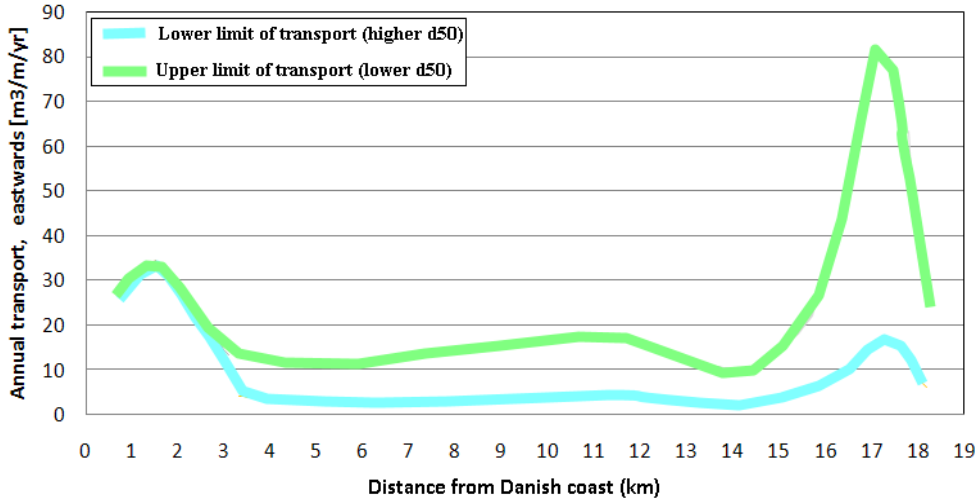

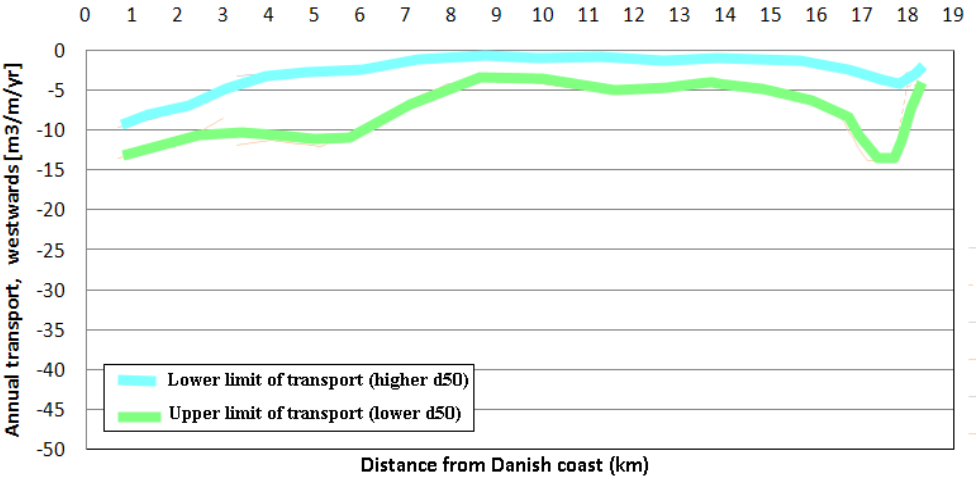

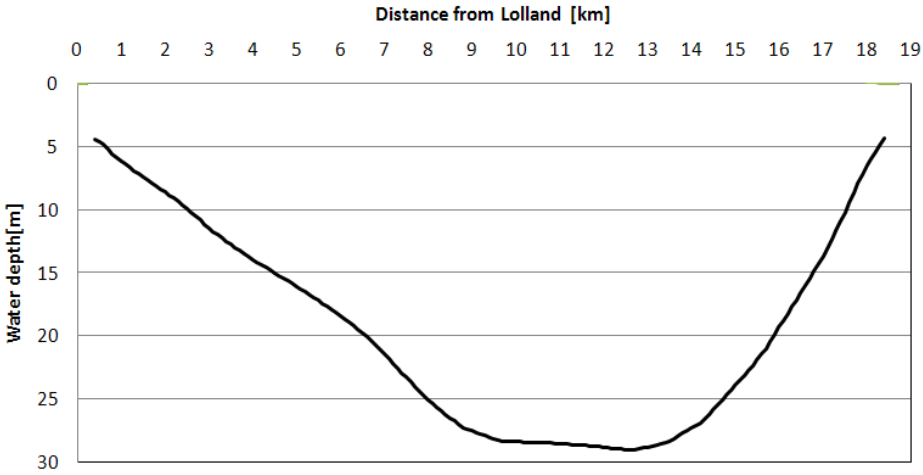

Figure 5.3 *Estimated annual sediment transport rates (2005) across the Fehmarnbelt in the alignment area in the eastward direction towards the Baltic Sea (upper figure) and in the westward direction towards the Great Belt (middle figure). The lower figure shows the water depth across the alignment.The cross section is shown in Figure 5.1*

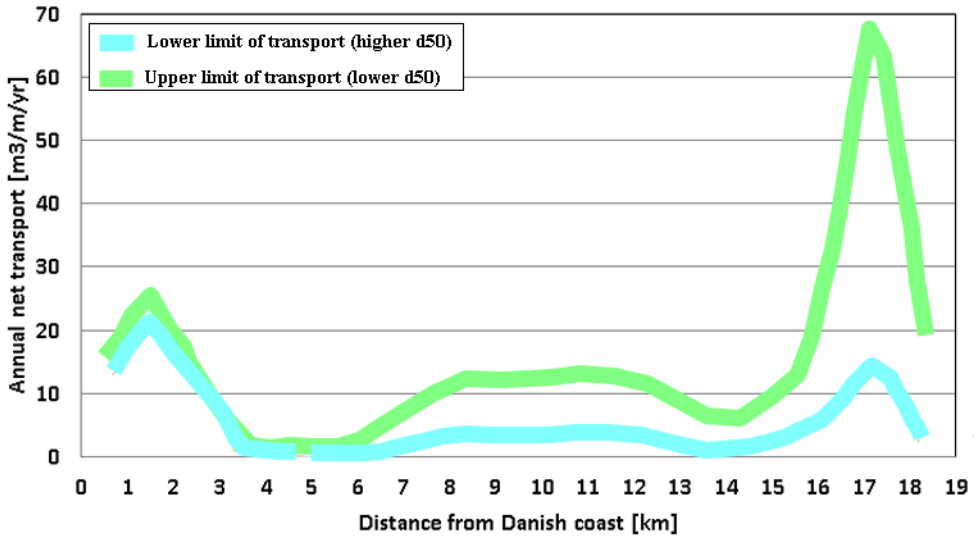

Figure 5.4 *Annual net sediment transport rates (2005) across the Fehmarnbelt in the alignment area. The cross section is shown in Figure 5.1. The net sediment transport is directed towards the Baltic*

Table 5.1 *Estimated annual sediment transport rates across the alignment, water depth > 4m*

	Water depth [mDVR90]	**Length [m]**	**Annual transport of non-cohesive sediment across the alignment [m^3/m/year]**			
Stretch			**Gross**	**Net**	**Eastwards**	**Westwards**
Danish side	4-12	2,500	15-45	10-25	10-35	5-15
Central area	>12 (DK) >20 (G)	12,500	5-25	1-15	3-20	2-12
German side	4-20	2,500	7-95	3-70	5-85	2-15

5.2 Sediment Mobility at Water Depths less than approx. 4 m

The littoral drift along the coasts of Lolland and Fehmarn has been analysed and are documented in (FEHY 2013a). Note: the littoral drift or sediment transport within the surf zone does not interact with the bed forms which exist outside of the surf zone. The littoral drift is however an important contribution to the overall sediment transport in Fehmarnbelt. The results regarding littoral drift are therefore briefly summarised in the following. The littoral drift calculations are based on wave statistics for the period 1989-2010.

Around Rødbyhavn

The shoreline east of Rødbyhavn is influenced by the harbour, which has blocked the east-going transport and thereby caused erosion of the coastal profile east of Rødbyhavn. The lack of by-pass around the harbour has also caused a situation, where the finer sediments have gradually been removed from the nearshore zone east of the harbour such that the sea bed material is coarser here than west of the harbour.

The littoral drift budget shows that the net sediment transport is eastwards in the range 10,000-20,000 m^3/year. The gross transport is in the order 15,000-25,000 m^3/year.

Figure 5.5 shows the distribution of the sediment transport in a profile east of Rødby. It is seen that the major part of the sediment transport takes place within 20 m of the shoreline.

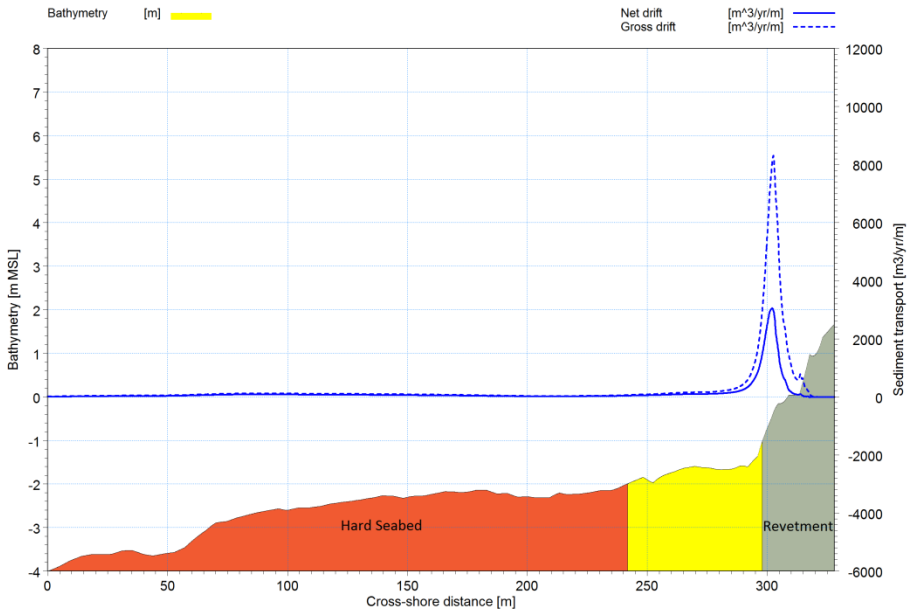

Figure 5.5 Distribution of near-shore net and gross sediment transport for a typical profile east of Rødby (Danish side)

East of Puttgarden Harbour

East of Puttgarden Harbour in the area of the planned landfall, the littoral drift calculations show that the net sediment transport is in the north-western direction, but small. The gross transport is calculated to be approx. 25,000 m^3/year whereas the net transport is in the range 0-2000 m^3/year towards the north-northwest.

Figure 5.6 shows the distribution of the transport along the profile on the German side. As for the Danish side there is no or little sediment transport for depths less than 2.5 m. As a major part of the transport is in the north-north-westerly direction towards the harbour, the effect of the harbour on the sediment transport will be insignificant.

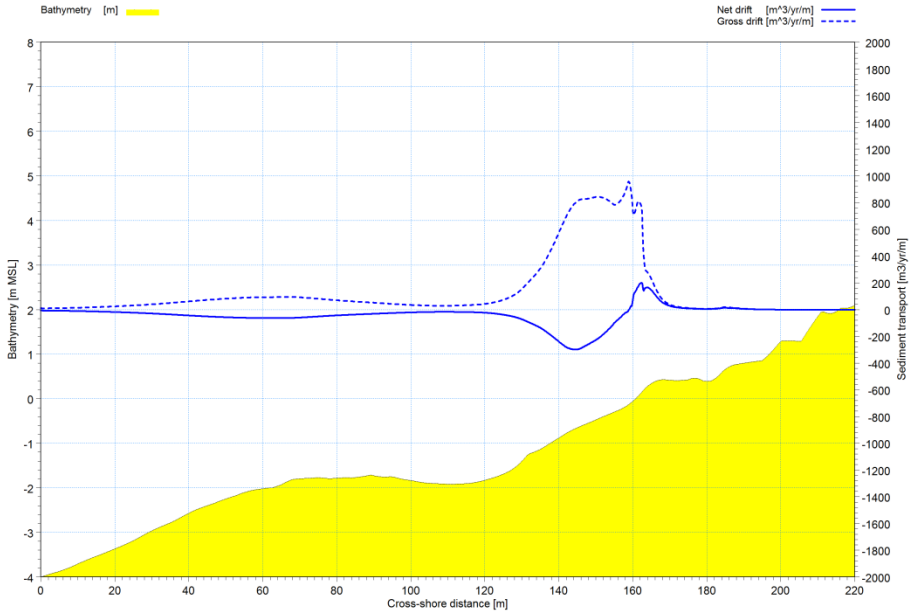

Figure 5.6 Distribution of near-shore net and gross sediment transport east of Puttgarden (German side)

The estimated longshore transport rates east of Rødby and Puttgarden are summarised in Table 5.2 and Table 5.3.

Table 5.2 Summary of estimated longshore sediment transport rates east of Rødbyhavn

	Gross transport [m^3/year]	**Net transport [m^3/year]**	**Eastwards transport [m^3/year]**	**Westwards transport [m^3/year]**
East of Rødbyhavn	15,000-25,000	10,000-20,000	12,000-22,000	2,000

Table 5.3 Summary of estimated longshore sediment transport rates southeast of Puttgarden Harbour

	Gross transport [m^3/year]	Net transport [m^3/year]	Eastwards transport [m^3/year]	Westwards transport [m^3/year]
East of Puttgarden Harbour	27,000	0-2,000	14,000	14,000-16,000

6 DESCRIPTION AND CLASSIFICATION OF BED FORMS

The bed forms on the sea bed of the Fehmarnbelt have been studied extensively. Parts of the bed forms are within Natura 2000 areas and are as such classified as protected morphological features.

Bed forms exist due to present or historical interactions between loose bed sediments and the flow. This interaction is analysed in Chapter 7. In the present section the bed forms are described and classified.

6.1 Classification of Bed Forms occurring in the Fehmarnbelt

Undulations of different types are found at a number of locations spread over the whole Fehmarnbelt. These undulations vary from isolated features in the central part of the Belt to more regular bed forms on the shoulders of the Belt.

Classification of bed forms is not international standard as such, and the description differs from geologists to engineers. Classification papers like that by (Dyer and Huntley 1999) and (Ashley 1990) provide some suggestions. The present description of the various bed form types found in the Fehmarnbelt follows the classification in the (Oxford Dictionary of Earth Sciences 2008).

I. Current ripples:

Ripples are small-scale ridges of sand produced by flowing water. The wave length or spacing of ripple crests is usually less than 50 cm and the heights are in a current dominated environment less than 5-8 cm.

Comments: Ripples cannot be seen on the multibeam measurements because of their small size, but can visually be observed from video recordings up to a water depth of at least 16-18 m.

II. Dune bed forms (mega ripples):

Mounds or ridges of sand which are asymmetrical, and are produced sub-aqueously by flowing water. The external geometry is similar to the above-mentioned ripples and the larger "sand waves" with a gently sloping upstream side (stoss) and a steeper downstream side (lee). The crest line elongation extends transverse to the flow direction and is sinuous or lunate in plan. The height varies between 0.1 m and 2 m, while the wave length (spacing) between dunes is 1-10 m. Size and growth are limited by water depth and, in general, dune height is less than one-sixth of the flow depth.

Comments: Transition between mega ripples and sand waves (next) is smooth. However, mega ripples are not identified on the multibeam measurements performed by Rambøll/Marin Mätteknik.

III. Sand wave:

Large-scale, transverse ridge of sand with the same external morphology as mega ripples. The spacing is 30-500 m and the height is 3-15 m.

Comments: Sand waves are the most common type of bed undulations found in the Fehmarnbelt. These sand waves can be divided into subgroups, depending on their orientation:

a) Flow transverse sand waves

Usually sand waves are flow transverse, i.e. the crests of the sand waves are perpendicular to the dominating flow direction. Even though the near-bed flow direction is quite variable, the dominating direction is not far away from the main alignment of the Fehmarnbelt.

b) Oblique sand waves

On the slopes it is observed that the sand waves are inclined at an angle to the main axis of the flow. In a number of locations such *oblique dunes* have been observed. These dunes behave differently from flow transverse dunes with respect to flow resistance, and are therefore categorized in its own group.

In the present case, the oblique dunes are spaced with a distance equal to or smaller than the flow transverse dunes in the bed with less transverse slope, i.e. 4-8 times the water depth. The angle which the dune front forms with the current is usually such that the dunes are inclined so the front at smaller water depth is ahead of the front at greater depths as also observed in the Fehmarnbelt. (Fredsøe 1974) demonstrated that the inclination is due to the transverse slope and the associated transverse gradient in the depth averaged flow velocity.

IV. Ribbons:

Ribbons are defined as "Straight to sinuous, thin bodies of sand, with a narrow width in relation to their length". Sand ribbons develop on sediment-poor shelves, and they are oriented nearly parallel to the flow. Sometimes the term is also used more generally to describe the large-scale geometry of a preserved sand body with a width to length ratio in excess of 1:100, and a thickness to width ratio greater than 1:10.

Comments: The orientation of the ribbons strongly depends on the flow velocity (e.g. Kenyon 1970). (Feldens et al. 2009) identified the ribbons in the Fehmarnbelt as depicted in Figure 6.1 which is based on earlier side-scan sonar data. It is seen that the ribbons form a significant angle with the current direction. (Feldens et al. 2009) suggest the ribbons are conduits for sediment because the sand waves are formed directly in extension of these ribbons. The occurrence of inclined sand waves is well-known from tidal sandbanks at the Dutch and Belgian coast, and is explained by (Huthnance 1982). (Huthnance 1982) predicted the banks to have a spacing of about 250 times the water depth. The spacing in the Fehmarnbelt (Figure 6.1) fits quite well with (Huthnance 1982) prediction.

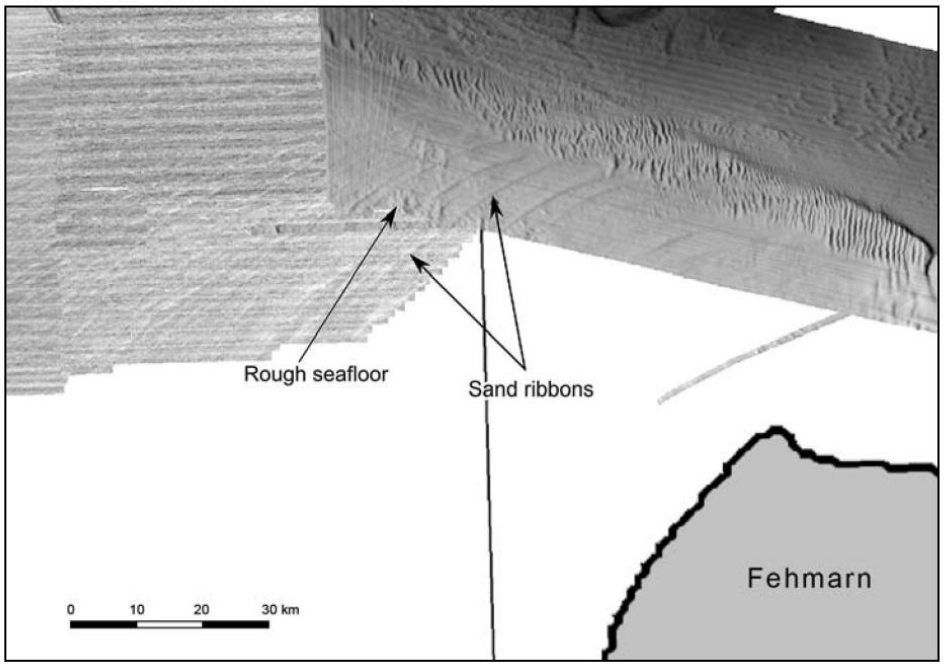

Figure 6.1 Ribbons identified in Feldens et al (2009)

V. Lunate bed forms (Isolated Crescentic bed forms)

In this deepest part of the Fehmarnbelt (water depths greater than 25 m) a large number of 3-dimensional features can be observed. The origin of these features is not obvious. In the North Sea and many other locations similar 3D features can be observed, sometimes with an opposite shape, namely a local deepening in the bed, the so-called Pockmarks, see (Judd and Hovland 2007). These Pockmarks are formed by seepage through the bed due to rising bubbles of mainly methane from below. Pockmarks have been reported in the nearby Eckernförde Bay by (Wever et al. 1975). Another common feature of isolated sand waves is the so-called comet marks, where the two downstream "legs", however, are almost parallel, while in the present case they form a large angle.

Another possibility is that the hills are relict sediment from the ice age, which later has been levelled out by current to form the present lunate shape. Relict sediment is in the Oxford Dictionary of Earth Sciences described by: *sand deposited by processes no longer active in the area where the sediment now occur. Relict sediment is remnants from an earlier environment and is now in disequilibrium. Subaquatic Relict bed form: a bed form that developed under hydraulic conditions very different from those today.* See also (Swift et al. 1971).

The shape indicates that they are modified by current from the western direction, which corresponds to the present conditions, while the current was in the opposite direction during the emptying of the Baltic Sea as described above.

If the sediment is relict it can either be finer or coarser than the surrounding sediment. Most probably these 3D lunate features consist of fine sediment on an otherwise more or less immobile bed. This seems to agree with the observations of the sea bed material in the area, which is described as "thin sandy mud".

This is also suggested by (Feldens et al. 2009) who from their seismic data clearly could observe that the sand waves are separated from the underlying units.

(Kleinhans 1999) demonstrated that graded sediment can form lunate bed forms with fine sediment on the top of sand waves.

It is noted that some of the areas covered with bed forms are protected under Natura 2000. The definitions in this connection and the specific areas are presented in Chapter 9.

6.2 Overview of Areas with Bed Forms in the Fehmarnbelt

Several areas with bed forms were identified in the Fehmarnbelt by extensive analysis of the multibeam bathymetry. The areas with the largest and most widespread bed forms, sand waves and lunate bed forms are mapped in Figure 6.2. The general parameters of the bed forms are stated in Table 6.1. The areas (ha) covered by the bed forms within the investigation area as well as within the so-called local area, which is used in the impact assessment of the Fixed Link projects as a reference area, are provided in the same table. The areas are indicated in Figure 6.2. The areas (ha) of the sea bed covered with large-scale bed forms within Natura 2000, where these are part of the conservation objectives (assigned Natura 2000 Code 1110) are also presented in Table 6.1.

Figure 6.2 and Table 6.1 have a third category of bed forms denoted: "other active bed forms". These are bed forms of significant size which cannot clearly be defined within one of the two main categories. They are most likely bed forms in a sedi-

ment sparser environment than the sand waves. They are located in areas with higher near-bed current speeds than the lunate bed forms, which is probably the reason why they have a different shape, see (Kenyon 1970).

Table 6.1 Bed form parameters and areas

	Water depth [m]	**Height [m]**	**Length [m]**	**Area [ha] within investigation area**	**Area [ha] within local area**	**Area [ha] within Natura 2000[1]**
Sand waves	10-25	0.25-4	25-400	3,160	1,261	1,120
Lunate bed forms	>25	~0.5	100-200	21,700	14,789	(10,800)
Other active bed forms	10-25	0.25-400	5-400	2,582	244	(1,500)

[1] Areas of bed forms within Natura 2000 areas, where sea bed forms are part of the conservation objectives (SCI DE 1631-392 and SCI DE 1332-301). Only the sand waves have been clearly assigned with the Natura conservation code 1110 Sandbanks within these areas, for which reason areas of lunate bed forms as well as other active bed forms within Natura 2000 are given in parenthesis in the above table.

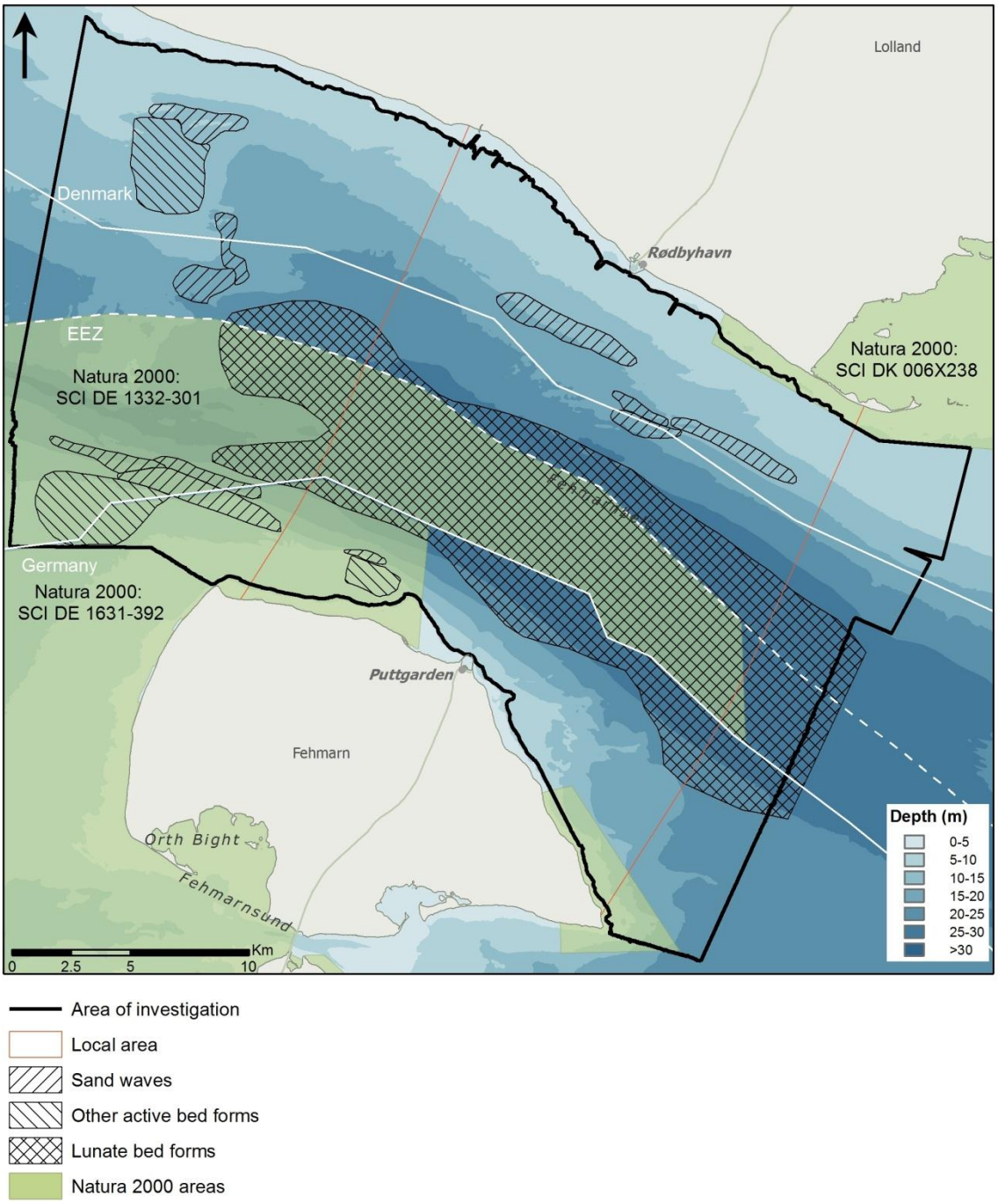

Figure 6.2 Areas of prominent bed forms in the Fehmarnbelt. The marine parts of Natura 2000 areas are shown

Maps of the local sea bed slope and the difference analysis are shown in Figure 6.3 and Figure 6.4, respectively. In these maps the bed forms clearly show the different characteristics they have (regularly varying slope and regular undulations). Large-scale maps of the detailed bathymetry and characteristics of the sea bed in the Fehmarnbelt are provided in Appendix A, Maps I-IX.

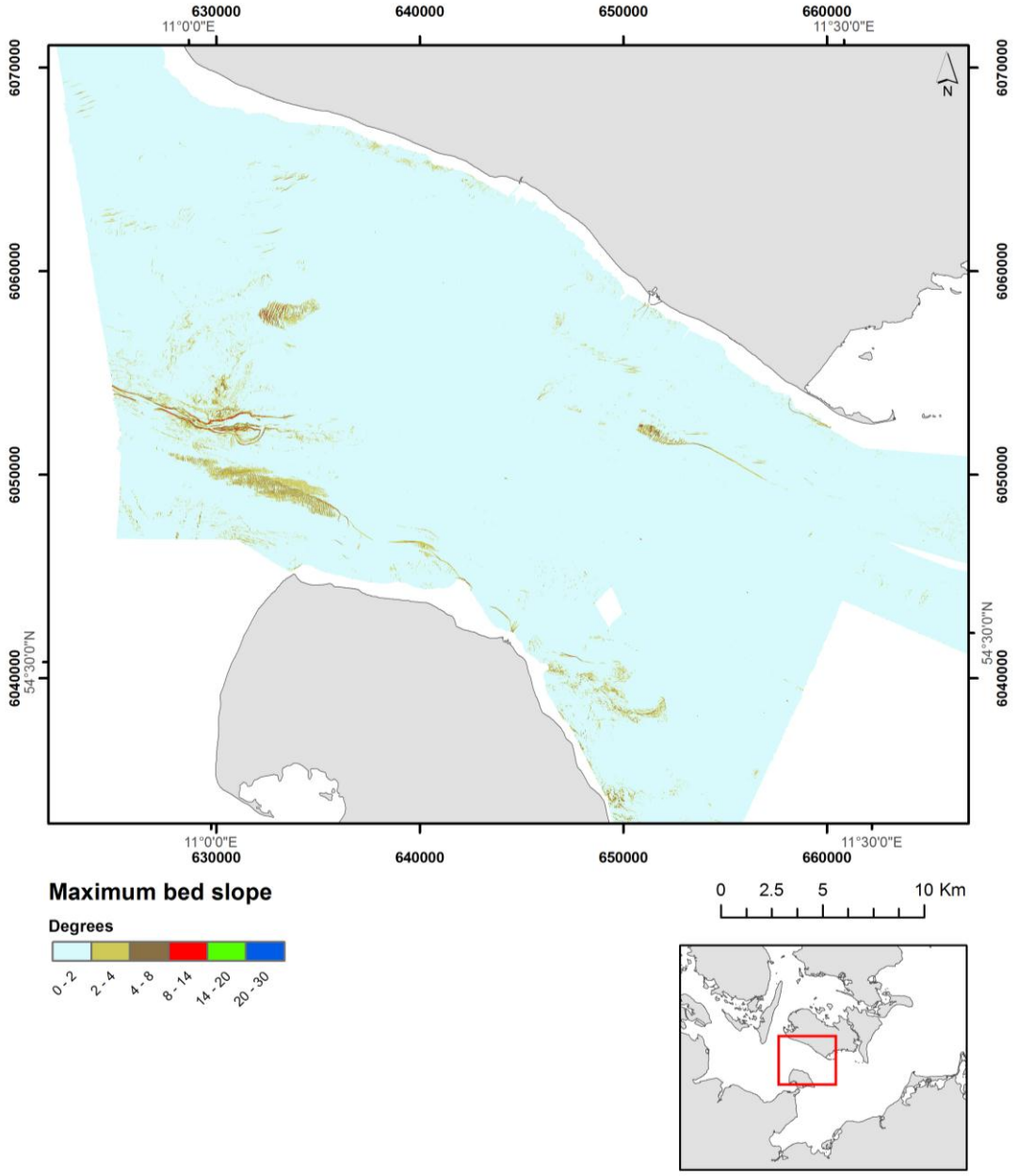

Figure 6.3 Maximum bed slope. Analysis of multibeam echo sounder data (2009)

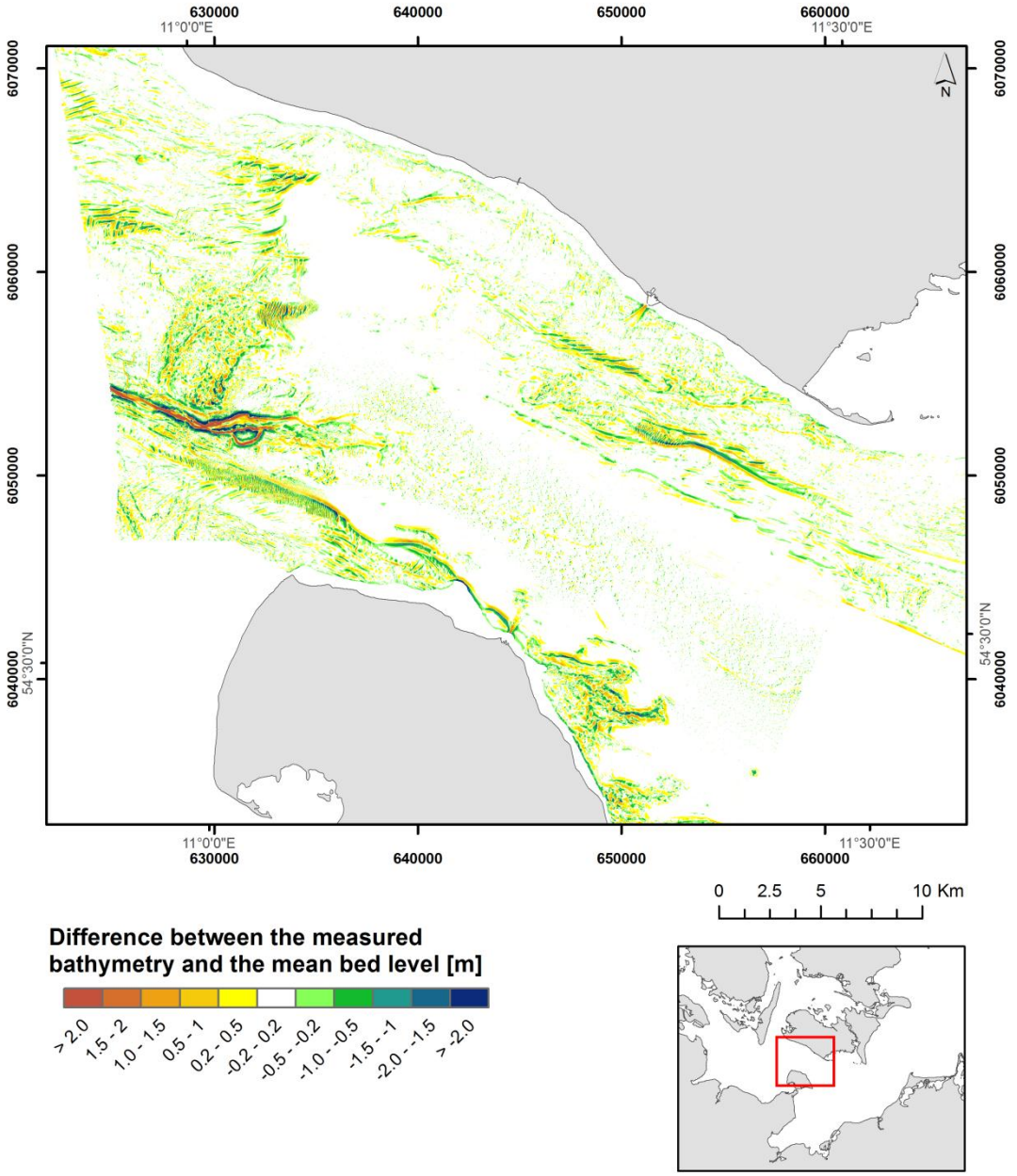

Figure 6.4 *Difference between the measured bathymetry and the mean bed level. The mean bed level is defined as the average bathymetry within a radius of 200 m. Analysis of multibeam echo sounder data (2009)*

Several earlier surveys have investigated the bed forms in the Fehmarnbelt.

Sand waves in the Langeland Belt are already described by (Werner and Newton 1975), where they used side scan sonar to survey the bottom. They repeated their survey after 14 months, and they concluded that no essential change could be observed. However, their survey was not detailed enough to conclude that the sand waves did not change geometry or location at all.

More recently a detailed survey in the Fehmarnbelt by (Fiedler (2000) using Klein side scan sonar is reported. Fiedler concluded that the sand waves are typical up to 3 m in height and have a wave length ranging from 12 to 100 m, and very similar to those found in Langeland Belt. The sand wave field reported above by (Fiedler 2000) is located 4-6 km west of the proposed corridor for the link.

(Feldens et al. 2009) also measured the detailed bathymetry of the Fehmarnbelt and mapped approximately 75 km^2. Figure 6.5 shows a detailed view of a 1.5 km wide and 6 km long area northwest of Fehmarn containing a large number of sand waves. This area is located further west than the area investigated by (Fiedler 2000).

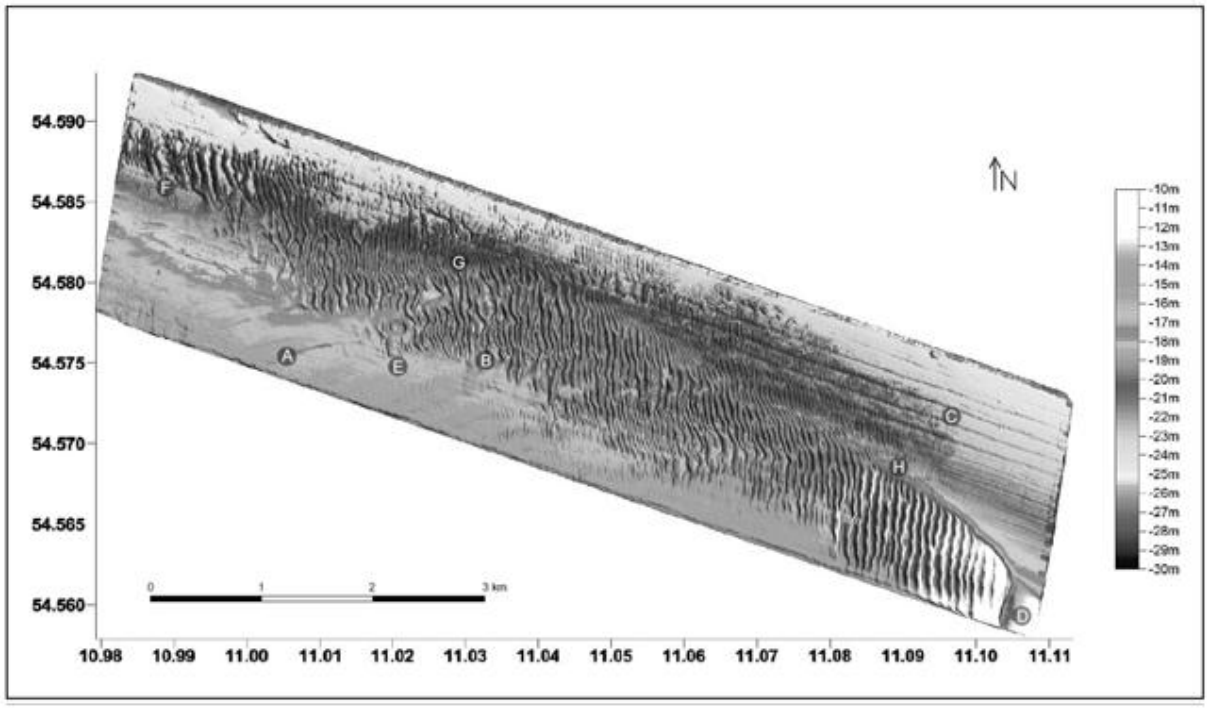

Figure 6.5 Sand wave field measured by (Feldens et al. 2009) using multibeam echo sounder

6.3 Detailed Description of Bed Forms in Different Parts of the Fehmarnbelt

In this section the bed forms of eight different areas will be described. Each area is 6 x 4 kilometres and four are located on the Danish side (named D1-4) and four are located on the German side (named G1-4), see Figure 6.6. Detailed maps with zooms of each of the areas are supplied in Appendix A.

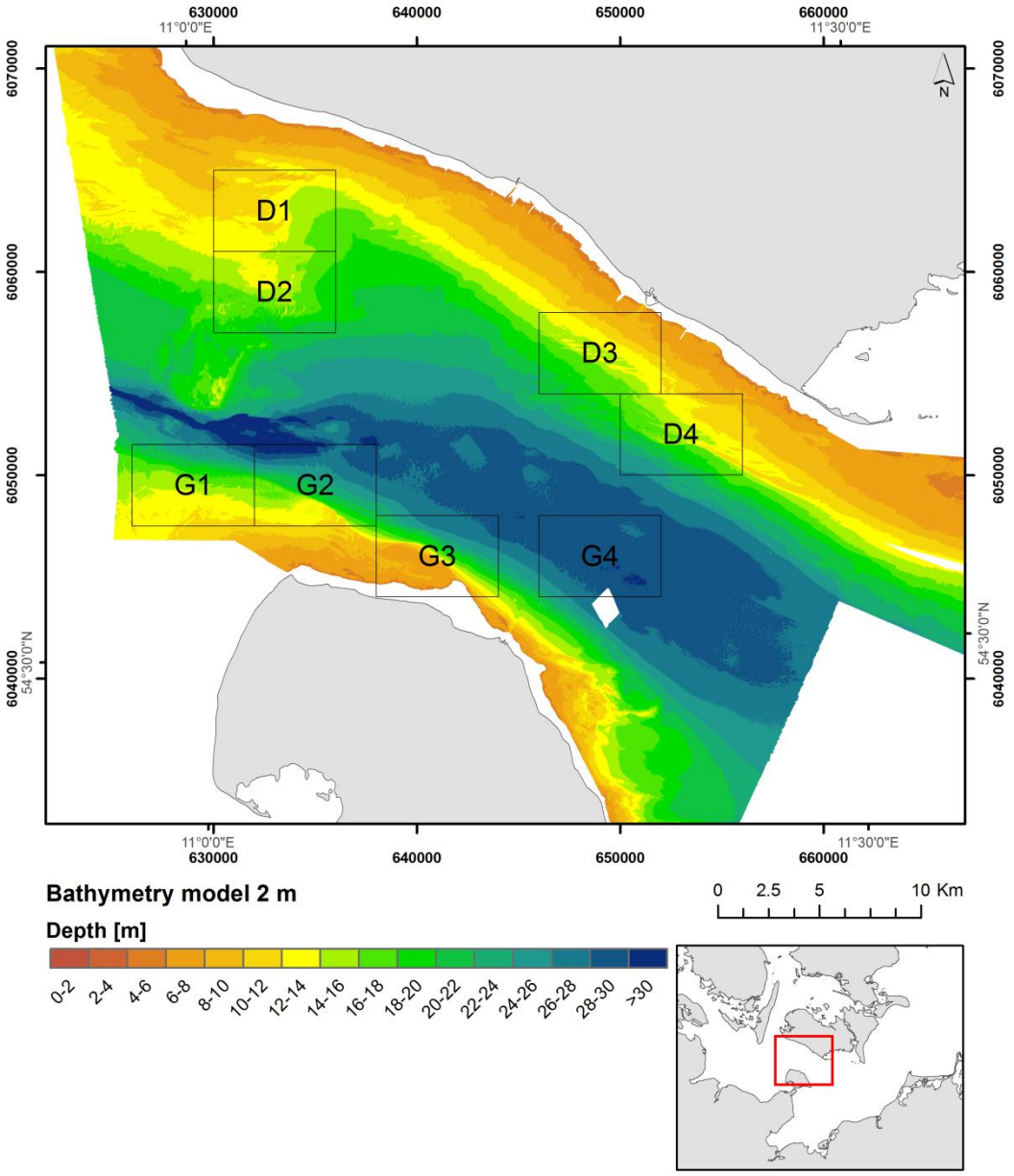

Figure 6.6 Areas containing bed forms which are described in detail

For every area a table with the typical bed form heights, lengths, steepness and orientations is given. The orientation of the sand waves is defined as the direction perpendicular to the crest lines relative to true north, see Figure 3.24. The maximum steepness will be given in two ways:

- The typically maximum steepness; defined as the general maximum steepness for the majority of the sand waves and for a significant length along each sand wave

- The local maximum steepness; defined as the largest steepness located in the sand wave field

Estimated migration rates are provided for sand wave fields near or in the alignment (areas D3, D4 and G4). A summary of bed form types and parameters for the respective sub-areas D1-D4 and G1-G4 are provided in Figure 6.7.

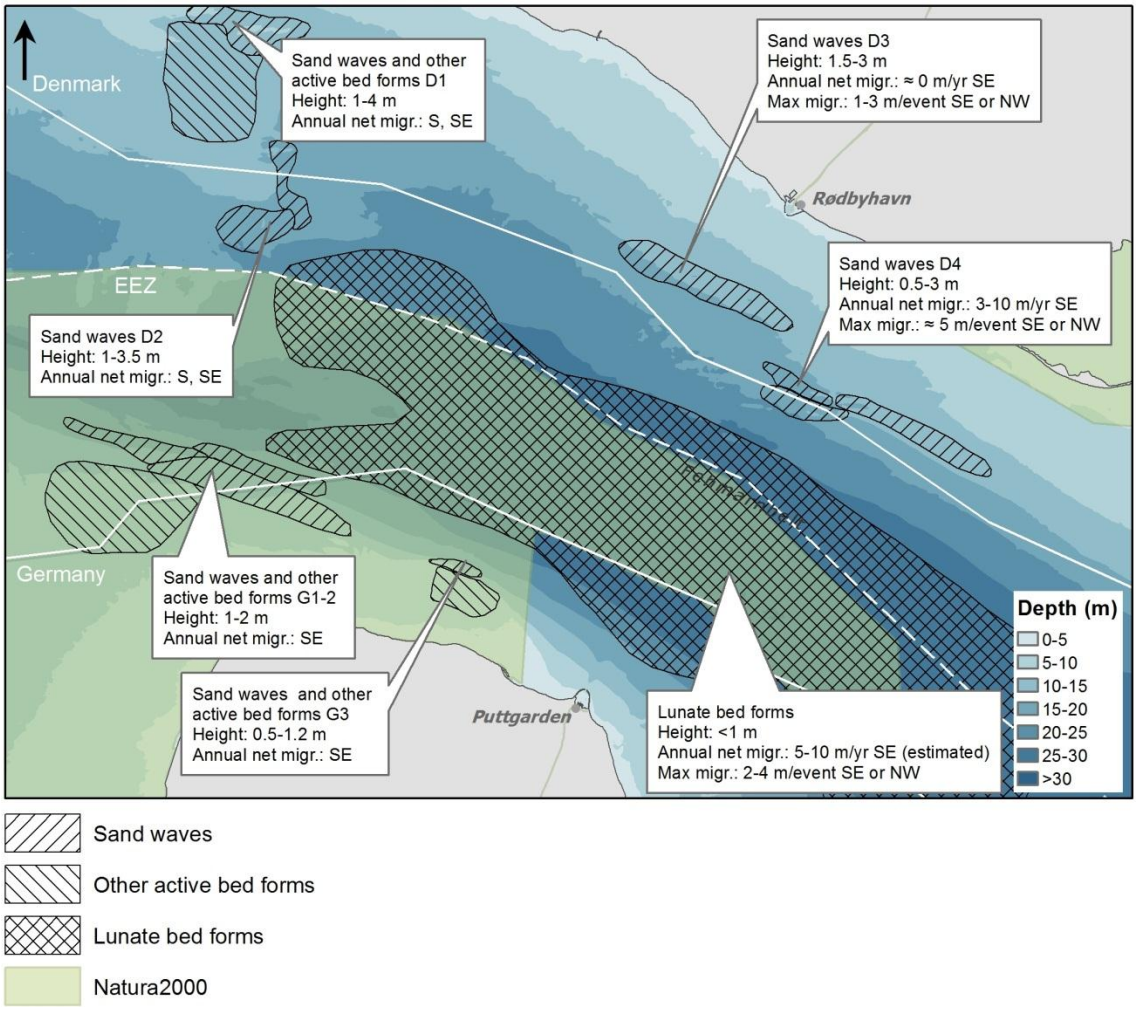

Figure 6.7 Main bed form areas in the Fehmarnbelt and their main characteristics. The maximum migration rates are related to events occurring 2-5 times a year and lasting approximately 2 days. Maps from the sub areas are included in Appendix A)

D1 (Map XI in Appendix A)

The northern and central parts of area D1 are characterised by a few sand waves and some less homogenous bed forms (other active bed forms), which vary a lot in shape and size, see overview in Figure 6.7 and detailed bathymetry in Figure 6.8. All bed forms in area D1 are oriented with their steepest bed slope facing the same direction of about 170 degrees N.

The largest bed forms by height are the sand waves located in the northern part. The heights of the sand waves are up to about 4 m, see vertical profile through one of the sand waves in Figure 6.10. The length is in the order of 300 m. These sand waves have also the steepest bed slope with a local steepness up to around 20 degrees. Figure 6.9 shows a profile from north to south through the sand waves in the north and the 'other active bed forms' in the central and southern part of D1. The profile shows that the wave heights are smaller for these bed forms but the lengths are up to 600 m. The bed slopes of these bed forms in this part of D1 are also significantly lower than the northern sand waves; only up to about 8 degrees.

A sand mining area is present within area D1 and clearly shows up as irregularities in the detailed bathymetry in Figure 6.8. The last large-scale extraction from the area was in 2006 with an extraction of 93,000 m^3. Extraction of the sea bed material is clearly seen in the multibeam survey as irregular patterns in the top of some of the

large sand waves, see Figure 6.8 (and in Figure 8.2 in Chapter 8 below). The multibeam survey was performed in 2009, i.e. three years after the extraction in 2006. The magnitude of the extraction is relatively small compared with the size of the individual bed forms. The sand waves therefore still persist more or less in their natural shape, although deep holes of several metres have been cut into parts of them extending over their full height. The bed forms are expected to regenerate naturally with time. However, this is a slow process due to the relatively low sediment mobility. The sand mining is further discussed in Chapter 8.

Table 6.2 Bed form parameters – D1(Sand waves and other active bed forms)

Height, H [m]	Length, λ [m]	Typical maximum steepness [deg]	Local maximum steepness [deg]	Orientation, α_d [deg. N]	Area [ha]
1-4	100-600	6-12	20.5	170	1,430

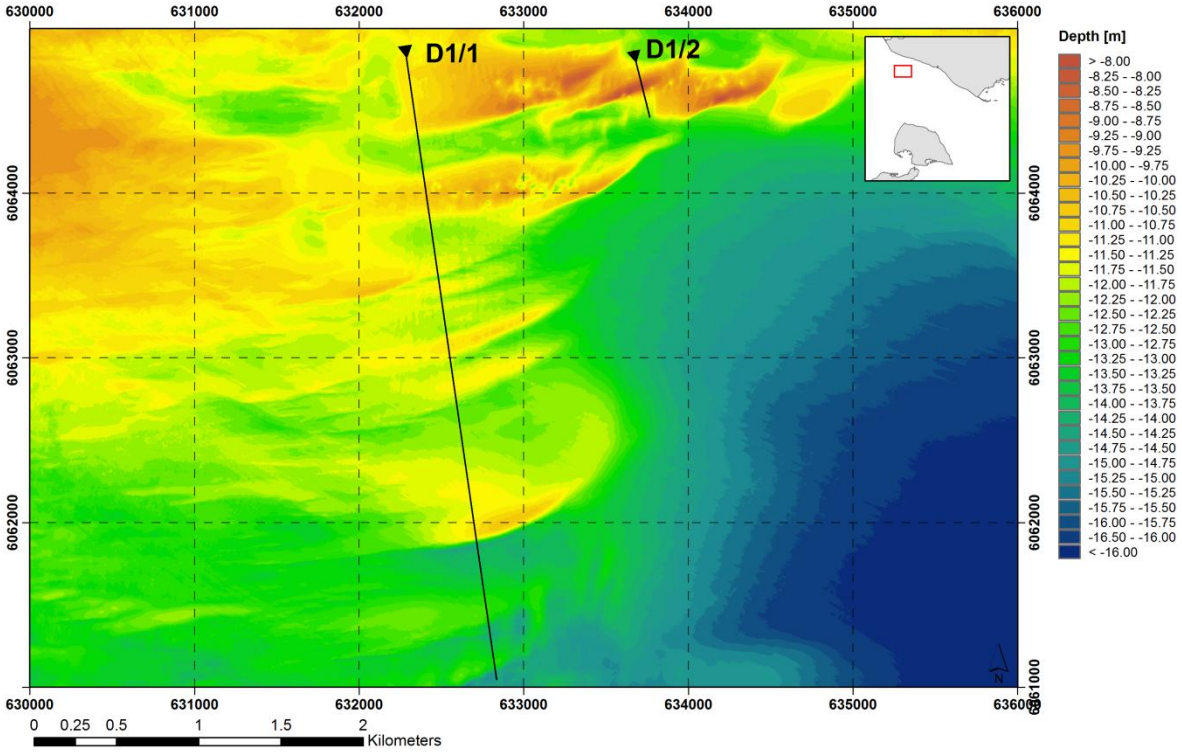

Figure 6.8 D1 – Bathymetry 8-16 m depths

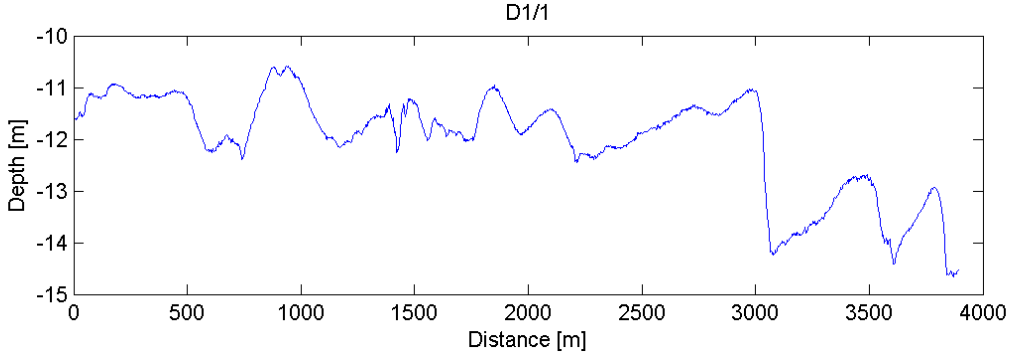

Figure 6.9 Profile along D1/1

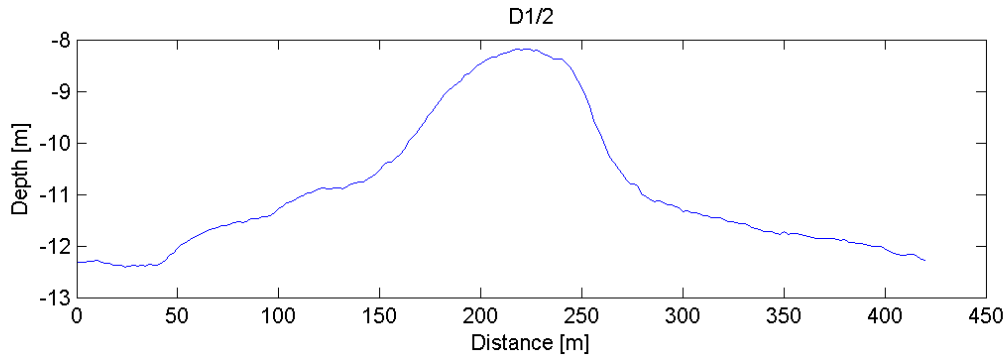

Figure 6.10 Profile along D1/2

D2 (Map XII in Appendix A)

Area D2 is characterised by a significant number of sand waves with heights up to 3.5 m located at 14-20 m water depth (see overview in Figure 6.7 and detailed bathymetry in Figure 6.11). The sand waves cover an area of approximately 3x2 kilometres. Figure 6.12-Figure 6.14 show diver photos of the sand wave field. The wave lengths of the sand waves are in the range 50-150 m and they are more homogenous with regard to shape and size than the bed forms in area D1.. In general, the sand waves are asymmetric with a steeper lee-side facing east (85-95 degrees N). The maximum steepness of the lee-side is usually 12-16 degrees, but a bed slope up to 18.9 degrees is observed in this area. Figure 6.15 shows a profile with sand waves with a height lower than 1 m and a wave length around 40 m. Figure 6.16 - Figure 6.18 show three profiles with larger sand waves which vary more in size and shape.

Table 6.3 Sand wave parameters – D2

Height, H [m]	Length, λ [m]	Typical maximum steepness [deg]	Local maximum steepness [deg]	Orientation, α_d [deg. N]	Area [ha]
1-3.5	50-150	12-16	18.9	90 (±5)	480

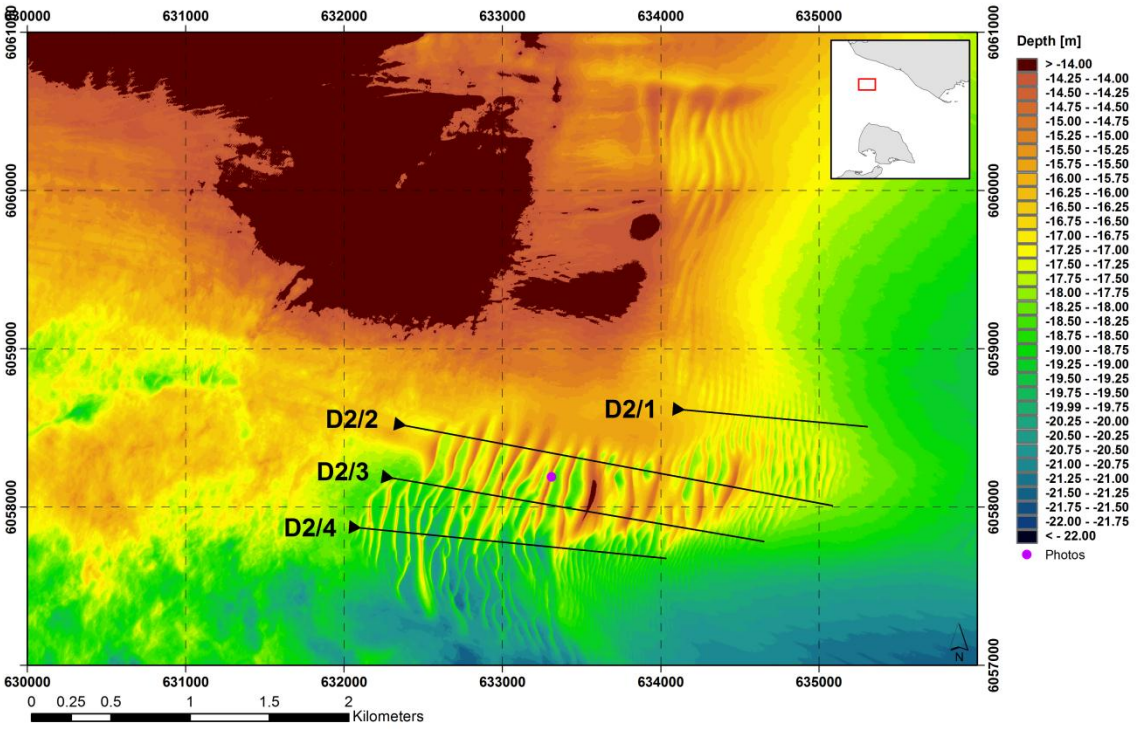

Figure 6.11 D2 – bathymetry 14-22 m depths

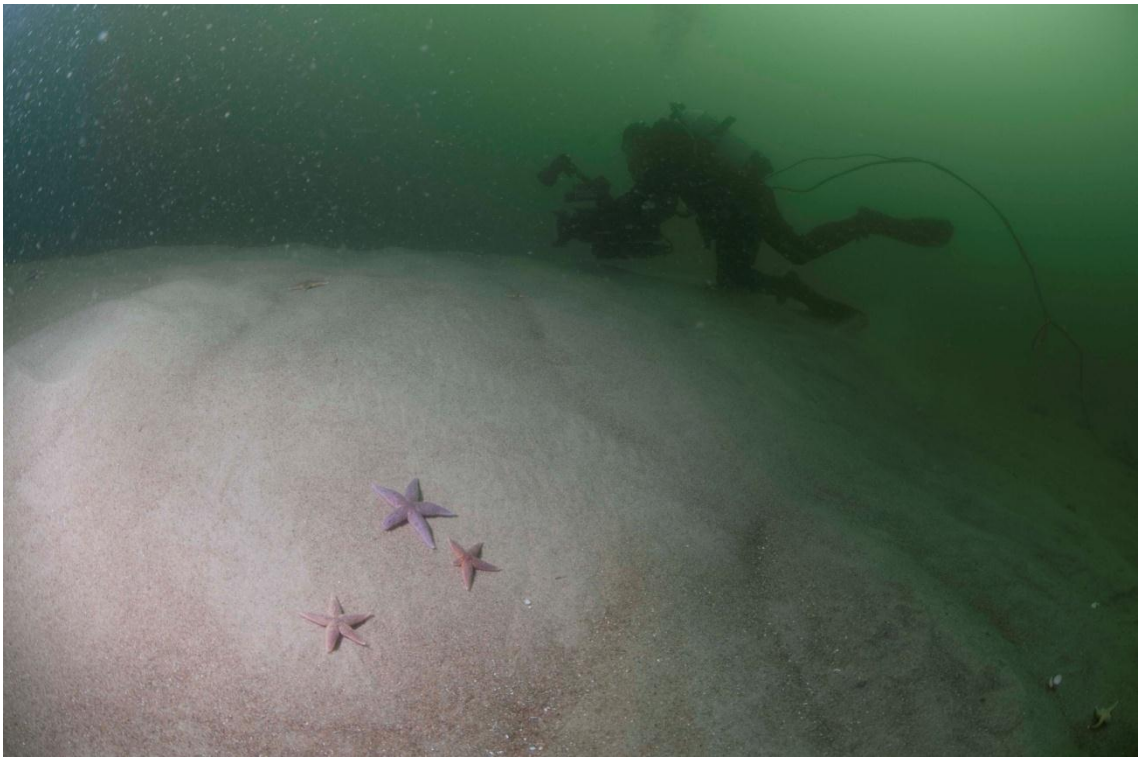

Figure 6.12 Photo 1 of sand wave from area D2 (©NaturFocus, personal communication)

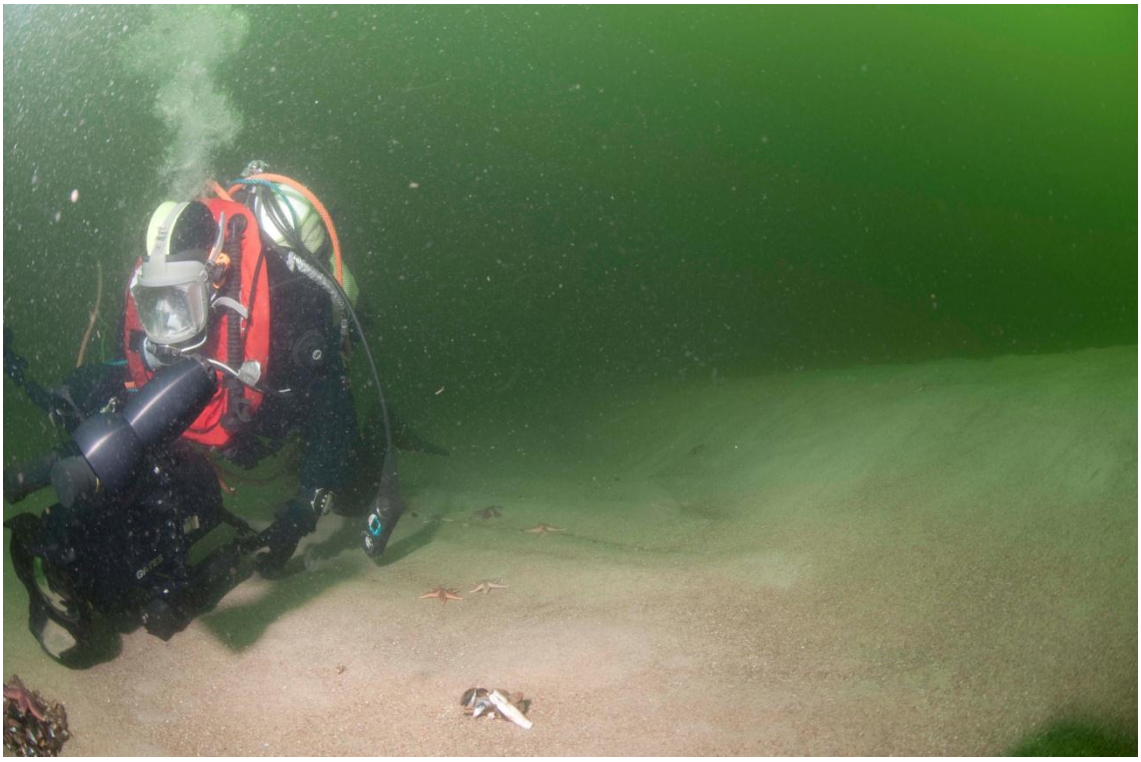

Figure 6.13 Photo 2 of sand wave from area D2 (©NaturFocus, personal communication)

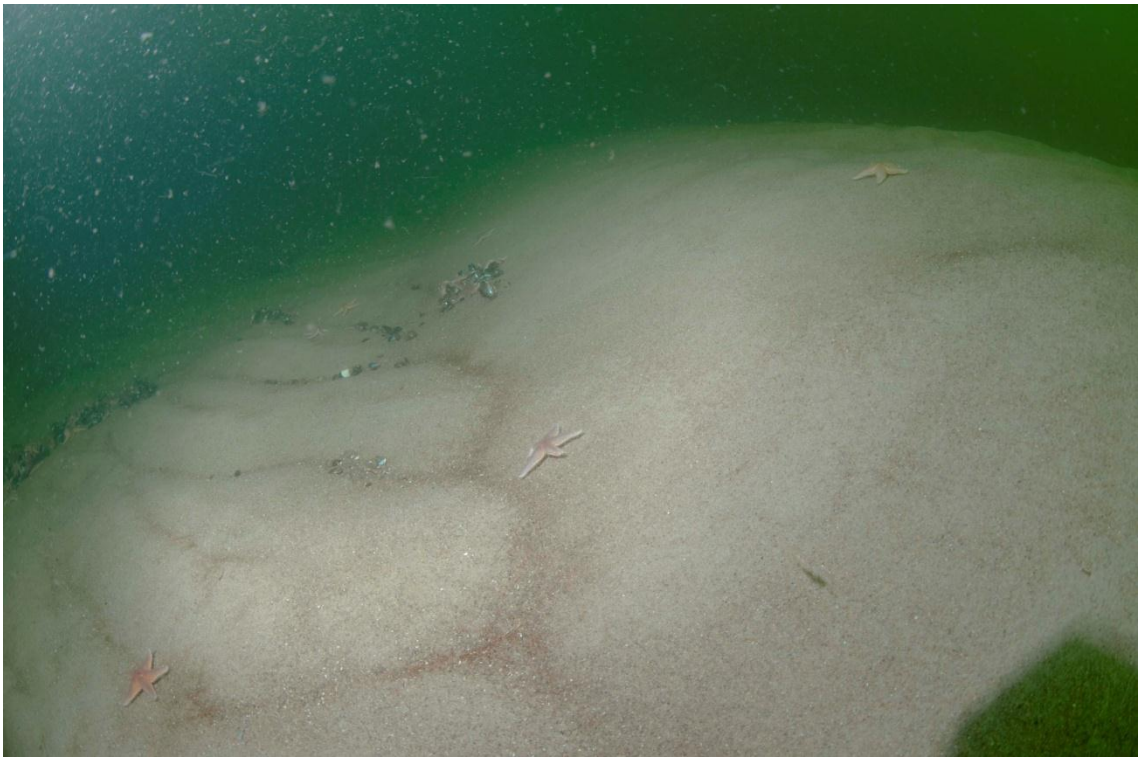

Figure 6.14 Photo 3 of sand wave from area D2 (©NaturFocus, personal communication)

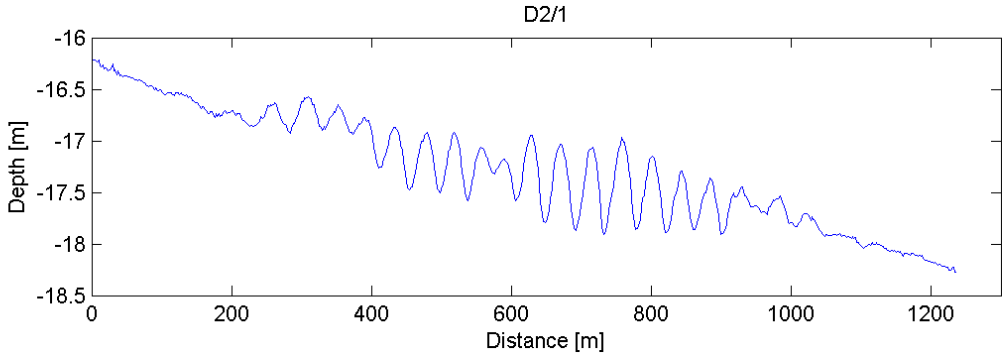

Figure 6.15 Profile along D2/1

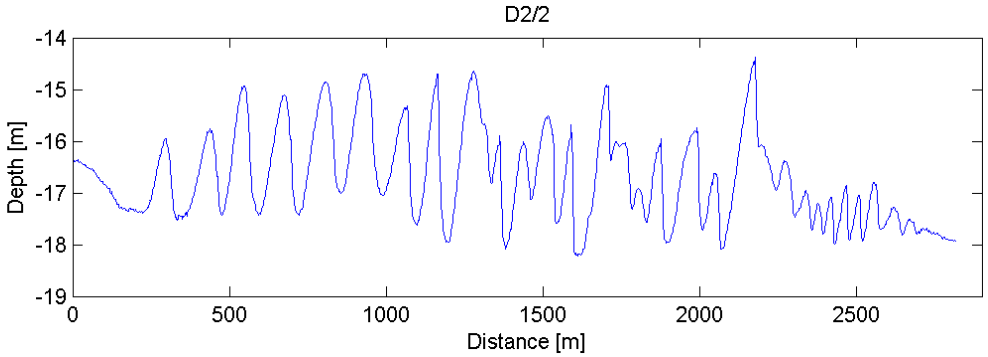

Figure 6.16 Profile along D2/2

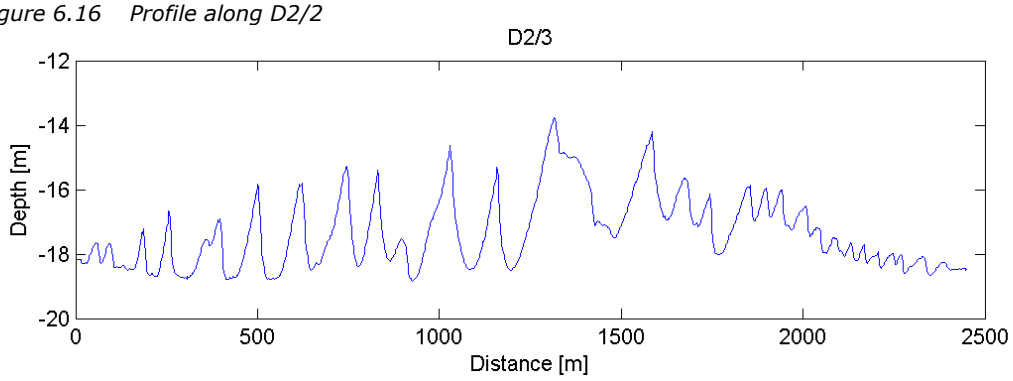

Figure 6.17 Profile along D2/3

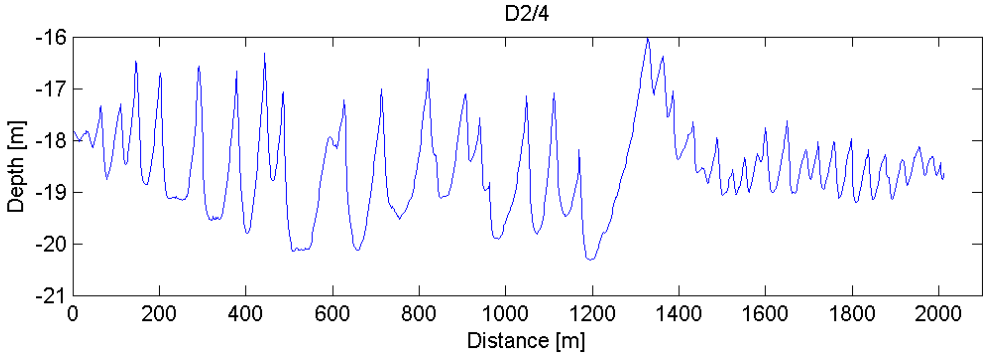

Figure 6.18 Profile along D2/4

D3 (Map XIII in Appendix A)
In area D3, there are about 8 large oblique sand waves at 12-15 m depth, see Figure 6.19. The heights of the bed forms are up to 3 m.

This sand wave field is characterised by its relatively few but long sand waves (length about 200-400 m) and resembles in this regard the large sand waves in the northern part of D1.

Each individual sand wave is oriented with their steeper bed slope facing approx. 180 degrees to true north, while the entire sand wave field extends in the NW-SE direction (the current direction).

These sand waves are also characterised by their relatively small steepness of their bed slope, which for most of the sand waves is in the range 3-5 degrees. The local maximum steepness is observed to 7.2 degrees.

The net migration rates of the sand waves are probably very small, less than a few m/year, as the net sediment transport rate in this area is small. The sand waves are, however, expected to be dynamic in the sense that they are expected to move slowly back and forth as the sea bed sediment is transported along the sea bed.

During individual events of 12-24 hours occurring a few times a year, however, volumes of sea bed material in the order of 3-5 m^3/m may be transported in either direction (east or west). During such events, the bed forms may migrate up to 1-3 m.

Table 6.4 Sand wave parameters – D3

Height, H [m]	Length, λ [m]	Typical maximum steepness [deg]	Local maximum steepness [deg]	Orientation, α_d [deg. N]	Area [ha]
1.5-3	200-400	3-5	7.2	180	570

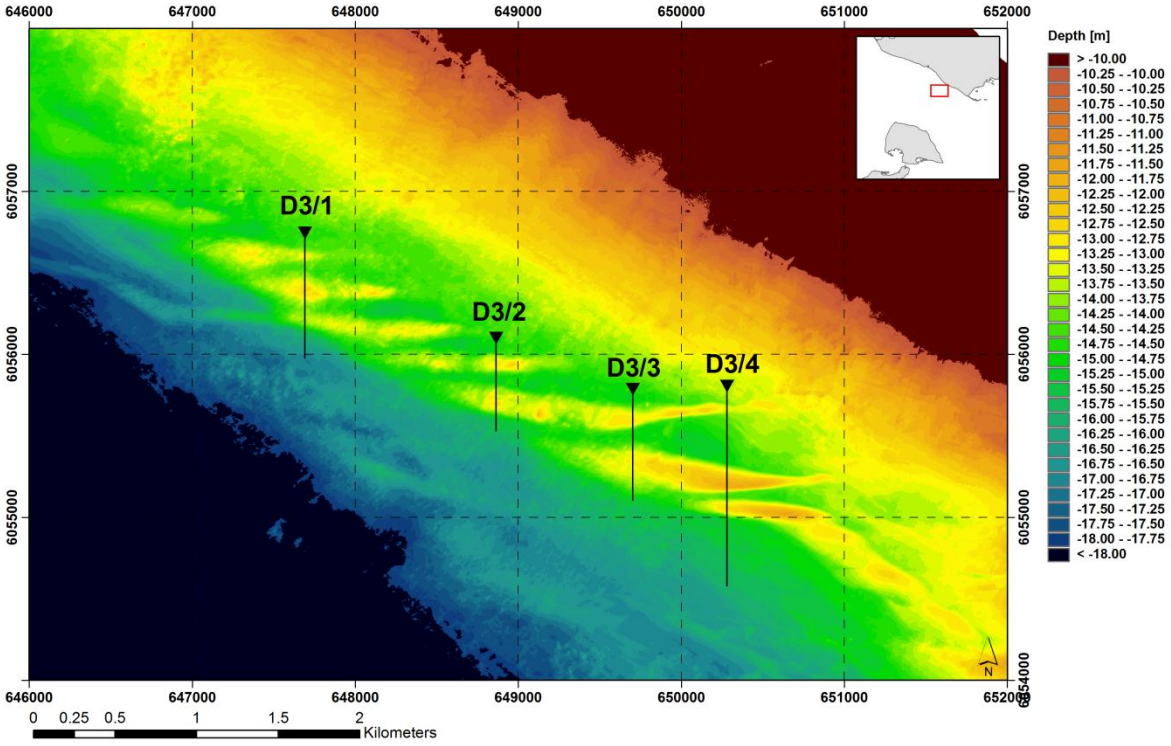

Figure 6.19 D3 - bathymetry 10-18 m depths

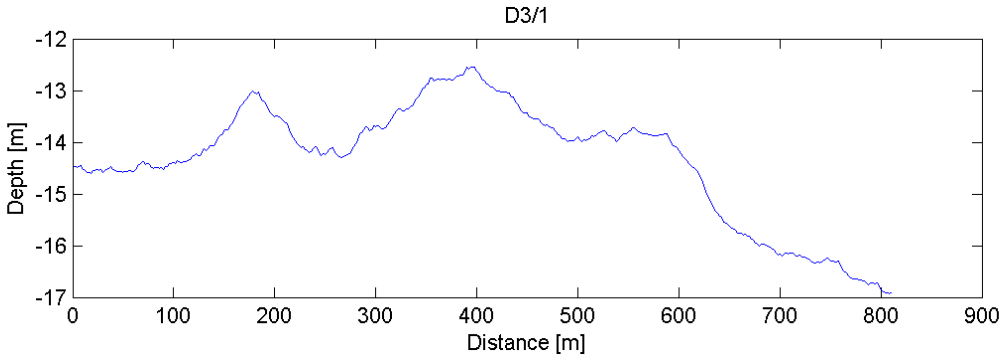

Figure 6.20 Profile along D3/1

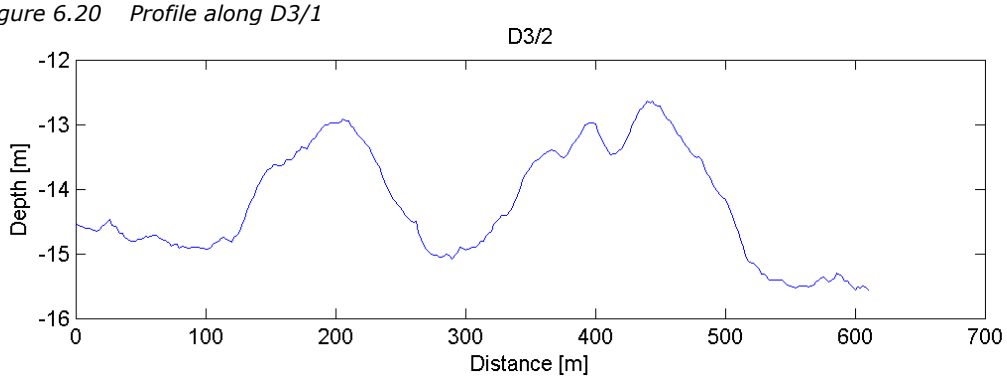

Figure 6.21 Profile along D3/2

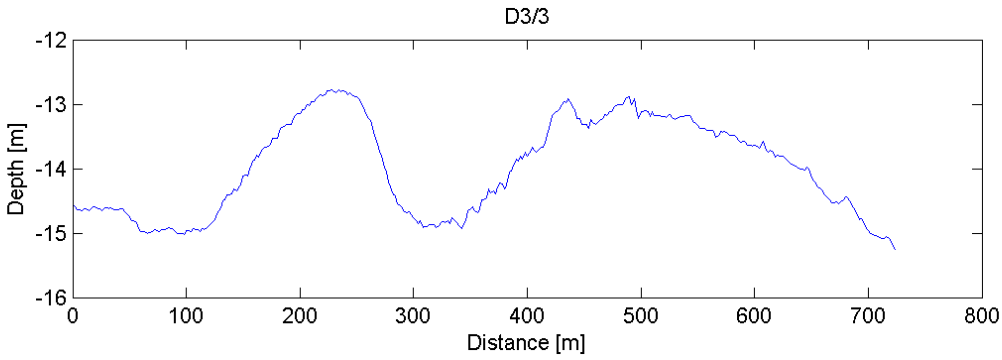

Figure 6.22 Profile along D3/3

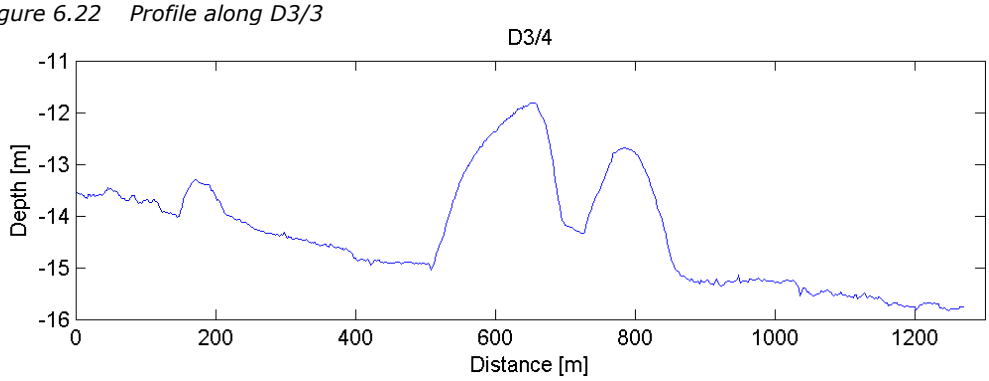

Figure 6.23 Profile along D3/4

D4 (Map XIV in Appendix A)

This area, at water depths ranging between 14 and 18 m, have three separate sand wave fields, see overview in Figure 6.7 and Figure 6.24. The sand wave fields in area D4 are characterised by a large number of smaller sand waves and some oblique sand waves. All the sand waves in area D4 have an orientation of about 120 degr. N, i.e. their steep sides are facing towards the southeast.

The most northwestern sand wave field has fairly small bed forms with a maximum height of 1.2 m and lengths of about 80 m as seen in the vertical profiles in Figure 6.25 and Figure 6.26. The bed slope steepness of these sand waves is rarely above 4 degrees, although they locally can reach up to 10 degrees.

The sand wave field to the southwest is shown in Figure 6.27 and Figure 6.28. This sand wave field includes sand waves with a height of 2 m and a length of 100 m. The maximum bed slope steepness of the bed forms is typically between 12 and 16 degrees but locally bed slopes up to 22.8 degrees are found.

The easternmost area of sand waves are composed of larger oblique sand waves with bed forms characteristics similar to the sand waves in area D3. They have heights up to 3 m, lengths of about 200-500 m and mild bed slopes.

A small net migration rate of up to about 10 m/year for the smallest sand waves (with heights of approximately 0.5 m) towards the Baltic Sea is expected for the sand waves in area D4, especially for the southernmost sand waves. Larger sand waves will annually migrate shorter distances.

During individual events of 12-24 hours occurring a few times a year, the bed forms may migrate in either direction up to about 5 m.

D4 includes a sand mining area. Substantial amounts of sand have been extracted from the area. Extraction of the sea bed material is clearly seen in the multibeam survey as areas within the sand wave field, where the sand waves are more or less eliminated, see Figure 6.24 and in cross section D4-4, see Figure 6.28. The multibeam survey was performed in 2009, three years after the last major extraction in 2006. The bed forms are expected to regenerate naturally with time due to the dynamic nature of the bed forms. In this case, the extraction area is large compared to the individual sand waves, which means that the sand waves need to reform completely. The bed forms have obviously not recovered fully during the three years 2006-2009, but signs of recovery can be found in the area as regular patterns of troughs and tops with a smaller length scale than the natural one can be identified in the extraction area. This agrees with the estimates of the sediment mobility in the area (in the order of 10 m^3/m/year in each direction, see Chapter 5). A gross migration of several times the length of the full size sand waves is expected for a full recovery, (Niemann et al. 2003). With the estimated sediment mobility and the size of the sand waves, this may take in the order of 10 years or more in this area. The sand mining is further discussed in Chapter 8.

Table 6.5 Sand wave parameters – D4 (western bed form fields)

Height, H [m]	Length, λ [m]	Typical maximum steepness [deg]	Local maximum steepness [deg]	Orientation, α_d [deg. N]	Area [ha]
0.5-3	50-100	12-16	22.8	120	290

Table 6.6 Sand wave parameters – D4 (eastern bed form field)

Height, H [m]	Length, λ [m]	Typical maximum steepness [deg]	Local maximum steepness [deg]	Orientation, α_d [deg. N]	Area [ha]
1-3	200-500	3-5	-	180	350

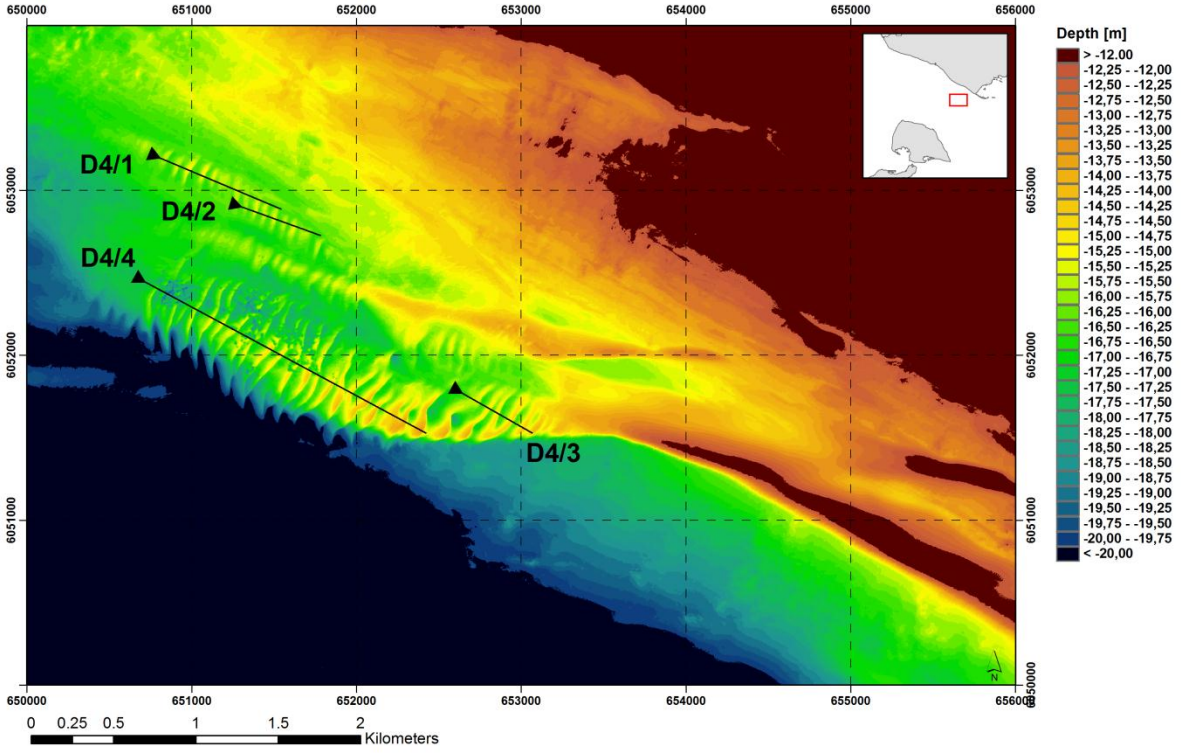

Figure 6.24 D4 – bathymetry 12-20 m depth

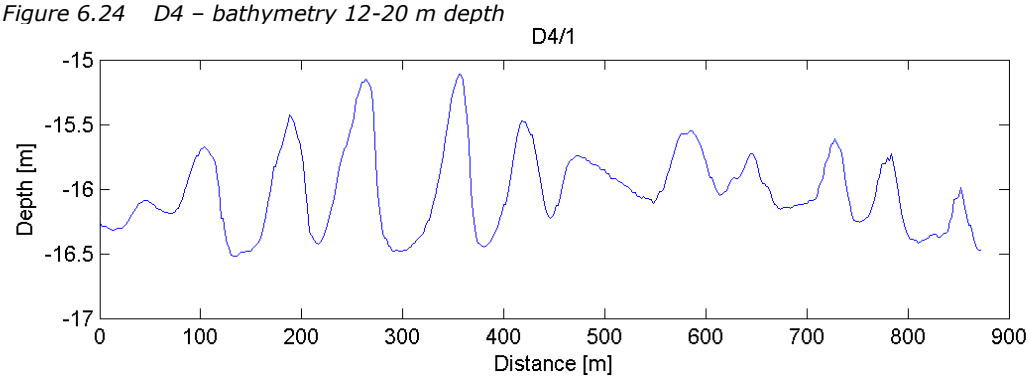

Figure 6.25 Profile along D4/1

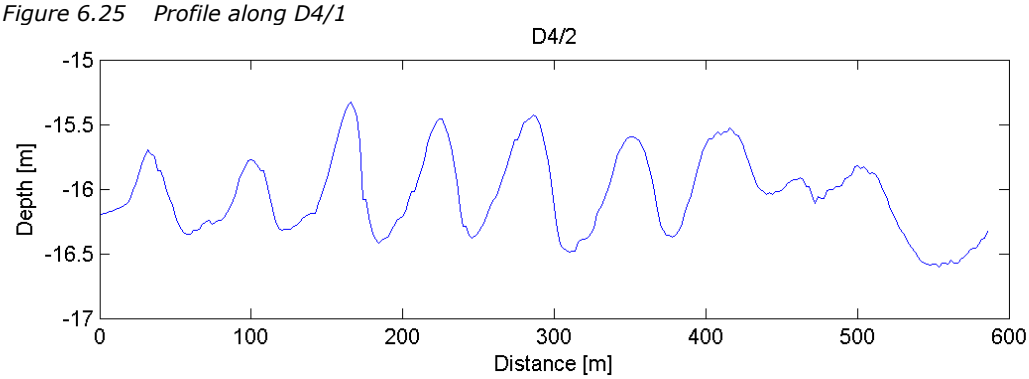

Figure 6.26 Profile along D4/2

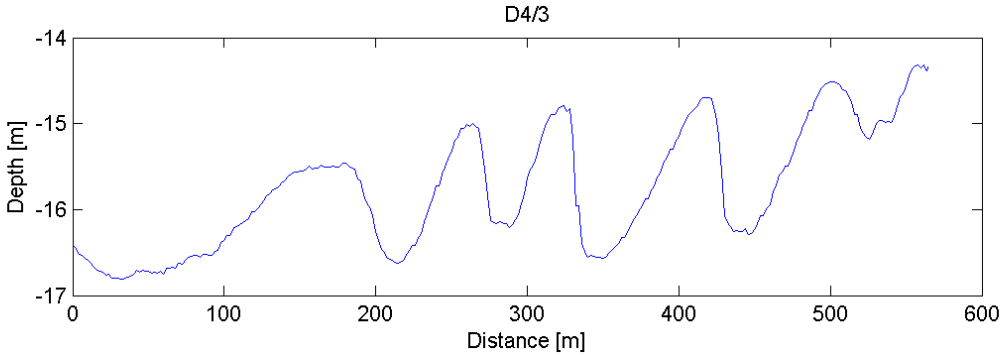

Figure 6.27 Profile along D4/3

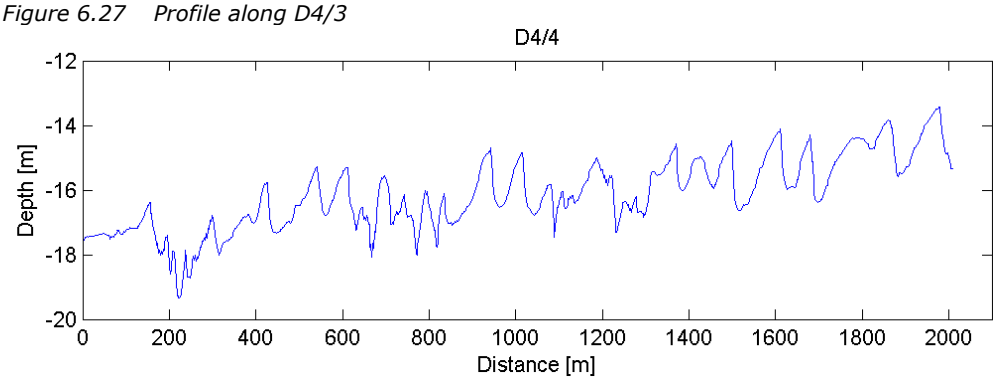

Figure 6.28 Profile along D4/4

G1-G2 (Maps XV-XVII in Appendix A)

Area G1-G2 is characterised by a large field of homogenous bed forms at water depths from about 11 to 24 m, see Figure 6.29. The sand wave field extends approximately 9 km in the W-E direction and 1.5 km in the N-S direction and is thereby the largest sand wave area in the Fehmarnbelt. The sand waves are located in an area where the water depth increases from about 11 m to 24 m in two terraces. However, it is hard to distinguish between the two terraces in the western part of the sand wave field, whereas it is very clear in the eastern part, see Figure 6.29.

The largest sand waves are located on the upper terrace at water depths 11-16 m with a height of up to 2.5 m. The most common heights on the upper terrace are 1.5-2 m, while the lengths usually are between 50-100 m. The bed form height on the lower terrace at water depths 15-24 m is up to about 1 m but is typically around 0.5 m. Lengths are in the range 25-50 m.

All sand waves are characterised by their asymmetric shape. The sand waves are almost all asymmetric with their lee side facing east. While the sand waves on the upper terrace are oriented approximately 90 degrees to true north, the sand waves on the lower terrace are oriented with an angle of 80 degrees.

Furthermore, some long sand ribbons exist in the south-western part of G1-2. These are categorized as 'other active bed forms' in the overview figure, Figure 6.7. They extend in the SW-NE direction (approximately 140 degrees N) and terminate in the north at the sand wave field. The sand ribbons are characterised by their relatively long length compared to their width. They are more non-homogenous bed features than the sand waves, as seen in the vertical profiles in Figure 6.33 and Figure 6.34. They have heights up to about 1 m, widths about 50-200 m and lengths of several kilometres.

Table 6.7 Sand wave parameters upper terrace – G1-G2

Height, H [m]	Length, λ [m]	Typical maximum steepness [deg]	Local maximum steepness [deg]	Orientation, α_d [deg. N]	Area [ha]
1-2	50-100	16-20	24.0	90	600

Table 6.8 Sand wave parameters lower terrace – G1-G2

Height, H [m]	Length, λ [m]	Typical maximum steepness [deg]	Local maximum steepness [deg]	Orientation, α_d [deg. N]	Area [ha]
0.5-1	25-50	4-7	12.8	80	460

Table 6.9 Bed form parameters of 'other active bed forms' – G1-G2 (sand ribbons)

Height, H [m]	Width, λ [m]	Typical maximum steepness [deg]	Local maximum steepness [deg]	Orientation, α_d [deg]	Area [ha]
0.5-1	50-200	-	-	140	1,270

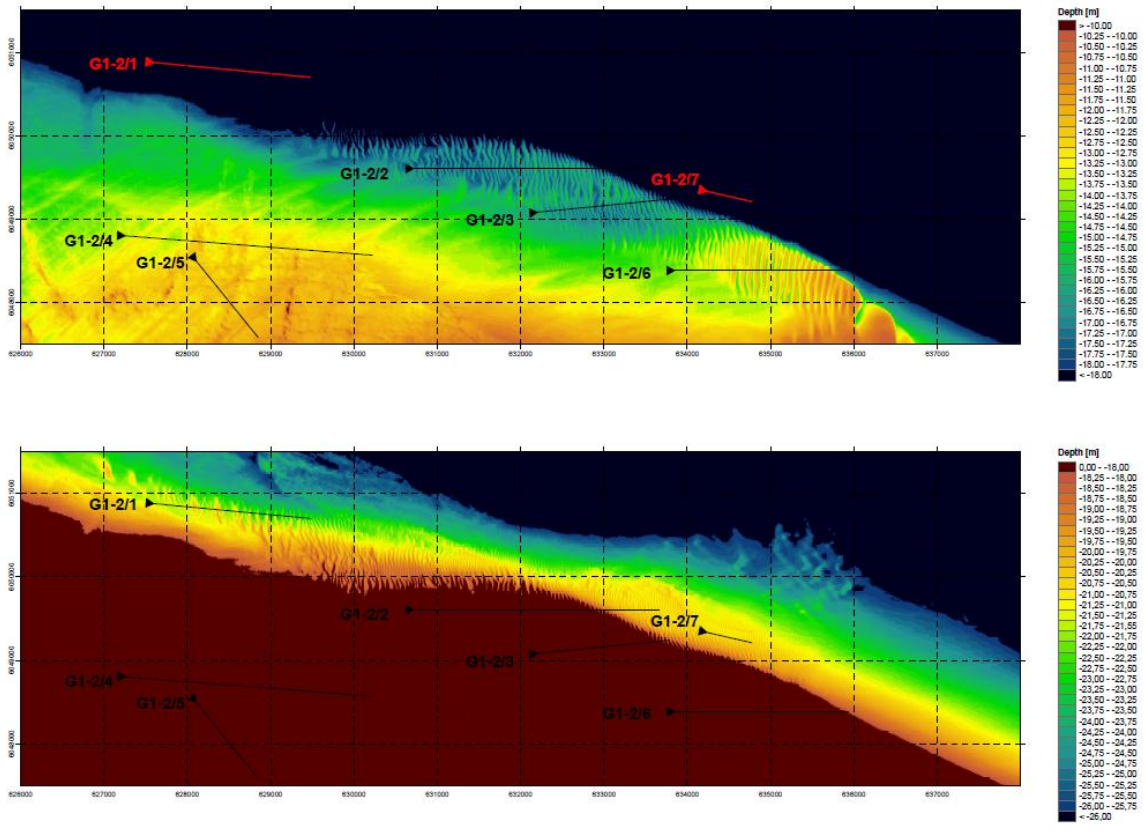

Figure 6.29 G1-G2 – A. bathymetry 10-18 m depth. B. Bathymetry 18-26 m depth

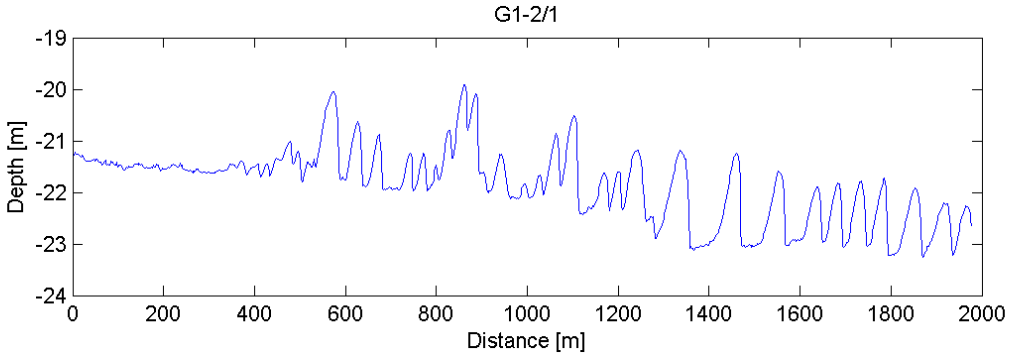

Figure 6.30 Profile along G1-2/1

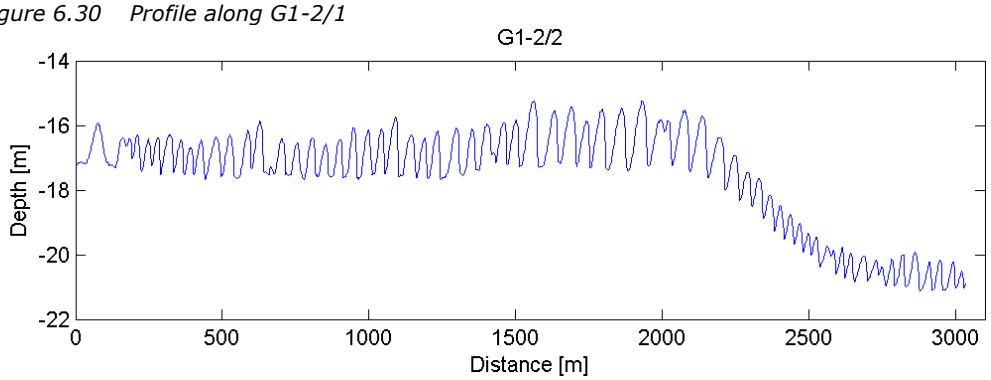

Figure 6.31 Profile along G1-2/2

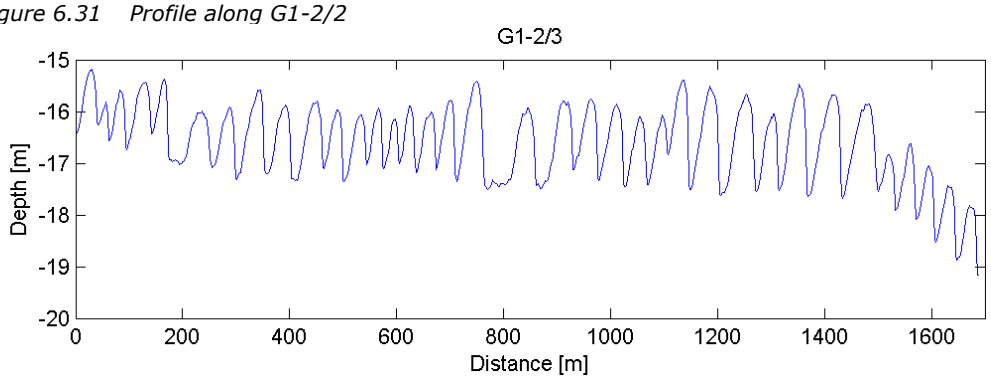

Figure 6.32 Profile along G1-2/3

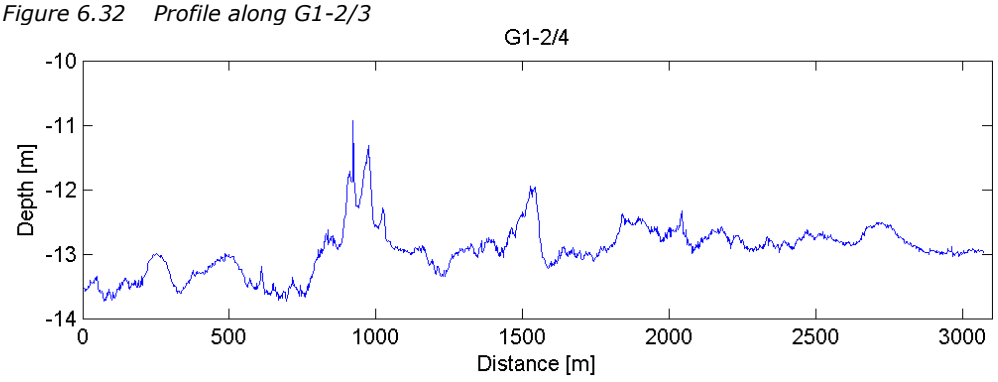

Figure 6.33 Profile along G1-2/4

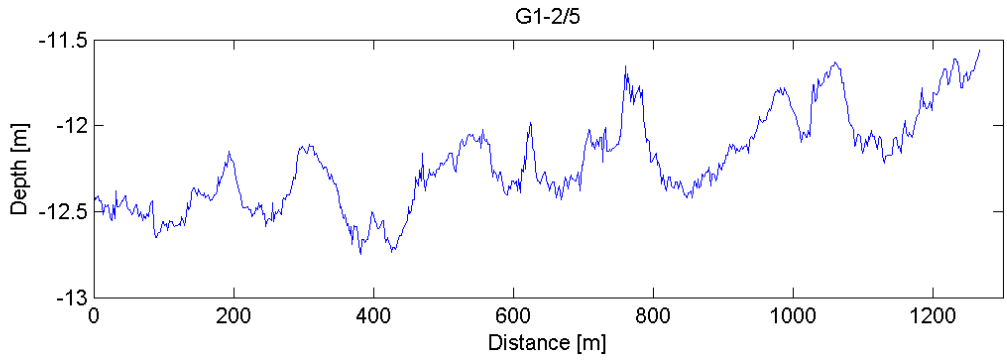

Figure 6.34 Profile along G1-2/5

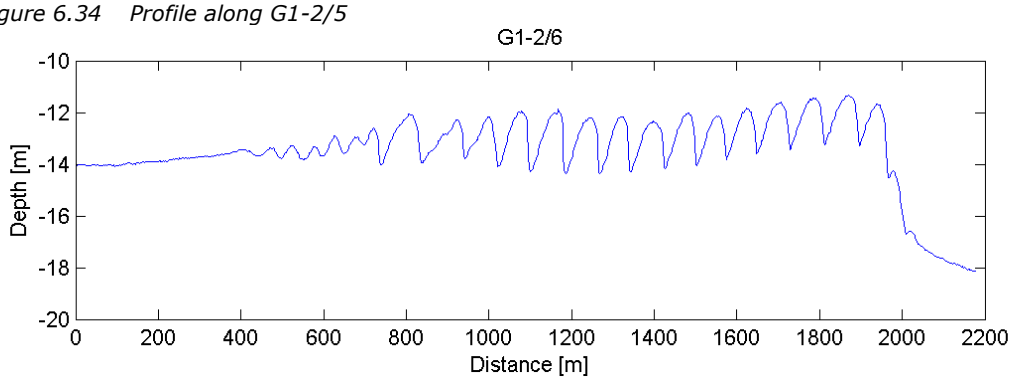

Figure 6.35 Profile along G1-2/6

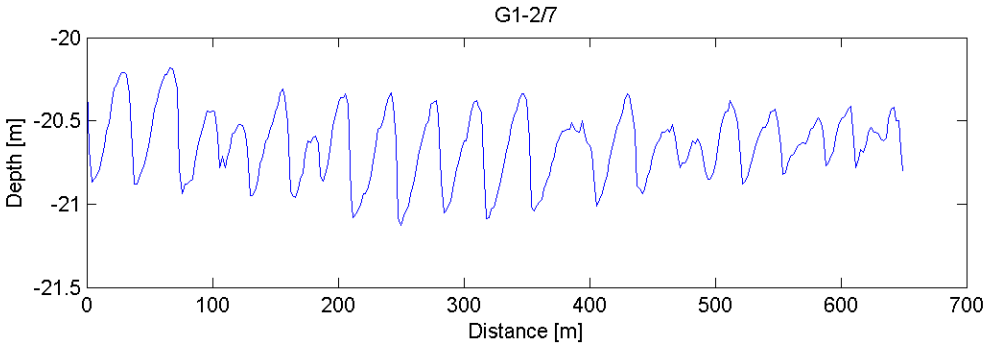

Figure 6.36 Profile along G1-2/7

G3 (Map XVIII in Appendix A)

Area G3 includes two fields of bed forms located on two different terraces. On the lower terrace some homogenous sand waves are located at water depths from 9.5 to 11 m. The heights are about 0.5-1 m and the s lengths are approximately 25-40 m. The sand waves are oriented with their lee-side facing east; about 95 degrees N. The typical maximum bed slope steepness is in the range 8-12 degrees but up 19.4 degrees is observed.

The bed forms on the upper terrace are much more scattered, less homogenous in their shape and pattern and random in size and shape compared to the sand waves on the lower terrace. The heights are approximately the same as for the sand waves on the lower terrace but the lengths are larger and the bed slope steepness significantly lower.

Table 6.10 Bed form parameters for upper terrace G3 (other active bed forms)

Height, H [m]	Length, λ [m]	Typical maximum steepness [deg]	Local maximum steepness [deg]	Orientation, α_d [deg. N]	Area [ha]
0.5-1.2	50-150	4-7	9.0	100	240

Table 6.11 Sand wave parameters lower terrace G3

Height, H [m]	Length, λ [m]	Typical maximum steepness [deg]	Local maximum steepness [deg]	Orientation, α_d [deg. N]	Area [ha]
0.5-1	25-40	8-12	19.4	95	50

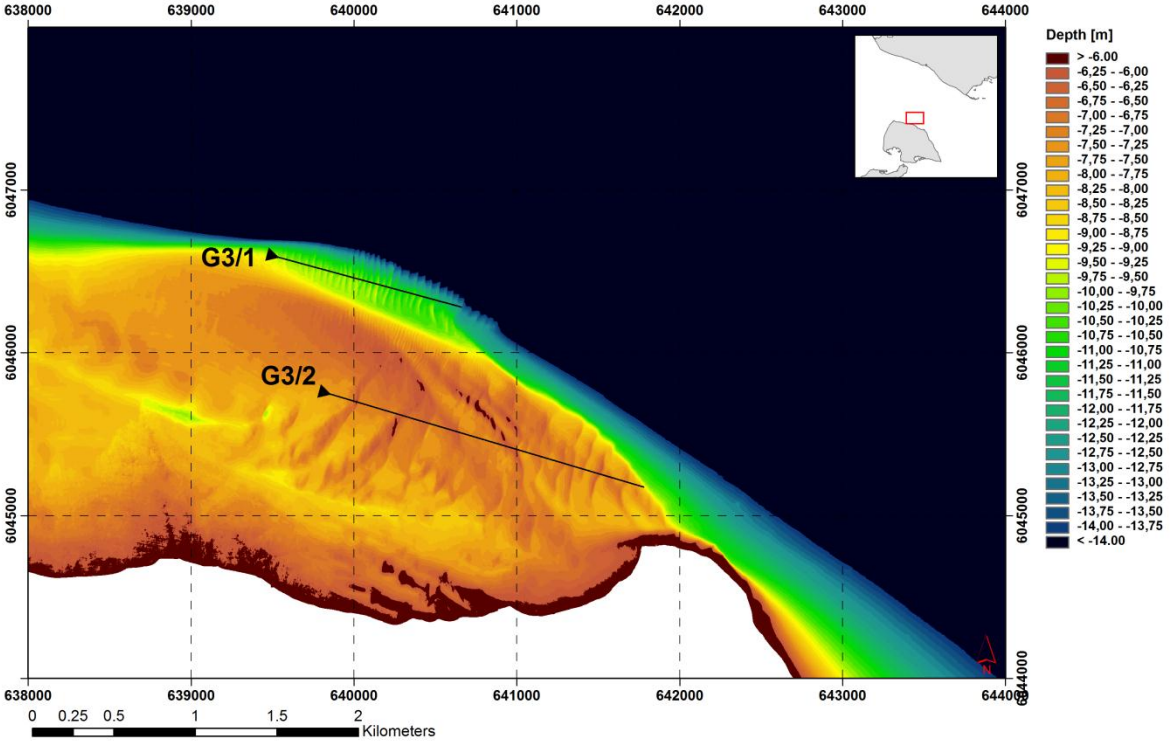

Figure 6.37 G3 – bathymetry 6-14 m depth

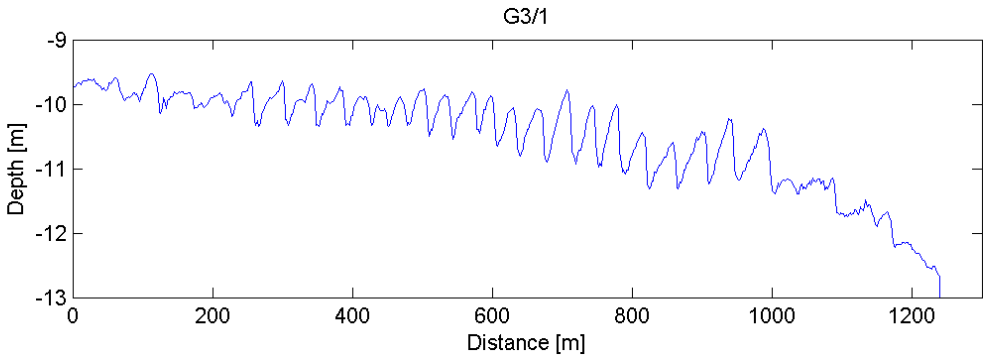

Figure 6.38 Profile along G3/1

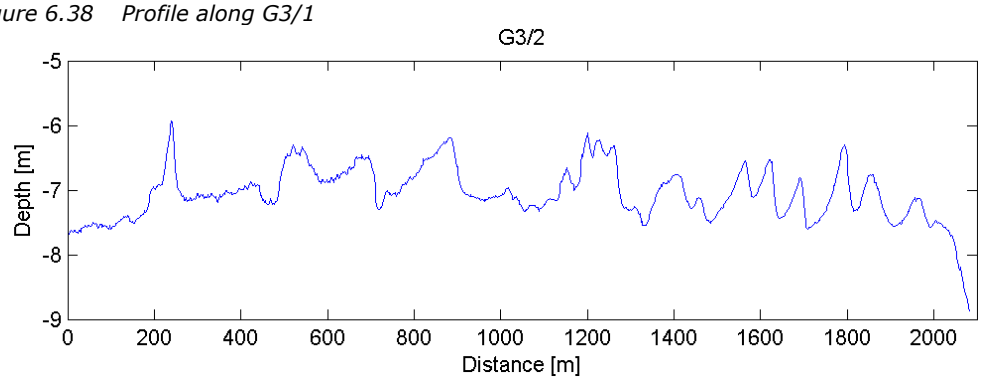

Figure 6.39 Profile along G3/2

G4 (Map XIX in Appendix A)

Area G4 is dominated by a great amount of lunate bed forms located at water depths of less than 25 m. The lunate bed forms are covering a large area of the deeper part of the Fehmarnbelt as mapped in Figure 6.2.

In contrast to the bed forms described previously in areas D1-D4 and G1-G3, the lunate bed forms are characterised by a much more 3-dimensional structure. The crescent bed forms usually consist of a "head" and two "legs". The head is typically elevated 40-60 cm above the surrounding area, but up to 1 m is also observed. The two legs are less pronounced than the head but are usually elevated 20-40 cm above the surrounding area. The length and width of the bed forms are both in the order of 100-150 m. Figure 6.41 and Figure 6.42 show close ups of the bathymetry of one of the lunate bed forms. Figure 6.43-Figure 6.45 shows several vertical profiles through one of the lunate bed forms. The shape of the bed forms as well as the net sediment transport in this area indicate that they are migrating eastwards in the direction of the Baltic Sea. The migration rate, however, is difficult to estimate, but in the order of 5-10 m/year towards the southeast is expected.

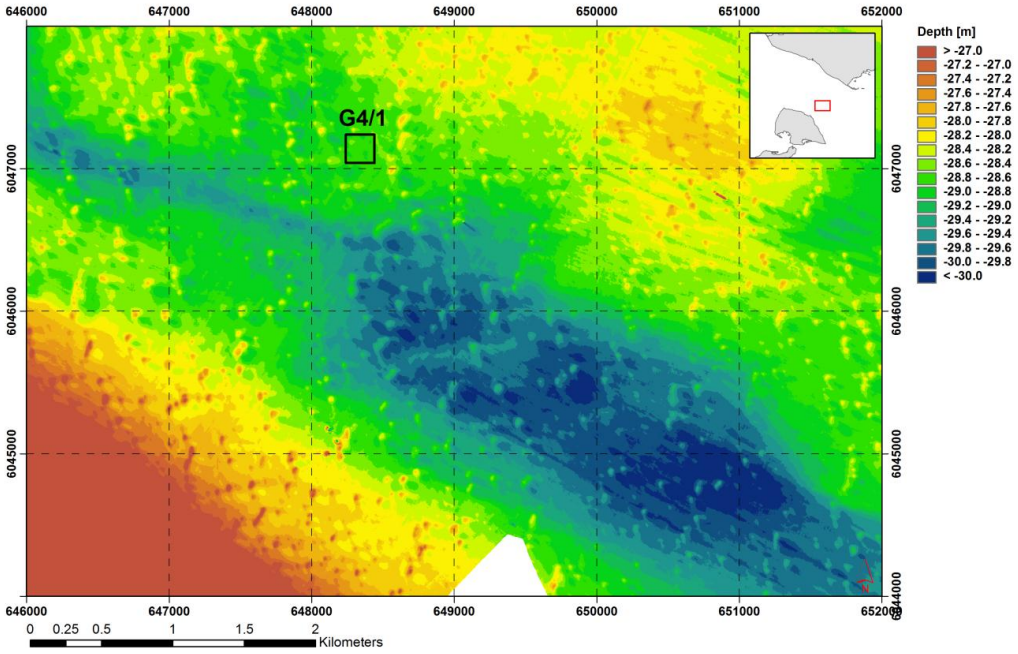

Figure 6.40 G4 – bathymetry 27-30 m depth

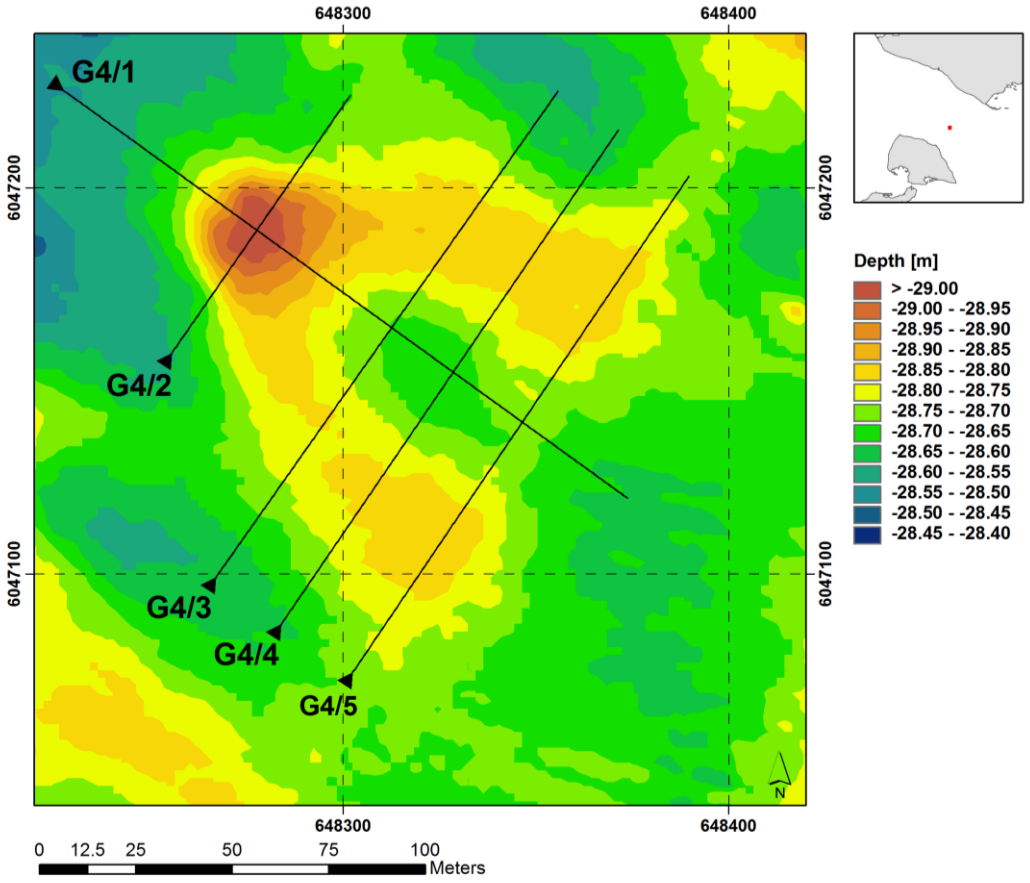
648300
648400
6047200
6047100
G4/1
G4/2
G4/3
G4/4
G4/5
Depth [m]
> -29.00
-29.00 - -28.95
-28.95 - -28.90
-28.90 - -28.85
-28.85 - -28.80
-28.80 - -28.75
-28.75 - -28.70
-28.70 - -28.65
-28.65 - -28.60
-28.60 - -28.55
-28.55 - -28.50
-28.50 - -28.45
-28.45 - -28.40
N
0 12.5 25 50 75 100
Meters

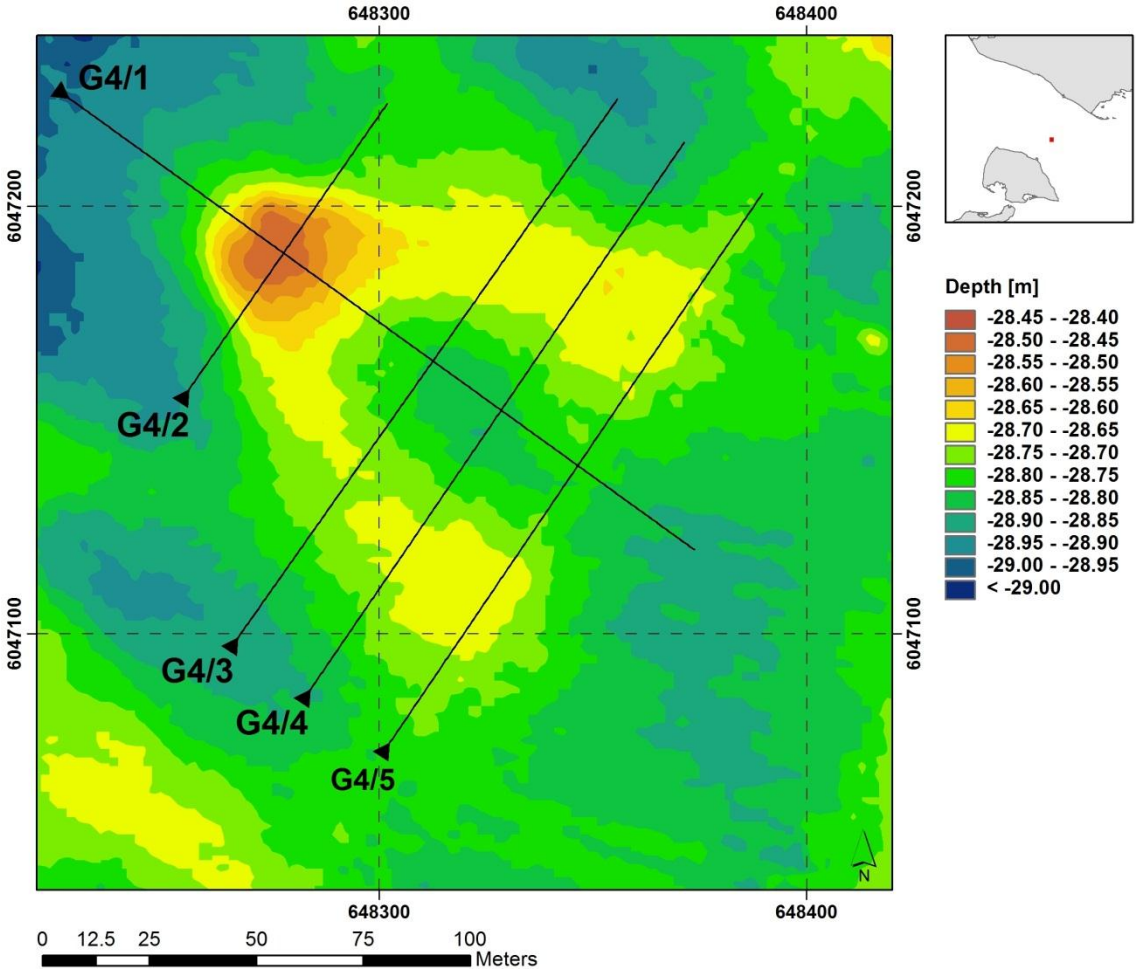

Figure 6.41 G4/1 Example of a lunate bed form

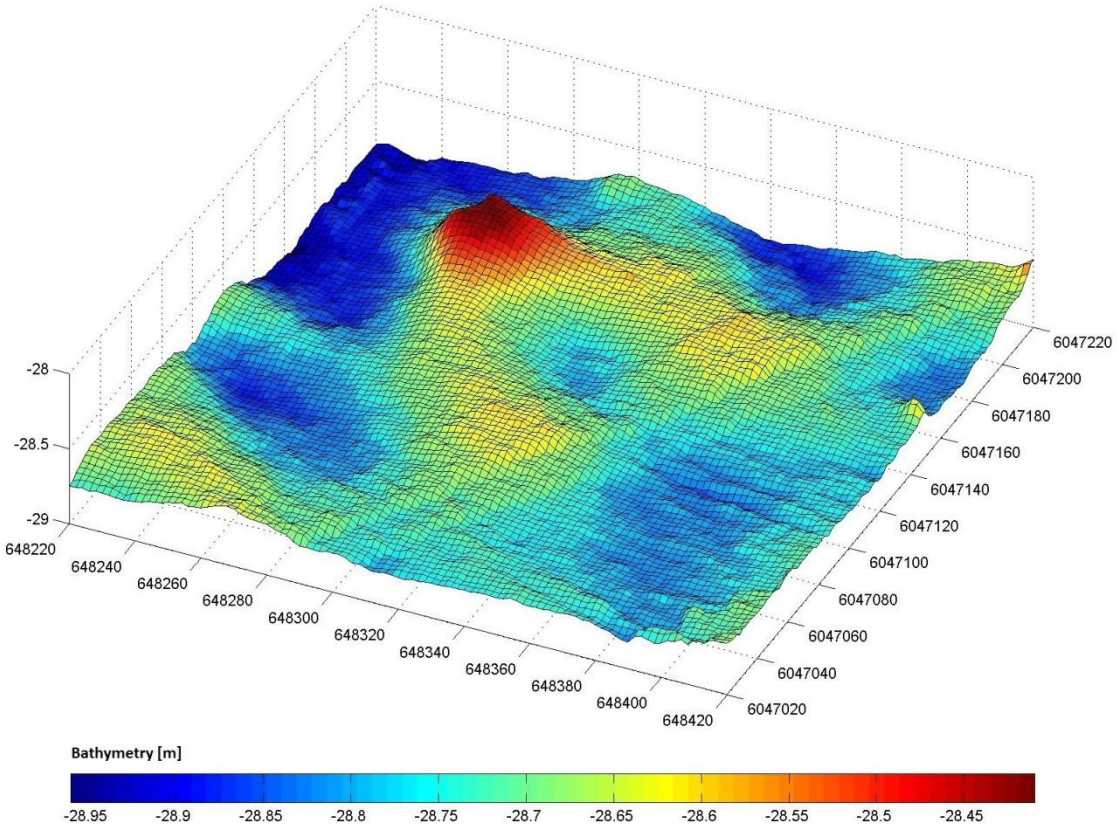

Figure 6.42 3D-view of a lunate bed form

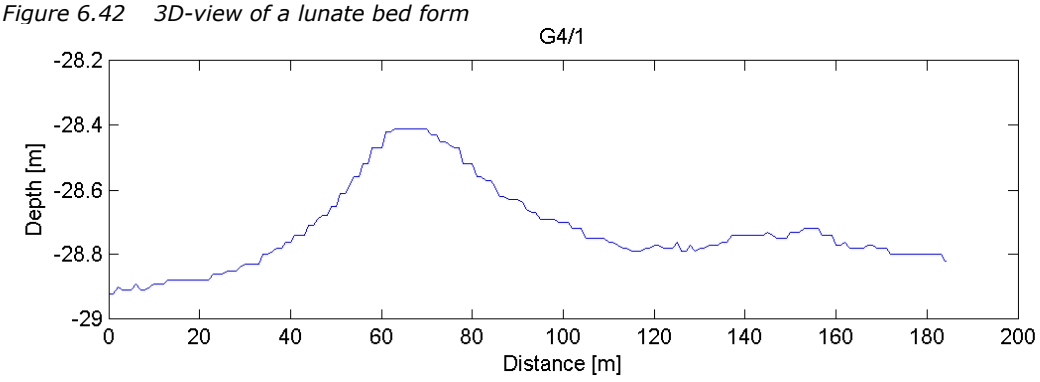

Figure 6.43 Profile along G4-1

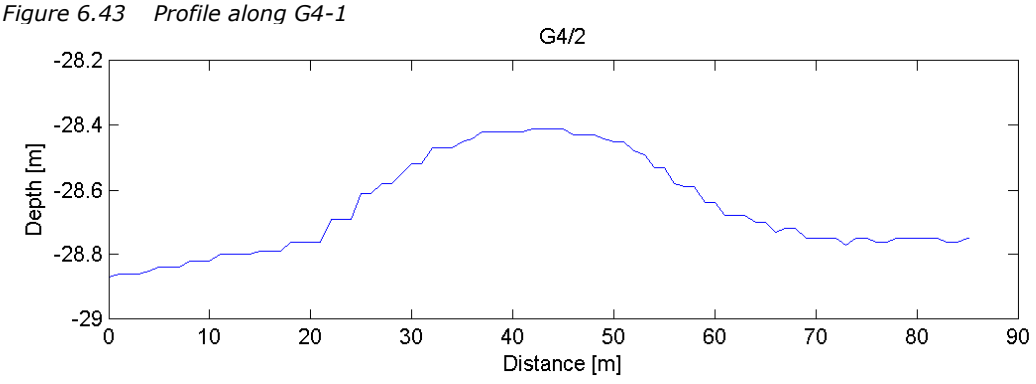

Figure 6.44 Profile along G4/2

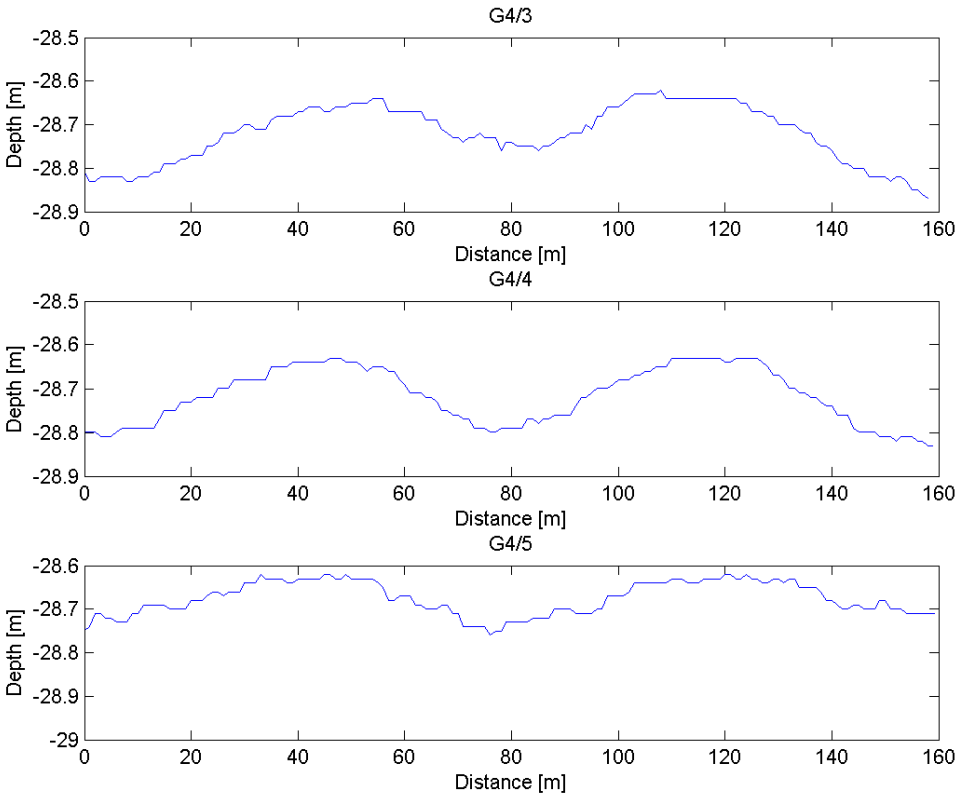

Figure 6.45 Profile along G4/3, G4/4 and G4/5

7 INTERACTION BETWEEN BED FORMS AND OVERALL FLOW

The bed forms in the Fehmarnbelt interact with the flow: the flow generates sediment transport which for certain flow conditions leads to the formation of bed forms and the bed forms constitute flow roughness elements or flow resistance. In this section the effect on the overall flow of the spatial variation in flow resistance due to bed forms is analysed. The applied methods for this analysis are outlined in Section 3.3.3.

7.1 Resistance Coefficients for Areas with Sand Waves

In the following results for the flow resistance in areas with sand waves are presented.

Flow resistance coefficients for skin friction, C_f, form drag, C_p and total drag, C_d (see definitions in Section 3.3.3) are computed for all transects in Section 6.3. Maps of the flow resistance imposed on the flow from the bed forms in individual areas are created.

Bed shear stress and near-bed pressure
An example of computed bed shear stress and pressure distribution along the bed forms in transect D4/1 is shown in Figure 7.1. It is seen that the pressure has a maximum in the trough and the pressure decreases along the upstream side of the sand wave. Nearly the same pressure distribution is achieved irrespectively of the current direction. With respect to the bed shear stress, the shear stress increases along the upstream side of the sand wave due to the contraction of the cross section together with a thinning of the turbulent bed boundary layer. It is seen that the pressure achieves numerically larger values than the bed shear stress; however, as it changes sign the integrated form drag actually becomes smaller than the integral of the flow resistance due to skin friction.

Flow resistance coefficients
The relation between the total computed drag and the skin friction, C_d/C_f, as a function of the skin friction, C_f, is shown in Figure 7.2. The skin friction, C_f, is basically unaffected by the presence of bed forms and C_d/C_f is hence the relative increase in the flow resistance due to the presence of bed forms compared to the situation without bed forms.

The flow resistance from the bed forms along the individual transects is thus seen to be less than 30% for all transects and combinations of bed roughness and current speeds. Furthermore, it is seen that the bed roughness has a pronounced influence on the skin friction and the form drag.

The flow resistance coefficients shown in Figure 7.2 form the basis for creating maps with the increase in flow resistance due to the bed forms. The transects have been grouped into geographical regions based on similarity in the resistance pattern and the average water depth.

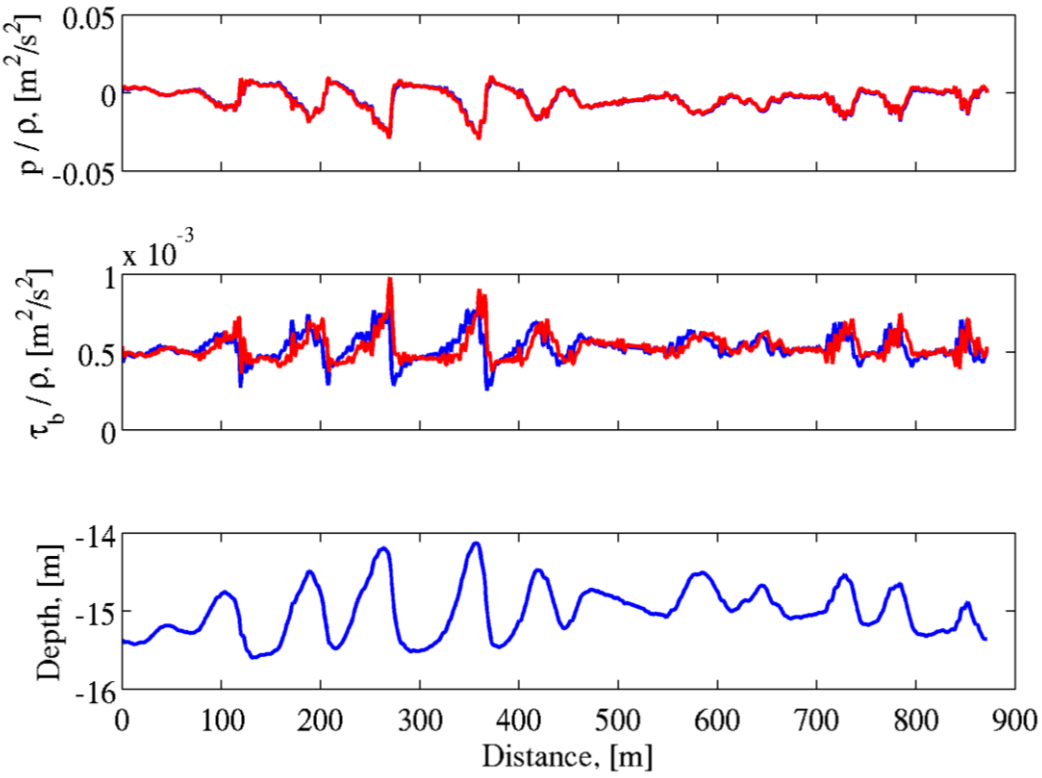

Figure 7.1 *The pressure and bed shear stress distribution along the transect D4/1. (Blue) Current in the positive x-direction. (Red) Current in the negative x-direction. The bottom panel shows the bed level. Results for an average velocity of 0.5 m/s and a bed roughness of 25 mm*

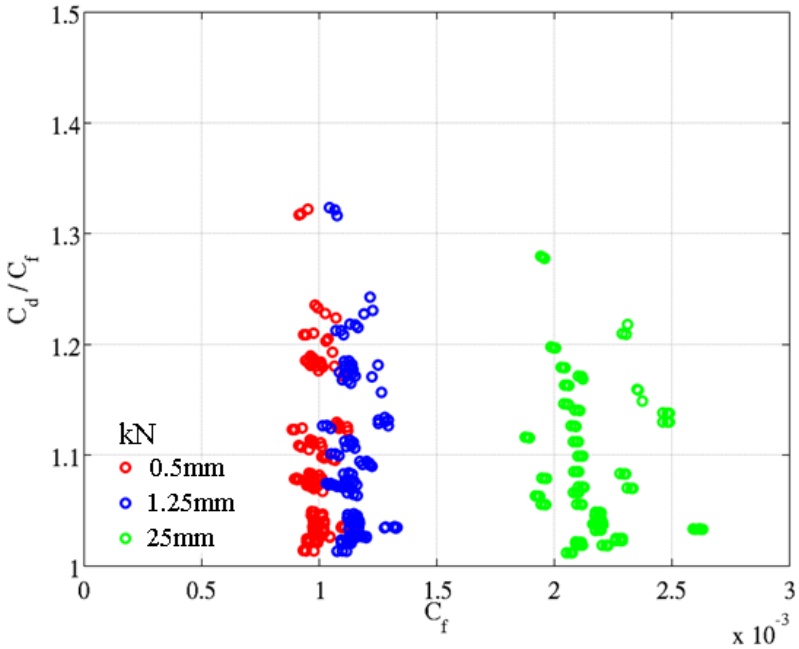

Figure 7.2 *The ratio between the total flow resistance and the one due to skin friction alone as a function of the skin friction coefficient. All combinations of transect, current velocities (0.3m/s, 0.5m/s and 0.7m/s) and bed roughness, k_N*

The maps of the relative flow resistance are provided in Figure 7.3 for the 'inflow' situation and in Figure 7.4 for the 'outflow' situation (inflow = towards the Baltic Sea). Results are shown for the runs with the lower values for the Nikuradse roughness parameter for the skin friction, k_N=0.5 mm. The values provided in the maps are the resistance coefficients for the in- and outflow situations, where the flow is perpendicular to the sand-wave crest lines, i.e. the resistance coefficients corresponding to L1 and L2 in Figure 3.24.

Comparing the flow resistance for region D1-R2 and G1-2-R1 it is seen that the relative resistance in the latter is considerably larger. The difference can be explained by the differences in the sand waves in the regions. In transect D1/1, the sand waves are long and generally with mild slopes and hence the flow resistance is dominated by skin friction contribution. The transects in G1-2-R1 (G1-2/2, G1-2/3 and G1-2/6) on the other hand, are covered with dunes and flow separation occurs which is not the case for D1-R1, hence the contribution from the form drag is larger.

The lack of flow separation also explains why the relative resistance is unaltered irrespective of the flow direction for D1-R1, whereas the flow separation is different depending on the flow direction over the transects in region G1-2-R1, thus the relative flow resistance becomes a function of the current direction. In the latter case it is the in-flow to the Baltic Sea which is subject to the largest flow resistance, which is also what appears to be the direction of propagation for those dune fields.

The test carried out with the higher bed roughness parameter for the skin friction, k_N=0.00125 m and k_N=0.025 m, instead of the roughness of k_N=5e-3, showed as expected a similar relative importance of the sand waves to the total flow resistance. Maps are supplied in Figure 7.5 and Figure 7.6 for the highest roughness, k_N=0.025 m.

Friction coefficients due to skin friction and form drag are presented in Table 7.1-Table 7.3 for each of the areas for each of the three values of the roughness parameter, respectively. The tables present the largest values of friction coefficients found for the three velocities which have been tested.

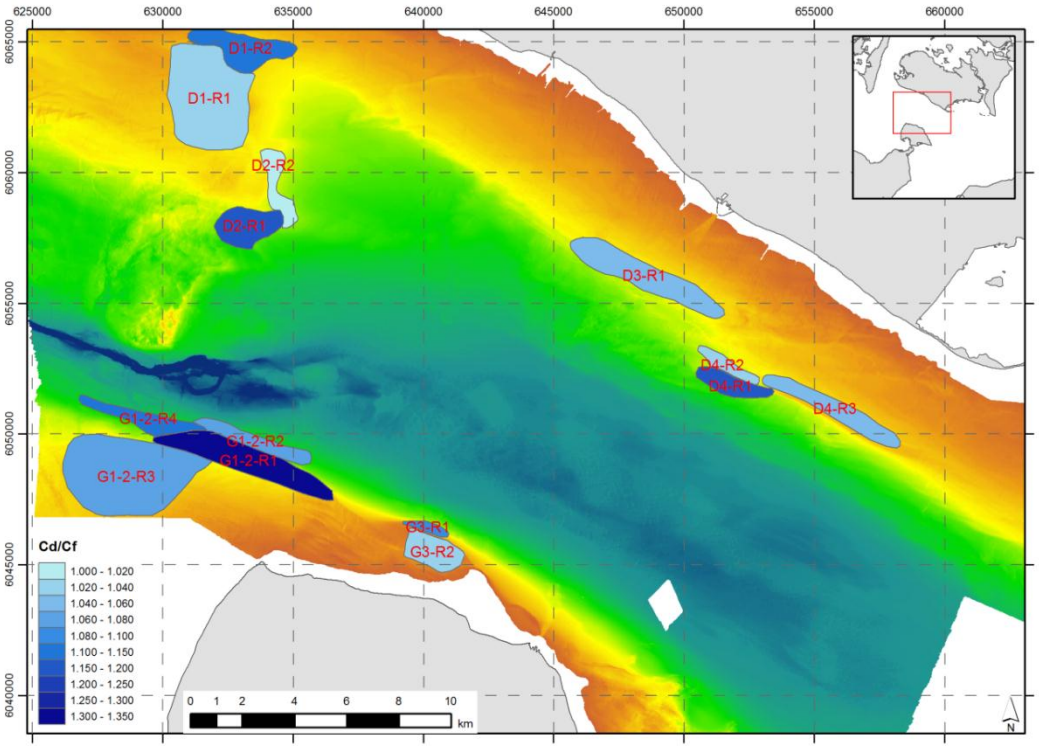

Figure 7.3 Map of Cd/Cf values for each sand wave field in case of inflow and for a bed roughness k_N of 0.5 mm

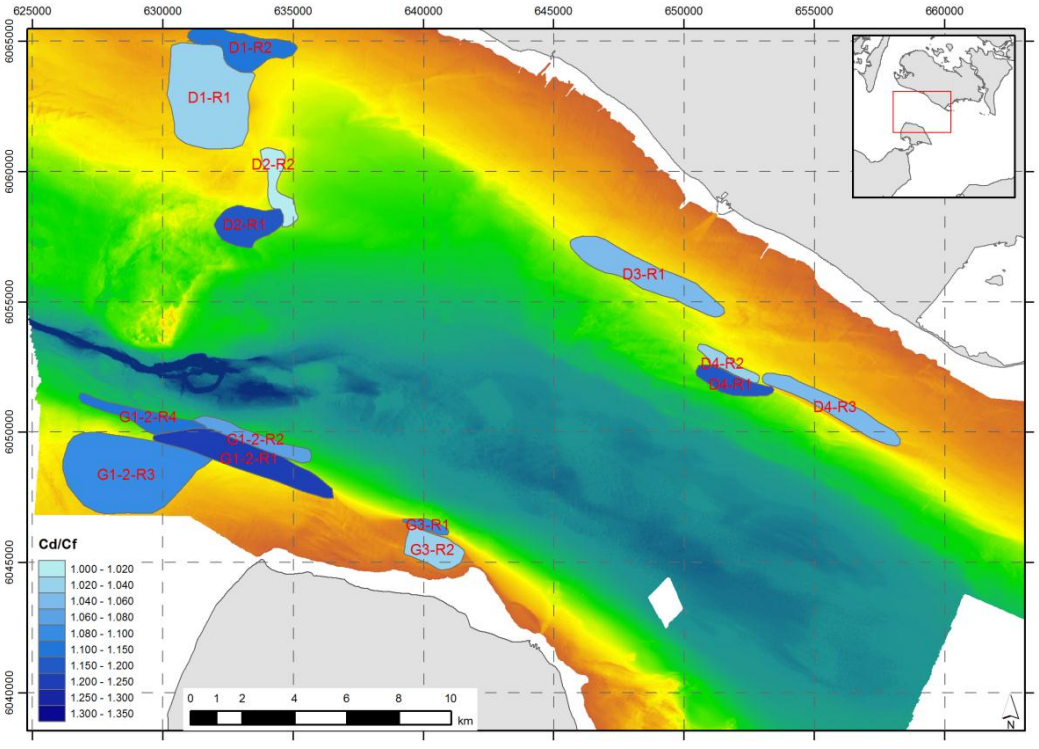

Figure 7.4 Map of Cd/Cf values for each sand wave field in case of outflow and for bed roughness of k_N=0.5 mm

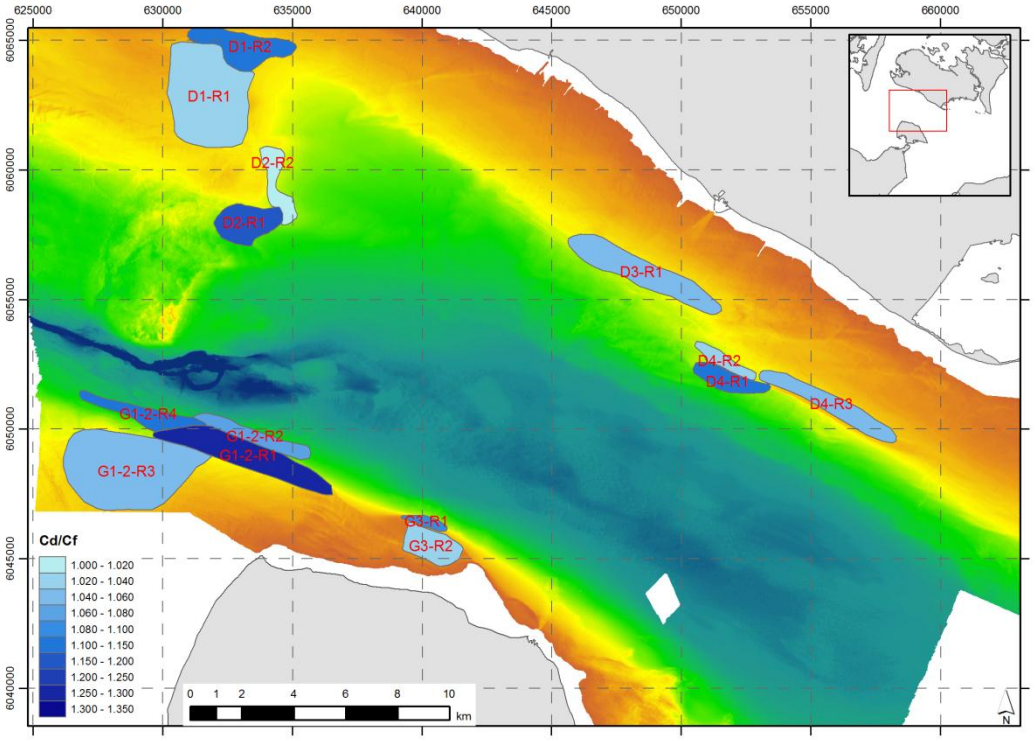

Figure 7.5 Map of Cd/Cf values for each sand wave field in case of inflow and for a grain diameter of 0.025 m

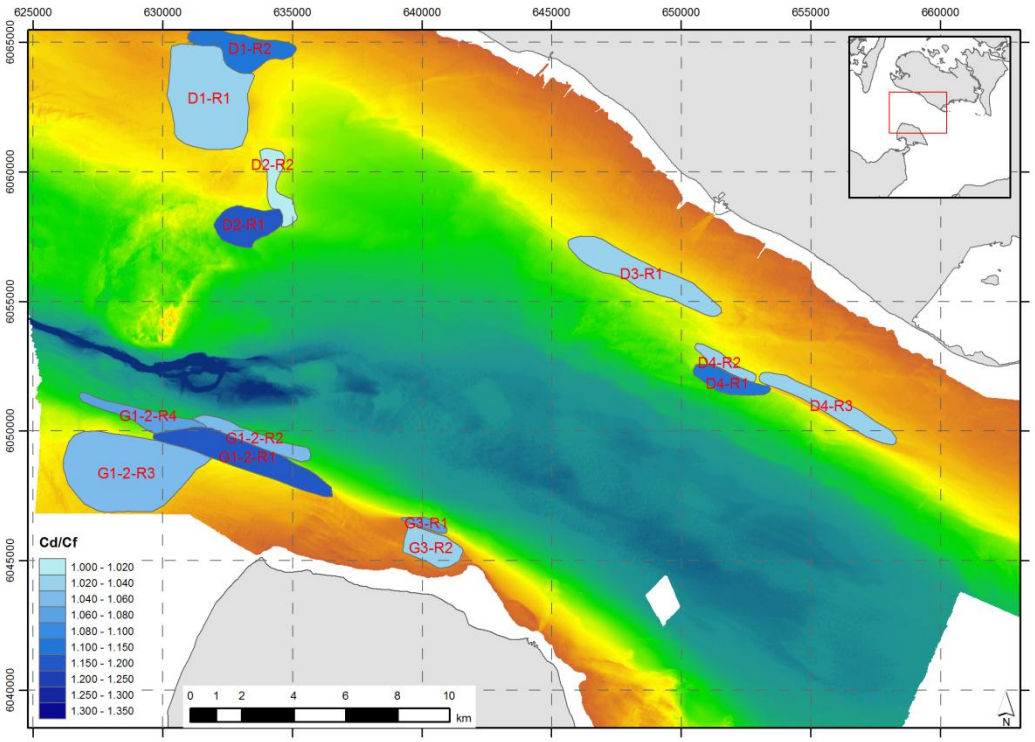

Figure 7.6 Map of Cd/Cf values for each sand wave field in case of outflow and for a grain diameter of 0.025 m

Table 7.1 The coefficients for skin friction and form drag and relative increase in total friction due to presence of bed forms. For a grain diameter of 0.2 mm

Area:	**Inflow:**				**Outflow**			
	Direction:	C_f	C_p	C_d/C_f	**Direction:**	C_f	C_p	C_d/C_f
D1-R2	170	0.00224	0.00028	1.13	350	0.00224	0.00027	1.13
D1-R1	170	0.00209	0.00006	1.03	350	0.00209	0.00005	1.03
D2-R1	85	0.00201	0.00037	1.19	265	0.00202	0.00037	1.19
D2-R2	90	0.00196	0.00003	1.01	270	0.00196	0.00003	1.01
D3-R1	180	0.00204	0.00009	1.05	0	0.00204	0.0001	1.05
D4-R2	120	0.00199	0.00005	1.02	300	0.00199	0.00005	1.02
D4-R1	120	0.00198	0.00036	1.19	300	0.002	0.00035	1.18
D4-R3	180	0.00204	0.00009	1.05	0	0.00204	0.0001	1.05
G1-2-R4	80	0.00186	0.00023	1.12	260	0.00191	0.0002	1.11
G1-2-R2	90	0.00188	0.00014	1.08	270	0.0019	0.00014	1.08
G1-2-R1	90	0.00214	0.00061	1.32	270	0.0022	0.00047	1.24
G1-2-R3	140	0.00204	0.00014	1.07	320	0.00204	0.00016	1.08
G3-R1	95	0.00212	0.0002	1.10	275	0.00214	0.0002	1.10
G3-R2	100	0.00229	0.00008	1.03	280	0.0023	0.00008	1.04

Table 7.2 The coefficients for skin friction and form drag and relative increase in total friction due to presence of bed forms. For a grain diameter of 0.5 mm

Area:	**Inflow:**				**Outflow**			
	Direction:	C_f	C_p	C_d/C_f	**Direction:**	C_f	C_p	C_d/C_f
D1-R2	170	0.00259	0.00034	1.13	350	0.00259	0.00033	1.13
D1-R1	170	0.0024	0.00006	1.03	350	0.0024	0.00006	1.03
D2-R1	85	0.00229	0.00042	1.19	265	0.00231	0.00041	1.18
D2-R2	90	0.00223	0.00003	1.01	270	0.00223	0.00003	1.01
D3-R1	180	0.00234	0.0001	1.04	0	0.00234	0.00011	1.05
D4-R2	120	0.00227	0.00005	1.02	300	0.00227	0.00005	1.02
D4-R1	120	0.00226	0.00039	1.17	300	0.00228	0.00038	1.17
D4-R3	180	0.00234	0.0001	1.04	0	0.00234	0.00011	1.05
G1-2-R4	80	0.0021	0.00026	1.13	260	0.00217	0.00022	1.10
G1-2-R2	90	0.00213	0.00016	1.07	270	0.00215	0.00015	1.07
G1-2-R1	90	0.00246	0.00069	1.32	270	0.00253	0.0005	1.22
G1-2-R3	140	0.00235	0.00015	1.07	320	0.00235	0.00017	1.08
G3-R1	95	0.00243	0.00023	1.09	275	0.00245	0.00022	1.09
G3-R2	100	0.00265	0.00009	1.04	280	0.00266	0.00009	1.04

Table 7.3 The coefficients for skin friction and form drag and relative increase in total friction due to presence of bed forms. For a grain diameter of 10.0 mm

Region Name:	**Inflow:**				**Outflow**			
	Direction:	C_f	C_p	C_d/C_f	**Direction:**	C_f	C_p	C_d/C_f
D1-R2	170	0.00498	0.00069	1.14	350	0.00498	0.00065	1.13
D1-R1	170	0.00458	0.00011	1.02	350	0.00458	0.0001	1.02
D2-R1	85	0.00421	0.00073	1.18	265	0.00425	0.00067	1.16
D2-R2	90	0.00415	0.00005	1.01	270	0.00415	0.00005	1.01
D3-R1	180	0.00441	0.00018	1.04	0	0.00441	0.00018	1.04
D4-R2	120	0.00423	0.00009	1.02	300	0.00424	0.00009	1.02
D4-R1	120	0.00421	0.0006	1.15	300	0.00424	0.00053	1.13
D4-R3	180	0.00441	0.00018	1.04	0	0.00441	0.00018	1.04
G1-2-R4	80	0.00379	0.00044	1.12	260	0.00394	0.00031	1.08
G1-2-R2	90	0.00388	0.00024	1.06	270	0.00393	0.00022	1.06
G1-2-R1	90	0.00462	0.00109	1.28	270	0.00475	0.00075	1.17
G1-2-R3	140	0.00446	0.0002	1.05	320	0.00446	0.00021	1.05
G3-R1	95	0.00461	0.00038	1.08	275	0.00467	0.00033	1.07
G3-R2	100	0.00525	0.00018	1.03	280	0.00526	0.00017	1.03

7.2 Flow Resistance in Areas with Lunate Bed Forms

The lunate bed forms, see Figure 6.40, in the deeper part of the Fehmarnbelt, are 3-dimensional by nature. Therefore a 3-dimensional flow model is adopted to estimate the flow resistance over the lunate bed forms.

In Figure 7.7 the contour of the lunate bed form is shown. The dimensions are based on an estimate of the typical dimensions of the individual bed forms and the typical distance between these. A current of 0.5 m/s is imposed in the direction shown in the Figure 7.7, i.e. 138 degrees true north.

Due to the limited steepness of the bed form, approximately 4/1000, the form drag is negligible compared to the shear stress and $C_d \approx C_f$. The simulation shows that the form drag merely contributes with 0.2% to the total flow resistance.

In Figure 7.8 the direction of the bed shear stress vector is shown, where all data for vectors in the interval 137.8°-138.2° true north have been removed to focus on shear stress vectors deviating from the mean current direction. The main features of this plot reveal that the near-bed flow is driven around the top of the lunate bed form, i.e. around the top located at (x, y) = (25 m, 25 m). However, the deviation from the current direction is seen to be small, less than 5 degrees.

Consequently, the flow resistance due the presence of lunate bed forms has been neglected.

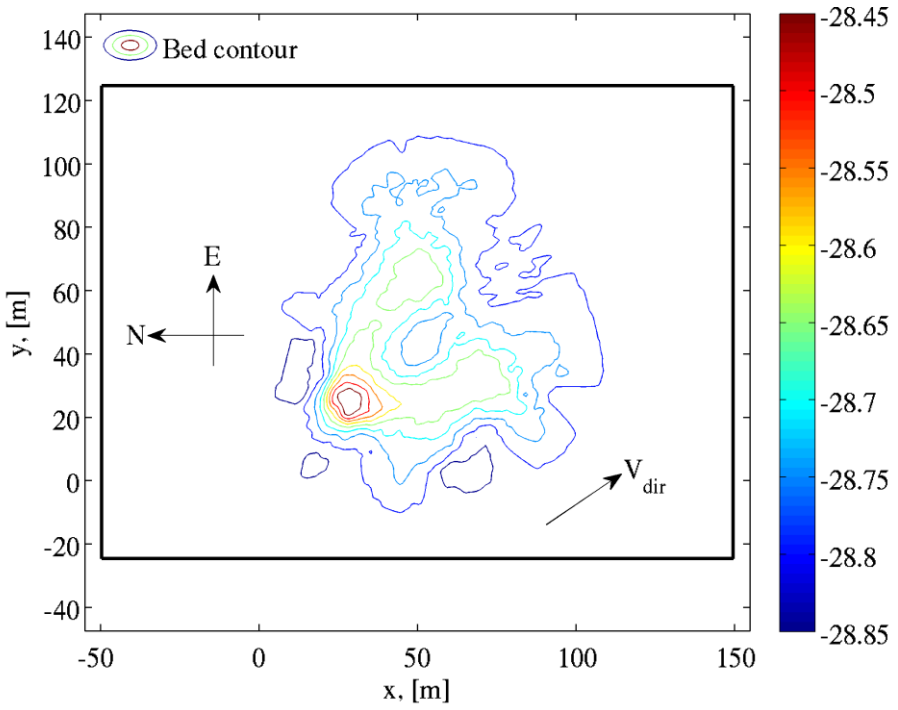

Figure 7.7 *The contour of the lunate shaped bed form. The domain is periodic in both the x- and y-directions. The domain boundaries are marked by a black box*

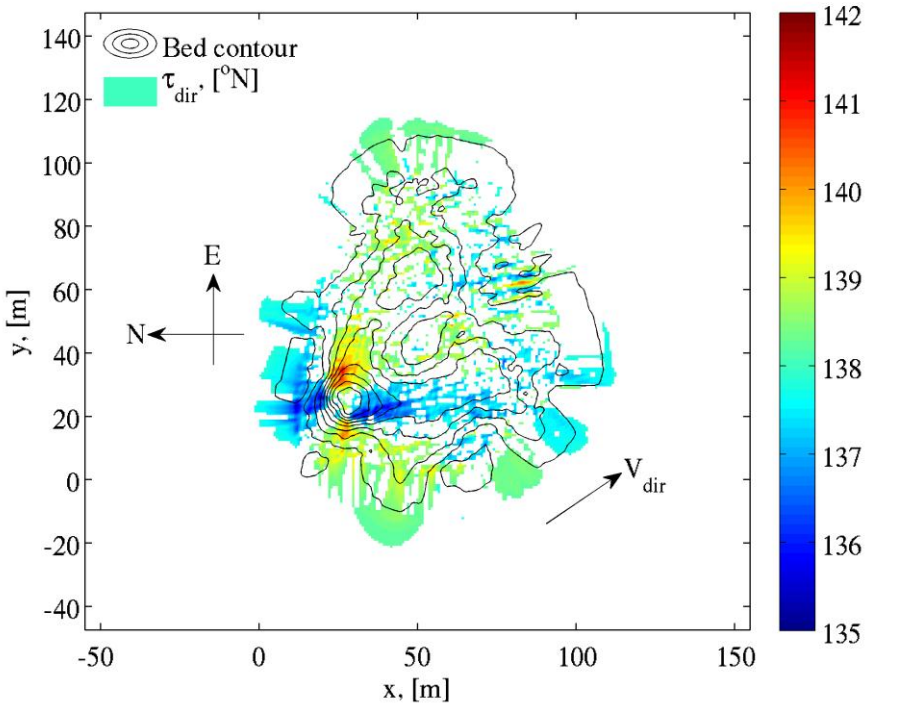

Figure 7.8 *The direction of the bed shear stress vector. The mean bed shear stress direction is 138 true north. Only directions smaller than 137.8° or larger than 138.2° are shown.*

7.3 Influence of the Bed Forms on the Overall Flow

In the following the hypothetical situation of no bed forms in the Fehmarnbelt is compared with the situation where the bed roughness is increased in the bed form areas of the Fehmarnbelt.

Results of the analysis of the influence of the bed forms are presented in the following:

- Regional influence: influence of the bed forms on the discharge through the Fehmarnbelt and the Øresund
- Local influence: redistribution of the discharge within the Fehmarnbelt caused by the bed forms

The analysis is carried out for two values of the global bottom roughness, $k_{a,g}$=0.05 mm and $k_{a,g}$=0.025 m (see Section 3.3.3). In the areas where sand waves have been identified the bottom roughness is increased to take into account the additional flow resistance from the sand waves.

The analysis leads to an estimate of the component of the flow which may be influenced in case of changes in the bed forms.

7.3.1 Regional influence: influence of the bed forms on the discharge through the Fehmarnbelt and Øresund

Due to the additional flow resistance from the sand waves, the discharge is found to be reduced for both inflow and outflow.

Figure 7.9 shows the correlation between the discharge through the Fehmarnbelt, Q, in the reference situation (without the influence of the sand waves, $k_{a,g}$=0.05 mm) and the change in the discharge, ΔQ, due to the sand waves. The discharges are evaluated across the transect between Rødbyhavn and Puttgarden Harbour. The discharges are defined as positive towards the Baltic Sea, and changes in the discharges are evaluated as:

$$\Delta Q = Q_{bed\ forms} - Q_{ref}$$

The reference discharges are evaluated without the influence of the bed forms in the simulations. It is seen that the decrease is larger for inflow than for outflow for the same magnitude of the discharge. A similar influence on the discharge is found for the larger bed roughness, $k_{a,g}$=0.025 m, in Figure 7.10.

The large influence from the sand waves on the inflow is mainly caused by the relatively large additional resistance which the sand waves in the south-eastern part of the Fehmarnbelt (area G1-2 – see Figure 6.29) impose on the flow. Additionally, the flow velocities are high in the German part of the Belt during inflow, which in combination with the high flow resistance factors from the sand waves in this area reduces the inflow to the Fehmarnbelt.

During outflow, the flow is more evenly distributed across the Fehmarnbelt transect. The sand wave areas with the largest flow resistance factors are located in the downstream part of the Fehmarnbelt, where the flow diverges around the island of Fehmarn reducing the flow speeds and hence the influence of the sand waves on the flow. The sand wave areas located near the tunnel alignment have smaller flow resistance factors.

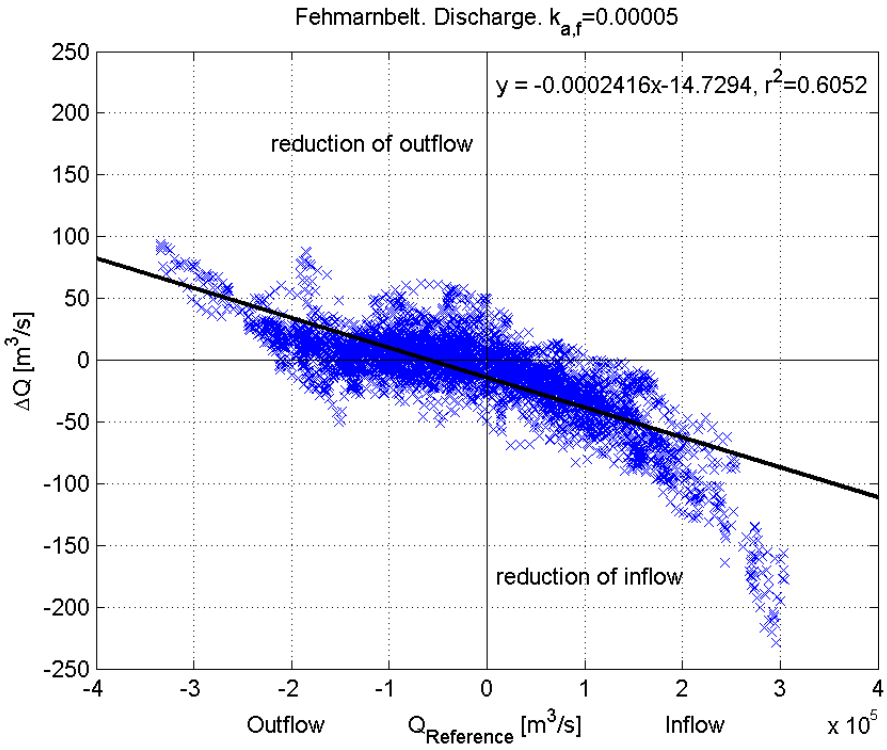

Figure 7.9 *Instantaneous discharge through the Fehmarnbelt ($Q_{Referemce}$, ΔQ) in case of a bottom roughness of $k_{a,g}$=0.05 mm. There is a marker for every 30 minutes throughout three months. 1/8-1/11 2009. $\Delta Q = Q_{bed\ forms} - Q_{ref}$*

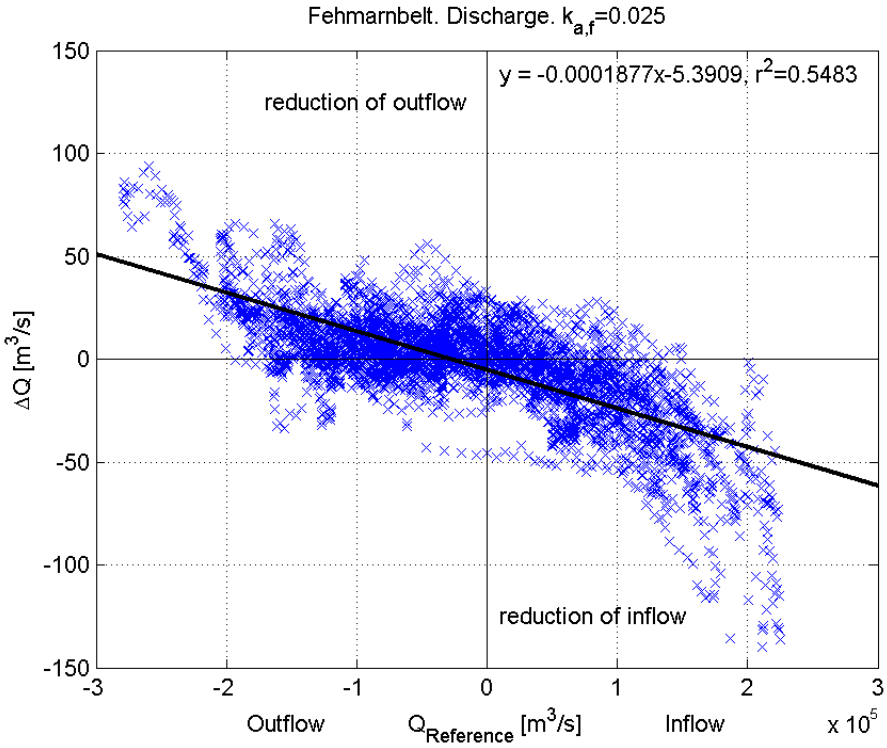

Figure 7.10 *Instantaneous discharge through the Fehmarnbelt ($Q_{Reference}$, ΔQ) in case of a bottom roughness of $k_{a,g}$=0.025 m. There is a marker for every 30 minutes throughout three months. 1/8-1/11 2009. $\Delta Q = Q_{bed\ forms} - Q_{ref}$.*

The difference between the influence of the sand wave areas in the inflow and outflow situation can also (to a minor extent) be explained by the larger form drag coefficients for inflow than for outflow, see Table 7.1-Table 7.3.

The relative importance of the form drag from the sand waves compared with the total flow resistance is higher in case of the small global bed roughness of 0.05 mm than for the larger bottom roughness of 0.025 m, and this explains the relatively larger reduction in the inflow for the smaller bottom roughness.

The accumulated discharge through the Fehmarnbelt in the simulation period, 1/7-1/11-2009, across the transect between Rødbyhavn and Puttgarden Harbour showed the following:

- The inflow discharge to the Baltic Sea through the Fehmarnbelt is reduced by approximately 0.3-0.4‰ of the total inflow in the simulation period.
- The outflow discharge is reduced by approximately 0.1‰ of the total outflow in the simulation period.

Details are summarised in Table 7.4 and Table 7.5 for the simulations with the small bottom roughness ($k_{a,g}$=0.05 mm) and the high bottom roughness ($k_{a,g}$=0.025 m), respectively.

By only considering the net discharges the sand waves have a relatively larger impact. Between 1 August and 1 November there is a net discharge of $133 \cdot 10^9\, m^3$ out of the Fehmarnbelt in case of the global bottom roughness of 0.05 mm. Due to the larger decrease in discharge through the Fehmarnbelt into the Baltic Sea than out, there is a net increase of discharge through the Fehmarnbelt of approximately $79 \cdot 10^6\, m^3$. This corresponds to an 0.6‰ increase compared to the net discharge.

Table 7.4 Influence from the bed forms to the accumulated discharges (inflow and outflow situations separately) in the simulation period through the Fehmarnbelt. Global bottom roughness $k_{a,g}$=0.05 mm. Simulation period: 01.08.2009-01.11.2009

Fehmarnbelt	Accum. discharge, Q [km^3]	Decrease [km^3]	Decrease [‰]
Inflow	+304.866	-0.116	-0.380
Outflow	-437.986	+0.037	+0.085

Table 7.5 Influence from the bed forms to the accumulated discharges (inflow and outflow situations separately) in the simulation period through the Fehmarnbelt. Global bottom roughness $k_{a,g}$=0.025 m. Simulation period: 01.08.2009-01.11.2009

Fehmarnbelt	Accum. discharge, Q [km^3]	Decrease [km^3]	Decrease [‰]
Inflow	+166.839	-0.046	-0.278
Outflow	-277.975	+0.027	+0.099

The simulations indicate that the increase in the net outflow through the Fehmarnbelt caused by the sand waves is to some degree compensated through the Øresund.

Table 7.6 and Table 7.7 show how an increased net outflow from the Baltic through the Fehmarnbelt is compensated by an increase of the inflow through the Øresund and a reduction in the outflow.

The net increase of discharge to the Baltic through the Øresund is about $14 \cdot 10^6\ m^3$ compared to the net increase in the outflow through the Fehmarnbelt from the Baltic Sea of $79 \cdot 10^6\ m^3$. The compensation through the Øresund is hence about 18%.

Note: in this analysis the effect of bed forms has been included as an *additional* roughness. This is the reason why the simulations lead to a slight change in the overall net (out-)flow from the Baltic Sea through Fehmarnbelt and Øresund. In case simulations had shown significant redistribution of flow due to spatial variations in roughness a more advanced comparison of results from modelling with and without spatial variations but with the same overall resistance would have been relevant.

Table 7.6 Influence from the bed forms in the Fehmarnbelt to the discharge through the Øresund (inflow and outflow situations separately). Bottom roughness $k_{a,g}$=0.00005 m. Simulation period: 01.08.2009-01.11.2009

Øresund	Accum. discharge, Q [km3]	Decrease/Increase [km3]	Decrease/Increase [‰]
Inflow	140.341	+0.009 (increase)	+0.063
Outflow	-213.951	-0.005 (decrease)	-0.026

Table 7.7 Influence from the bed forms in the Fehmarnbelt to the discharge through the Øresund (inflow and outflow situations separately). Bottom roughness $k_{a,g}$=0.025 m. Simulation period: 01.08.2009-01.11.2009

Øresund	Accum. discharge, Q [km^3]	Decrease/Increase [km^3]	Decrease/Increase [‰]
Inflow	118.356	+0.005 (increase)	0.046
Outflow	179.331	-0.004 (decrease)	0.025

7.3.2 Local influence: redistribution of the discharge within the Fehmarnbelt caused by the bed forms

The change in the flow distribution along five transects, see Figure 7.11, due to the bed forms is calculated. Furthermore, the redistribution of the flow across the depth is determined for two of the five transects. As shown in the previous sections, the sand waves have larger influence on the discharge in case of the smaller global bottom roughness of 0.05 mm and this roughness is hence selected in the analysis below.

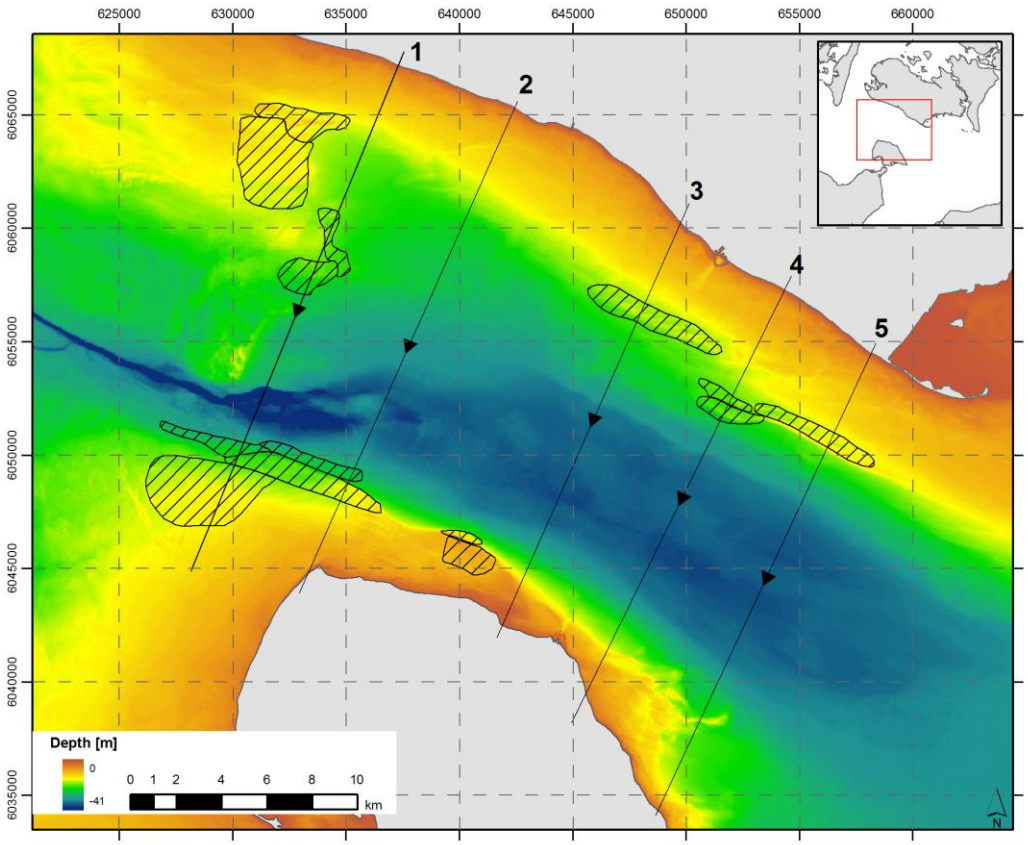

Figure 7.11 Model Bathymetry with areas of sand waves and discharge lines

Figure 7.12 and Figure 7.13 show the change in the depth integrated discharge due to the bed forms through the five transects for accumulated inflow and outflow situations, respectively. An 'inflow situation' is defined as a time step, where the integrated discharge across the Fehmarnbelt is directed towards the Baltic Sea and an 'outflow situation' vice versa.

In case of inflow, a decrease in flow is seen on the German side (Figure 7.12). This is due to the large, in both size and additional resistance, sand wave fields in the south-eastern Fehmarnbelt (G1-2) and to a smaller degree the sand wave field 4-5 km west of the alignment area (G3). The decrease is largest across transect 2 as the flow has passed almost the entire fields. The decrease in the flow is less powerful further west. The decrease in flow on the German side can be seen as a redistribution of the flow resulting in an increase on the Danish side. However, the decrease on the German side of the belt is larger than the increase towards the Danish side and causes a total reduction of the inflow to the Baltic as shown in the previous section.

In case of outflow (Figure 7.13), the sand waves cause a (smaller) reduction in the outflow on the Danish side due to the increased flow resistance from the sand wave fields near the alignment on the Danish side (D3, D4). This is compensated by an increase in the flow in the German part of the Fehmarnbelt.

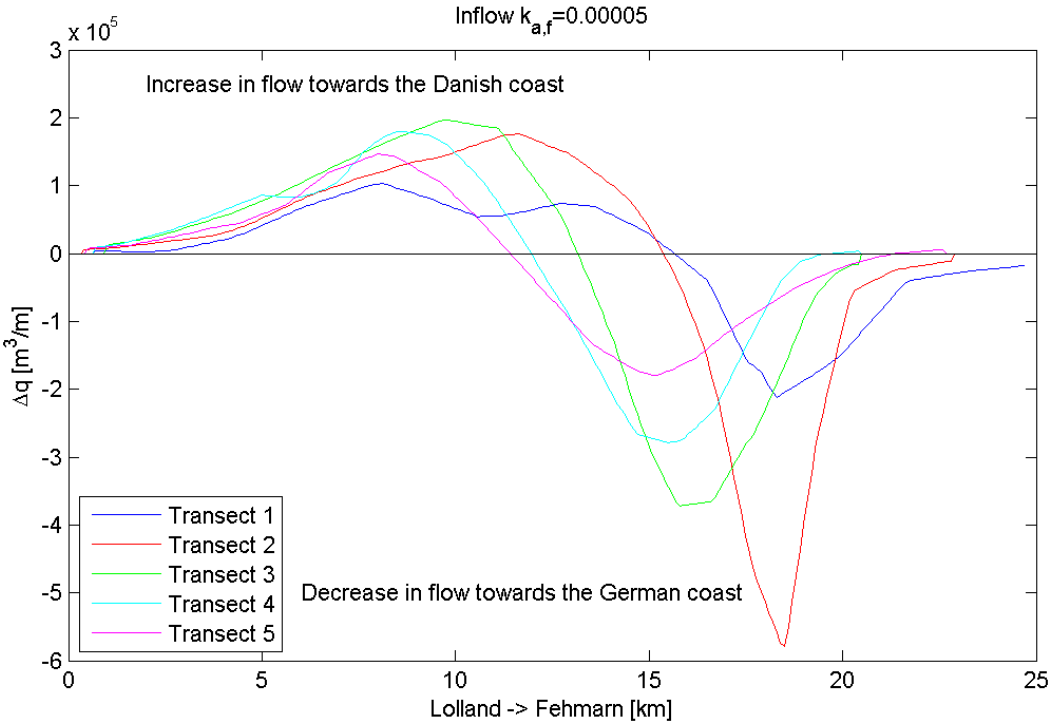

Figure 7.12 Change in depth-integrated accumulated discharge for inflow situations for five transects across the Fehmarnbelt in the period 1/7-1/10-2009. $\Delta q = |q_{bed\ forms}| - |q_{ref}|$

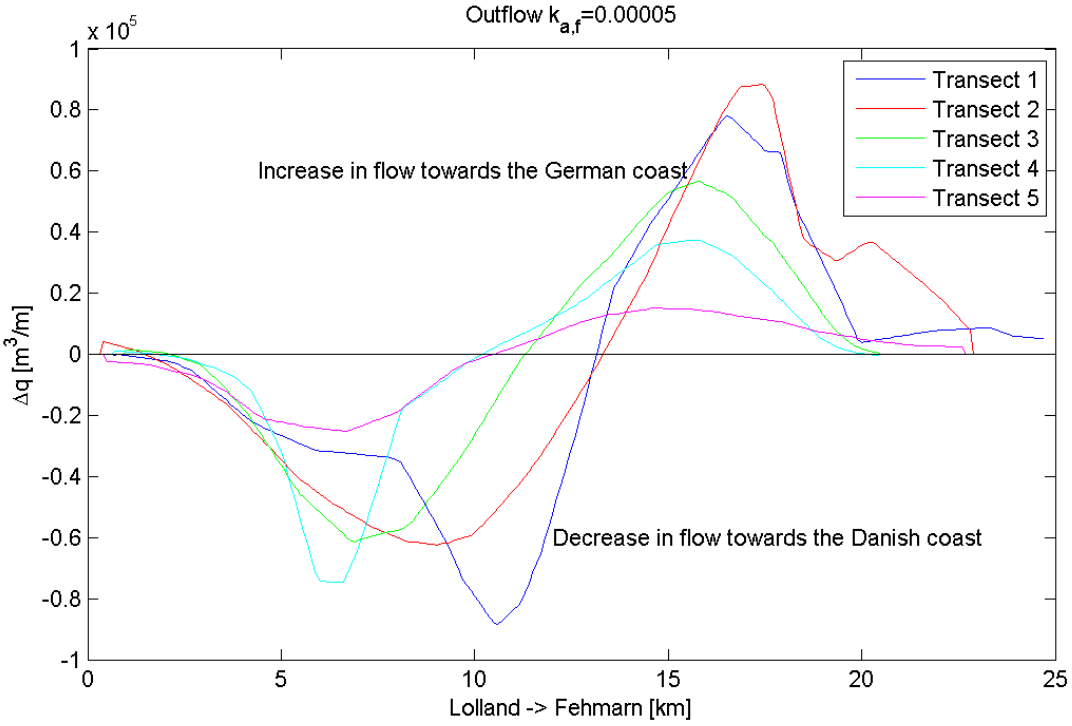

Figure 7.13 Change in depth-integrated accumulated discharge for outflow situations for five transects across the Fehmarnbelt in the period 1/7-1/10-2009. $\Delta q = |q_{bed\ forms}| - |q_{ref}|$

A different way of illustrating the changed flow field due to the additional flow resistance from the bed forms is by looking at the change in the current speeds across the Fehmarnbelt. Figure 7.14 and Figure 7.15 show the averaged current speeds for transect 2 in the western part of the Fehmarnbelt in case of flow situations in and out of the Baltic Sea, respectively.

Maximum averaged current speeds at the surface are up to 0.5 m/s. On the Danish side of the Fehmarnbelt downstream of transect 2 there is a large area with water depths less than 10 m. From the Danish shoreline this area extends approximately 8 km into the Belt and deflects the flow towards the German side during inflow situations. The high velocities are therefore concentrated on the German half of the Belt and the bottom velocities are low on the Danish side. In case of outflow, the near-bed velocities are approximately the same across the entire transect.

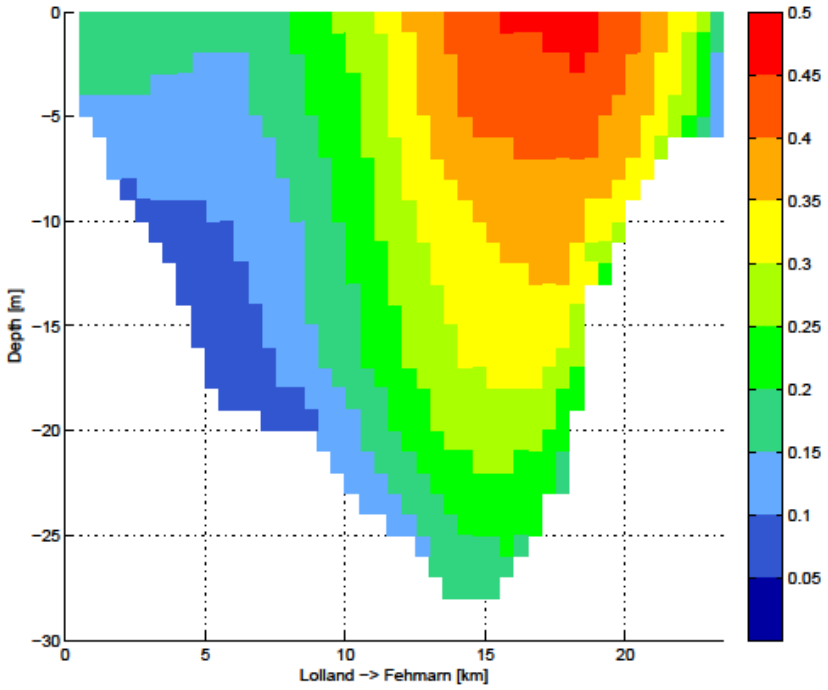

Figure 7.14 Transect 2: averaged current speeds, in m/s during inflow situations to the Baltic Sea. Extracted from Lolland to Fehmarn. Reference situation without sand waves

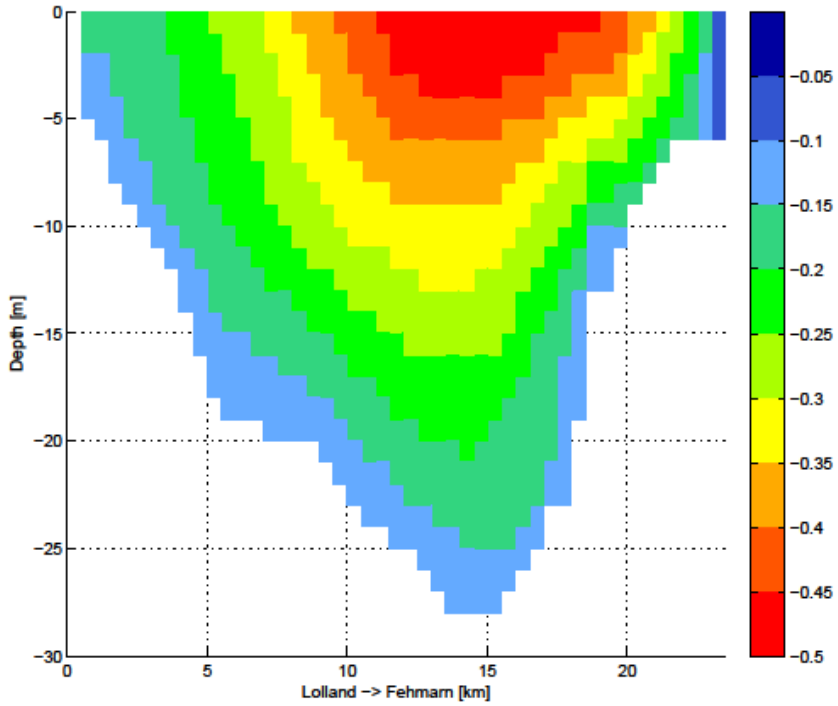

Figure 7.15 Transect 2: averaged current speeds, in m/s during outflow situations to the Baltic Sea. Extracted from Lolland to Fehmarn. Reference situation without sand waves

Figure 7.16 and Figure 7.17 show the difference in the time averaged flow between a simulation with sand waves and a simulation without sand waves for inflow and outflow, respectively. In case of inflow, the flow passes (upstream of transect 2) sand wave fields on both the German side and the Danish side of the Fehmarnbelt. However, the sand wave fields on the German side are superior in both sizes as well as in additional resistance, and the flow velocities are higher towards the German side. Furthermore, transect 2 is located across the western end of the sand wave fields on the German side while the sand waves on the Danish side are located further downstream of transect 2. This results in a redistribution of the flow, i.e. a decrease on the German side and an increase on the Danish side. The redistribution influences the entire water column and is not only limited to a certain height above the sand waves. The decrease is largest just above the sand waves and the local maximum decrease is in the order of 1 cm/s. This corresponds to a local decrease of 3-4% in the flow speed. The increase is more equally distributed than the decrease. The maximum local increase is less than half the maximum local decrease.

In case of outflow, the redistribution of the flow is opposite the one for inflow. In this case the dominating sand wave fields (upstream) are located on the Danish side of the Fehmarnbelt. This results in a decrease in the flow on the Danish side and a decrease on the German side. However, as transect 2 is across the German sand wave field, G1-2, there is a local decrease of about 0.1-0.2 cm/s just above the sand waves. In general, the redistribution of the flow is far less in case of outflow compared to inflow across transect 2.

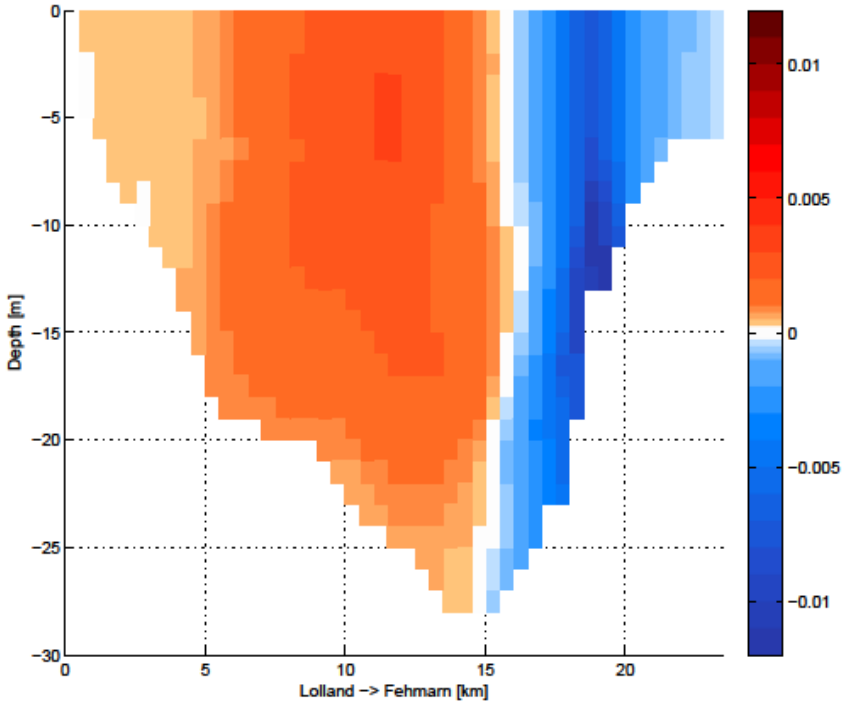

Figure 7.16 Transect 2: difference in average current speeds $\Delta CS = |CS_{bed\ forms}| - |CS_{ref}|$ for inflow situations (in m/s) to the Baltic Sea. Negative values/blue colours correspond to a decrease in the current speed and positive values/red colours correspond to an increase in the current speed

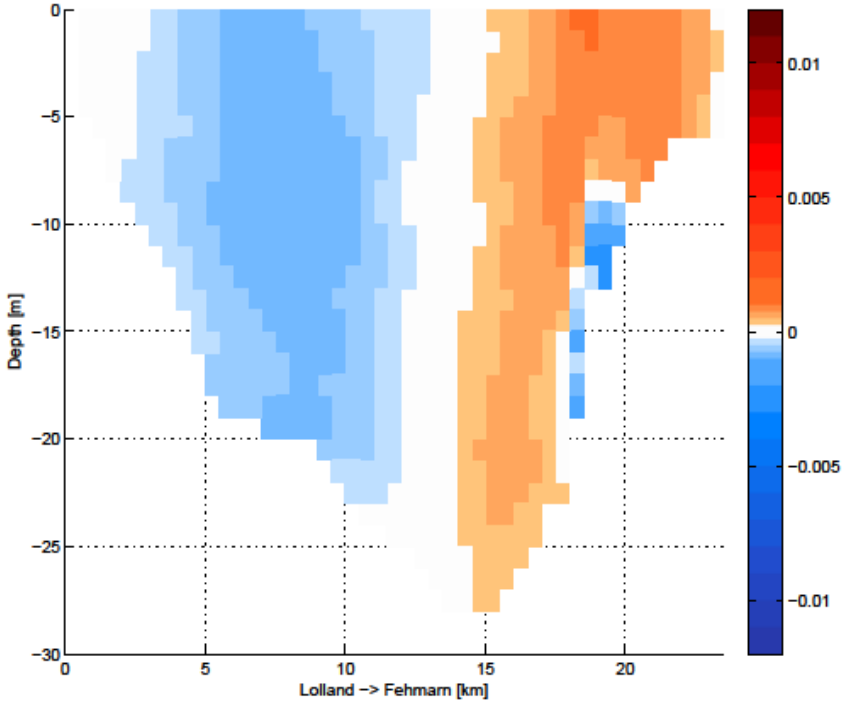

Figure 7.17 Transect 2: difference in average current speeds $\Delta CS = |CS_{bed\ forms}| - |CS_{ref}|$ for outflow situations (in m/s) from the Baltic Sea. Negative values/blue colours correspond to a decrease in the current speed and positive values/red colours correspond to an increase in the current speed

For transect 4 located between Rødby and Puttgarden Harbours, the averaged flow speeds are shown in Figure 7.18 (inflow situations) and Figure 7.19 (outflow situations), and the change in the current speeds imposed by the bed forms is shown in Figure 7.20 (inflow) and Figure 7.21 (outflow). In case of inflow the German side of the Fehmarnbelt is also exposed to a decrease in the current speeds due to the up-stream sand wave fields, but not as pronounced as in transect 2, however. The influence of the G1-2 sand wave field is causing higher flow velocities in transect 4 towards the Danish side; however, a local decrease in flow velocities is seen in the current speeds near the bed above the sand wave field on the Danish side.

In case of outflow only the influence from the sand wave fields on the Danish side can be recognized as a decrease in the flow speeds towards the Danish side and an increase towards the German side.

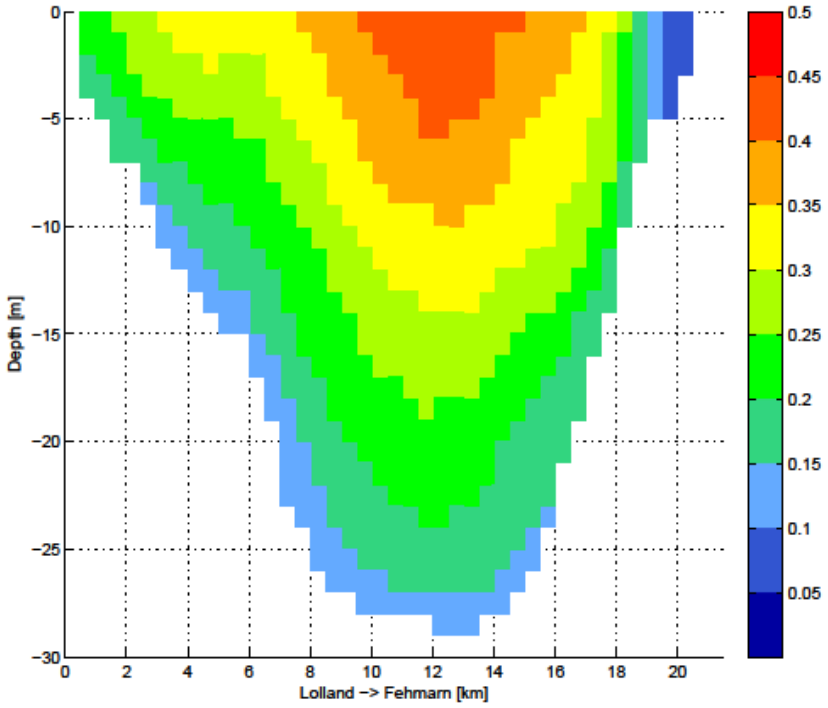

Figure 7.18 Transect 4: averaged current speeds, CS (in m/s) during inflow situations to the Baltic Sea. Extracted from Lolland to Fehmarn. Reference situation without sand waves

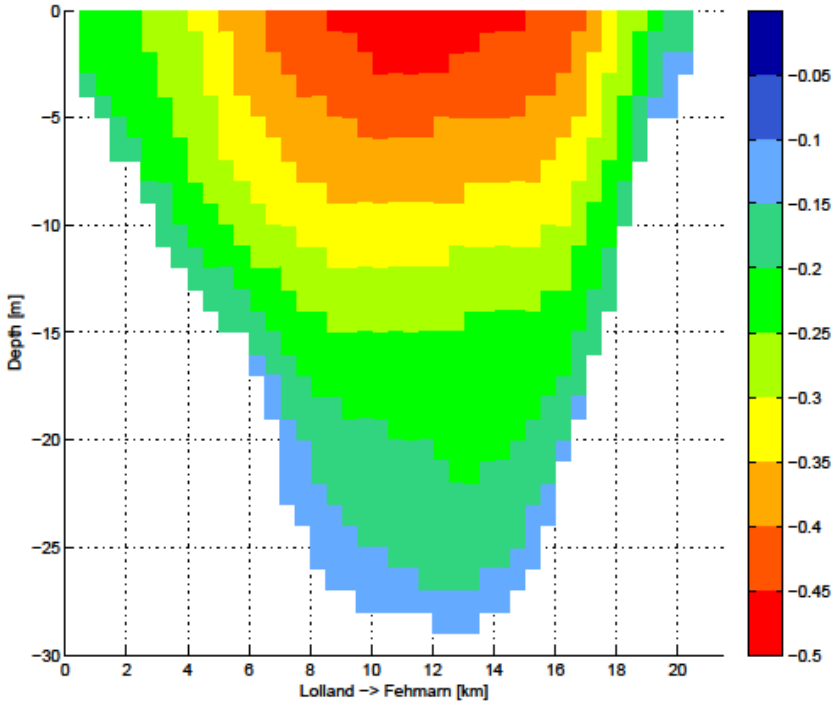

Figure 7.19 Transect 4: averaged current speeds, CS (in m/s) during outflow situations from the Baltic Sea. Extracted from Lolland to Fehmarn. Reference situation without sand waves

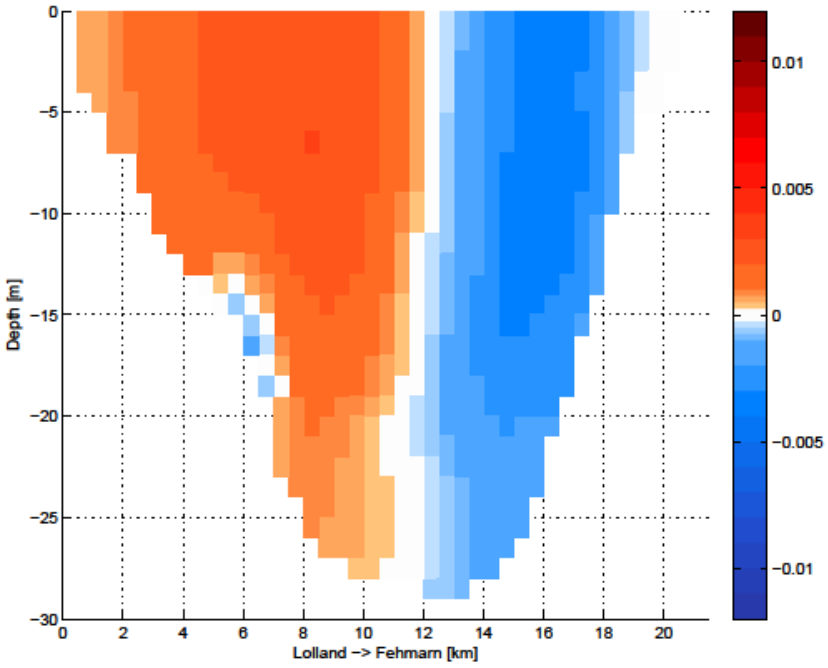

Figure 7.20 Transect 4: difference in average current speeds $\Delta CS = |CS_{bed\ forms}| - |CS_{ref}|$ for inflow situations (in m/s) to the Baltic Sea. Negative values/blue colours correspond to a decrease in the current speed and positive values/red colours correspond to an increase in the current speed

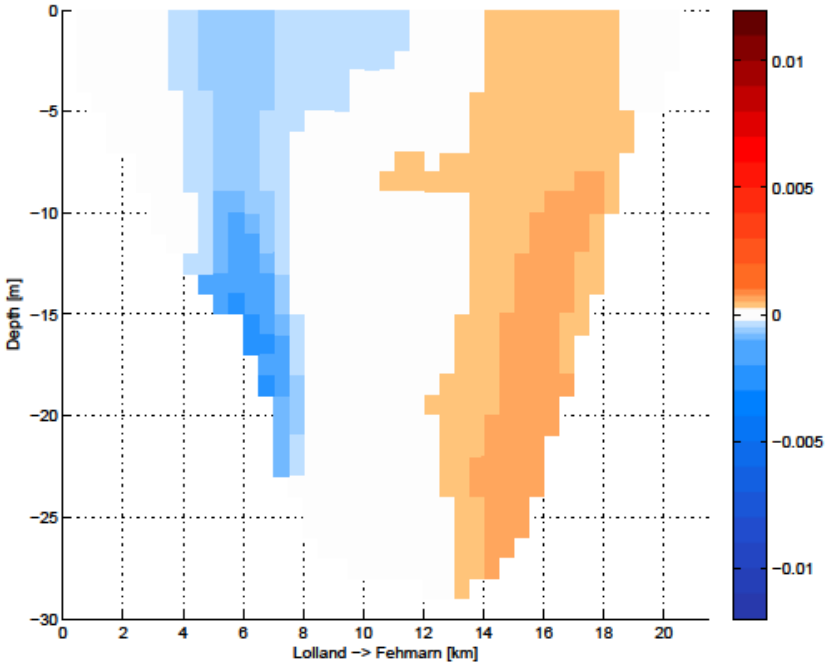

Figure 7.21 Transect 4: difference in average current speeds $\Delta CS = |CS_{bed\ forms}| - |CS_{ref}|$ for outflow situations (in m/s) from the Baltic Sea. Negative values/blue colours correspond to a decrease in the current speed and positive values/red colours correspond to an increase in the current speed

8 *PRESENT PRESSURES*

Sand mining and disposal of dredged material are the only present pressures on the sea bed forms. Mining of sea bed material takes place from two of the sand wave fields on the Danish side with permission from the Ministry of Environment, Agency for Spatial and Environmental Planning (in Danish: Naturstyrelsen). Disposal of material dredged in Rødby and Gedser Harbours takes place within an area west-south west of Rødbyhavn. This site is located at the boundary of one of the sand wave fields on the Danish side. The two sand mining areas and the disposal site are shown in Figure 8.1.

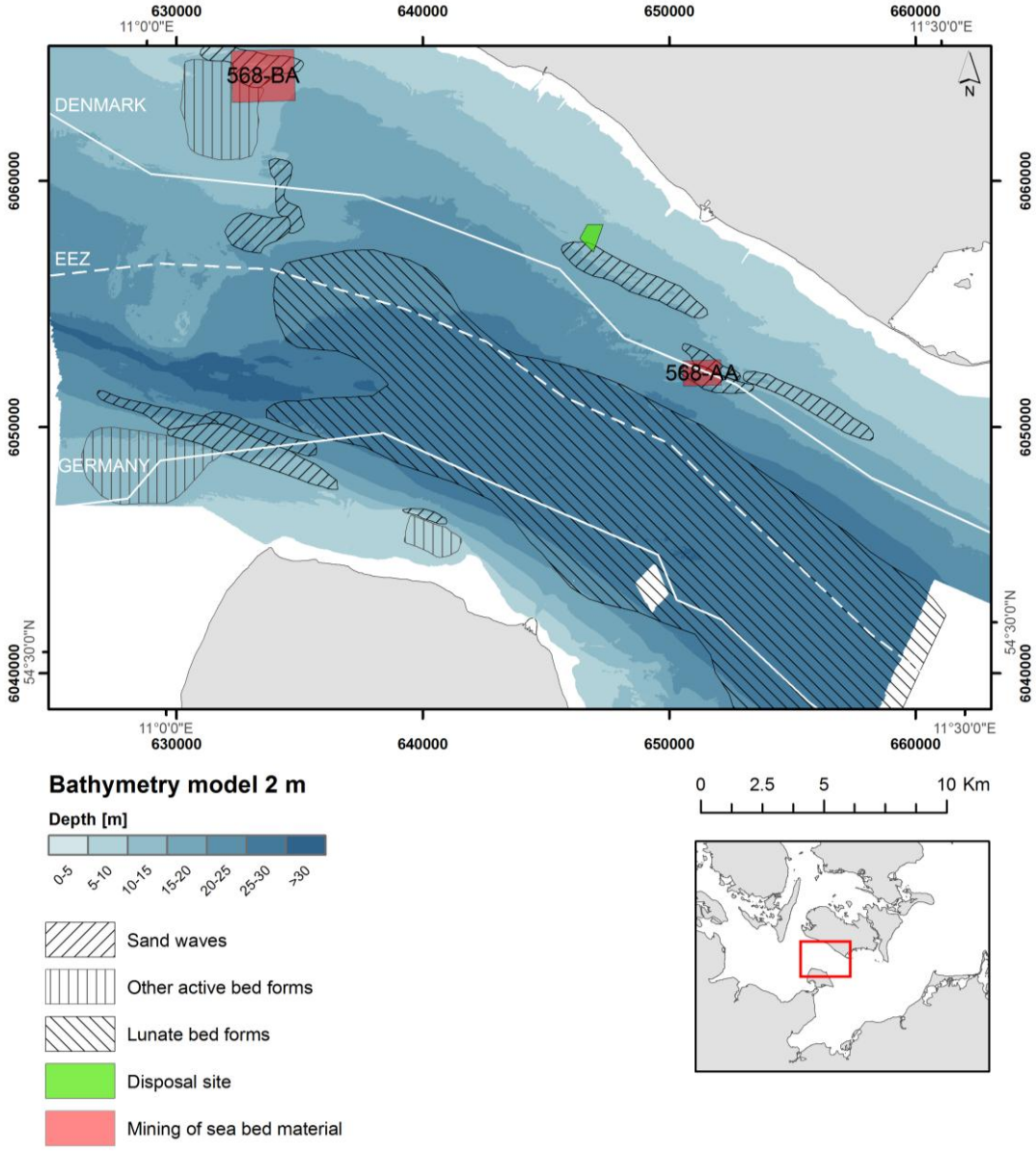

Figure 8.1 Areas with permission for mining of sea bed material and disposal site. Information from Ministry of Environment, Agency for Spatial and Environmental Planning

Sand mining within area D1

Volumes of sea bed material extracted from the sand waves in area D1, see Figure 6.2, are listed in Table 8.1. The last large-scale extraction from the area was in 2006 with an extraction of 93,000 m^3. Extraction of the sea bed material is clearly seen in the multibeam survey as irregular patterns in the top of some of the large sand waves, Figure 8.2. The multi beam survey was performed in 2009, i.e. three years after the extraction in 2006. The magnitude of the extraction is relatively small compared with the size of the individual bed forms. The sand waves therefore still persist more or less in their natural shape, although deep holes of several metres have been cut into parts of them extending over their full height. The bed forms are expected to regenerate naturally with time. However, due to relative low sediment transport rates in the area the bed forms have not recovered much over the three years 2006-2009.

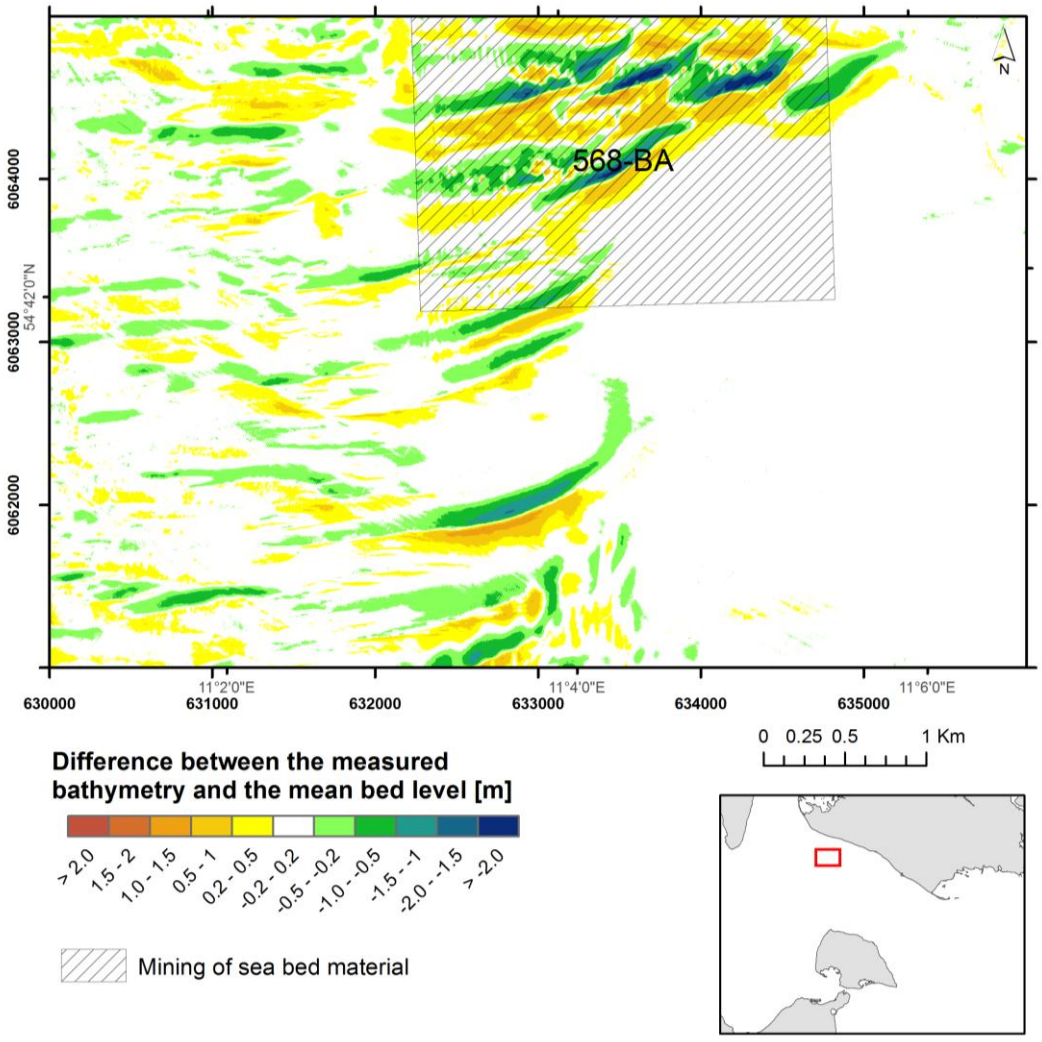

Figure 8.2 *Mining of sea bed material from sand waves in area D1 is clearly seen in the difference plot. Difference between the measured bathymetry and the mean bed level. The mean bed level is defined as the average bathymetry within a radius of 200 m. Analysis of multibeam echo sounder data (2009)*

Table 8.1 Volumes of sea bed material extracted from Mining area 568-BA in the period 1997-2009. Data from Ministry of Environment, Agency for Spatial and Environmental Planning

	Mining area 568-B/568-BA				
	Sand (0-4 mm) [m³]	**Gravel (0-20 mm) [m³]**	**Stones (6-300 mm) [m³]**	**Fill [m³]**	**Others [m³]**
1997	150	1260	0	4880	0
1998	150	0	0	0	0
1999	100547	3940	10	30515	0
2000	2395	0	1920	0	0
2001	41182	230	0	548	0
2002					7974
2003	0	7130	0	1815	0
2004	1000	340	0	1080	0
2005	4670	340		1020	
2006	330			93270	
2007	0	0	0	0	
2008					
2009	0	340	0	0	

Sand mining within area D4

Volumes of sea bed material extracted from the sand waves in area D4, see Figure 6.2, are listed in Table 8.2. The last extraction from the area was in 2006 with an extraction of 30000 m^3 and before that the last major extraction was in 1999 with 98000 m^3. Extraction of the sea bed material is clearly seen in the multi beam survey as areas within the sand wave field, where the sand waves are more or less eliminated, see Figure 8.3. The disturbance of the sand waves is also seen in cross section D4-4, see Figure 6.28. The multi beam survey was performed in 2009, i.e. three years after the last extraction in 2006. The bed forms are expected to regenerate naturally with time due to the dynamic nature of the bed forms. In this case, the extraction area is large compared to the individual sand waves. The bed forms have obviously not recovered fully during the three years 2006-2009, but signs of recovery can be found in the area as regular patterns of troughs and tops with a smaller length scale than the natural ones identified in the extraction area. This agrees with the estimates of the sediment mobility in the area (in the order of 10 m^3/m/year in each direction, ref. Chapter 5). A migration of several times the length of the full size sand waves is expected for a full recovery Niemann et al (2003). With the estimated sediment mobility and the size of the sand waves, this may take in the order of 10 years or more in this area.

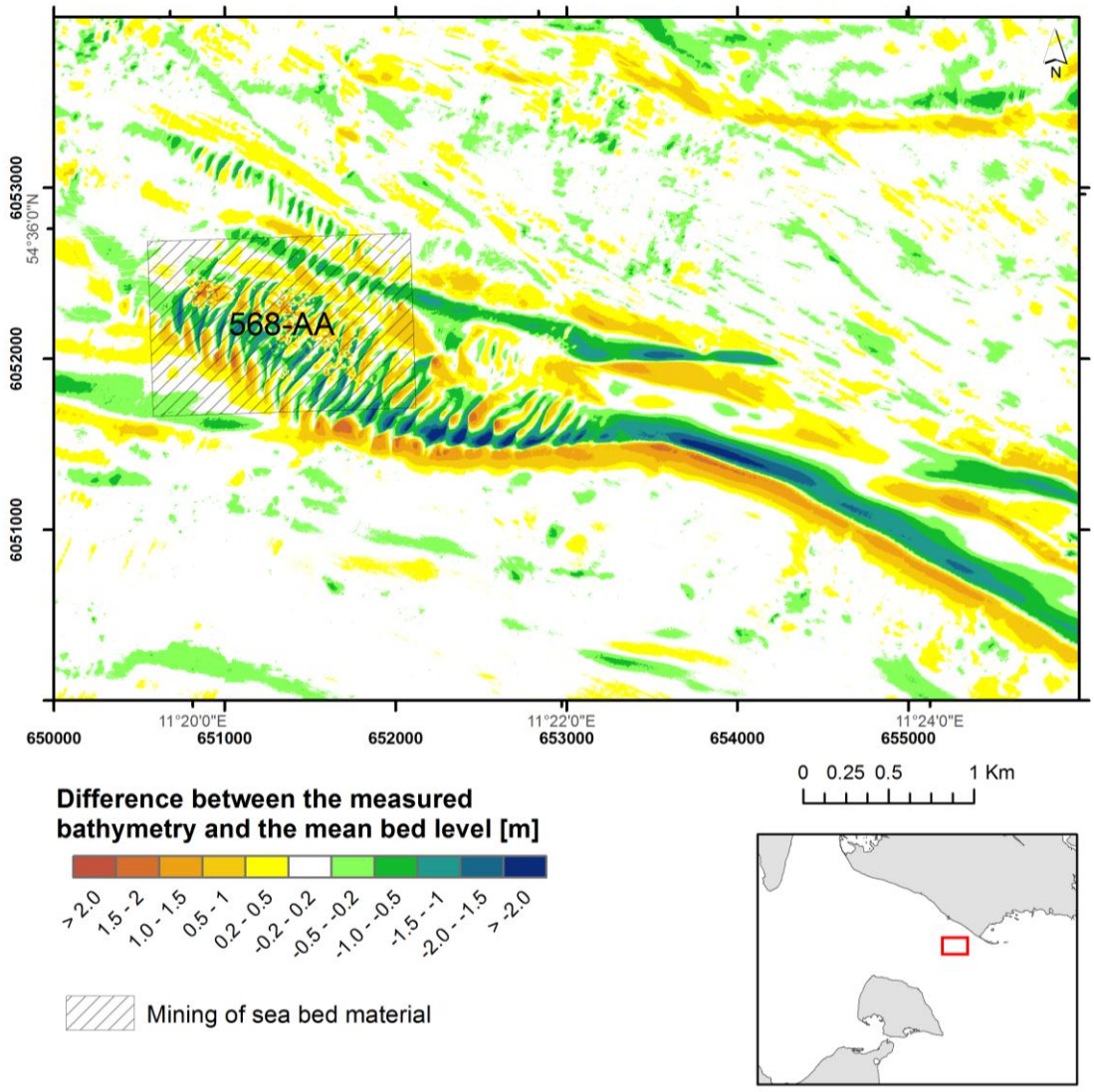

Figure 8.3 *Difference between the measured bathymetry and the mean bed level. The mean bed level is defined as the average bathymetry within a radius of 200 m. Analysis of multibeam echo sounder data (2009)*

Table 8.2 *Volumes of sea bed material extracted from Mining area 568-AA in the period 1997-2009. Data from Ministry of Environment, Agency for Spatial and Environmental Planning.*

	Mining area 568-A				
	Sand (0-4 mm) [m³]	**Gravel (0-20 mm) [m³]**	**Stones (6-300 mm) [m³]**	**Fill [m³]**	**Others [m³]**
1997	300	0	0	0	0
1998	0	0	3965	0	0
1999	0	0	0	98234	0
2000					
2001	821	2530	0	0	0
2002					
2003	0	0	0	4405	0
2004	3285	0	0	0	0
2006					30166
2007	0	0	0	0	0

Disposal of sediment at the boarder of area D3

A disposal site is located at the boundary of sand wave area D3, see Figure 6.2. The disposal site is not expected to have any impact on the sand waves.

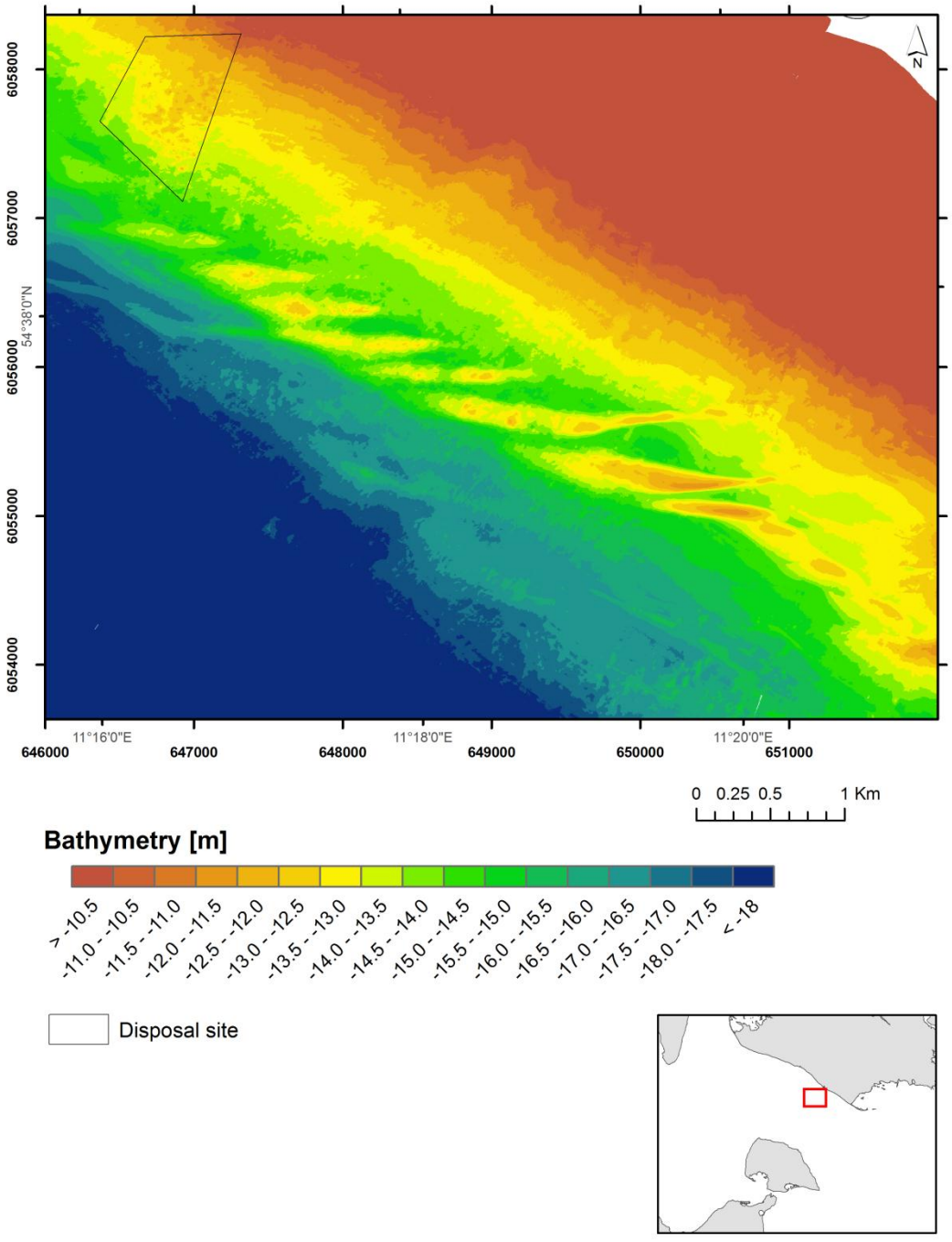

Figure 8.4 Disposal site west of Rødbyhavn located near the sand waves in area D3

9 ASSESSMENT OF IMPORTANCE

Sea bed forms are active morphological elements on the sea bed outside of the nearshore zone. The sea bed forms are the result of interaction between loose sediments on the sea bed and the flow above the sea bed. Bed forms only exist where the currents are strong enough to move the sediment. The sea bed vegetation is therefore sparse in areas with active bed forms.

The importance of the sea bed forms has been assessed based on the conservation objectives of the Natura 2000 areas occurring within the area of investigation and for the hydrodynamic conditions in the Fehmarnbelt area.

Some areas within the Fehmarnbelt area have been protected with large-scale, morphological active bed forms as conservation objectives under Natura 2000. These areas are accordingly used in the assignment of importance levels for sea bed morphology.

The bed forms act as roughness elements on the flow. The fact, that they are not evenly distributed in the Fehmarnbelt leads to a spatial variation in the flow resistance. The sensitivity of the distribution of flow through the Belt to spatial flow resistance has been quantified. It is found that the redistribution due to spatial variation of flow resistance corresponds to changes in the mean in-flow and mean outflow current speeds which are less than 0.01 m/s, see Chapter 7. The importance of the bed forms on the overall hydrodynamics is therefore concluded to be negligible.

The importance levels and descriptions are summarised in Table 9.1 and mapped in Figure 9.1.

Table 9.1 Importance levels for the Marine Soil component:Sea bed morphology

Importance level	Description
Very high	Sand wave areas within Natura 2000 areas, where these are part of the conservation objectives
High	Other sea bed areas with prominent large-scale, morphologically active bed forms (sand waves/lunate bed forms/other prominent bed forms) not included under the 'Very high' category
Medium	All other sea bed areas, which are not heavily influenced by anthropogenic activities as mentioned under the "Minor" category
Minor	Areas under heavy anthropogenic influence, including dredged navigation channels, disposal sites, areas with sand and gravel mining and harbours

The justification for Table 9.1 and Figure 9.1 is as follows:

- *Very high importance level*
  Certain areas with bed forms are protected as a special case of the habitat type "Sandbanks" (Natura 2000 Code: 1110) within the Natura 2000 areas SCI DE

1332-301 and SCI DE 1631-392. The Natura 2000 Code 1110 is related to "Sandbanks which are slightly covered by sea water all the time".

For this reason areas with sand waves, where the sea bed has explicitly been classified with the Natura 2000 Code 1110, have been assigned a very high importance level for the Marine Soil component Sea Bed Forms. Within German territory, such mapping of Code 1110 is only available for one of the above-mentioned Natura 2000 areas (SCI DE 1332-301). The official mapping of Code 1110 within this area has mapped bed forms, which are classified as 'sand waves' in the present work. For this reason, also sea bed areas within the German Natura 2000 area SCI DE 1631-392, which are classified as sand waves in the present work, have been assigned with a very high importance level following the mapping of Natura 2000 Code 1110 carried out in Natura 2000 areas SCI DE 1332-301. No areas with Natura code 1110 have been mapped within the area of interest within Danish territory.

- *High importance level*
  Sand waves, lunate bed forms and other active bed forms are large-scale and prominent morphological features on the sea bed and contribute as such to the diversity of the sea bed morphology in the Fehmarnbelt. Areas with such bed forms (outside the Natura 2000 areas) are therefore assigned a high importance level.

- *Medium importance level*
  All other marine areas with no specific conservation status related to morphological active bed forms and which are not under influence of heavy anthropogenic activities have been given the classification of Medium importance level.

- *Minor importance level*
  All areas under heavy influence of anthropogenic activities, including areas with raw material extraction (mining of sand and gravel), disposal sites, harbours and dredged navigation channels.

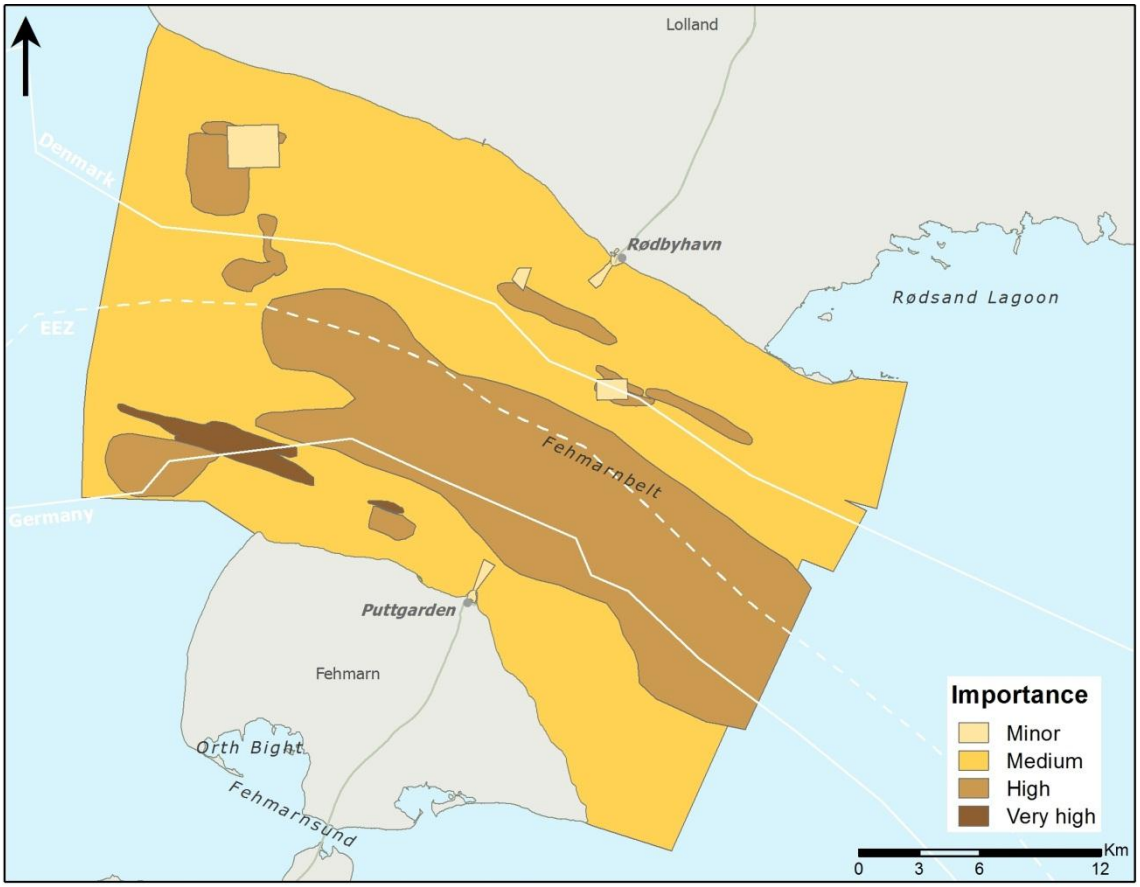

Figure 9.1 Importance levels for the Marine Soil component Sea bed morphology.

10 *REFERENCES*

Allaby M (2008). Oxford Directionary of Earth Sciences.

Ashley GM (1990). Classification of Large-scale subaqueous bedforms – a new look at an old problem. Journal of Sedimentary Petrology. Volume: 60 Issue: 1 Pages: 160-172.

Blayo, E. and Debreu L. (2005) Boundary conditions from the point view of characteristic variables. Elsevier, Ocean modelling 9 (2005) pp 231-252

Bundesamt führ Naturschutz. http://www.bfn.de/habitatmare/de/schutzgebiet-fehmarnbelt.php

Deigaard, R. and Fredsøe, J. (1992). Mechanics of Coastal Sediment Transport . Advanced Series on Ocean Engineering – Volume 3. World Scientic.

DHI. MIKE 21 and MIKE3 Flow Model FM. Hydrodynamic Module. Short description. http://www.mikebydhi.com/~/media/Microsite_MIKEbyDHI/Publications/PDF/MIKE213_FM_HD_Short_Description.ashx

Dyer and Huntley (1999). The origin, classification and modelling of sand banks and ridges. Continental Shelf Research 19 (10) 1285-1330.

Feldens, P., Schwarzer, K., Hübscher, C. and Diesing, M. (2009). Genesis and sediment dynamics of a subaqueous dune field in Fehmarnbelt (south-western Baltic Sea). Marburger Geographische Schiften, Heft 145, pp 80-97.

FEHY (2013a). Fehmarnbelt Fixed Link EIA. Marine Soil - Baseline. Volume III. Coastal Morphology along Fehmarn and Lolland. Report no. E1TR0056.

FEHY (2013b). Fehmarnbelt Fixed Link EIA. Marine Water - Baseline. Volume II. Hydrography of the Fehmarnbelt area. Report no. E1TR0057.

FEHY (2013c). Fehmarnbelt Fixed Link EIA. Marine Water - Baseline. Volume II. Suspended Sediments. Report no. E1TR0057.

FEMA(2013). Fehmarnbelt Fixed Link EIA. Flora and Fauna - Baseline. Volume III. Marine Benthic Biology - Integrated Habitat Mapping of the Fehmarnbelt area. Report no. E1TR0020.

Fredsøe, J (1974). The development of oblique dunes, part3 and part 4, Prog.Rep. 33 and 34, ISVA, DTU.

Fredsøe, J. (1982). "Shape and Dimensions of Stationary Dunes in Rivers." Journal of the Hydraulics Division, ASCE 108(8): 932-947.

Fiedler (2000). Seitensichtssonarmosaik des Rippelfeldes nördlich Fehmarn Messfarhrt mit MzB(k) "Breitgrund". Forschungsanstalt der Bundeswehr für Wasserschall-und Geophysik, Technischer Bericht TB 2000-15.

Hebsgaard, M., Ennemark, F., Spangenmark, S., Fredsøe, J. and Gravesen, H. (1994). Scour Model tests with Bridge Piers. Pianc Bulletin No 82.

Huthnance, JM (1982). On one mechanism forming linear sandbanks. Estuarine Coastal and Shelf Science 14(1) 79-99.

Judd A and Hovland M. (2007). Seabed Fluid Flow Cambridge Academic Press. The Impact on Geology, Biology and the Marine Environment.

Kenyon (1970). Sand Ribbons of European Tidal Seas. Marine Geology 9, 25-39.

Kleinhans (1999). The Relation between Bedform Type, Vertical Sorting in Bedforms and Bedload Transport During Subsequent Discharge Waves in Large Sand Gravel

Bed Rivers with Fixed Banks. Netherlands Centre for Geo-ecological Research (ICG), Utrecht University, Dept. of Physical Geography www.geog.uu.nl/fg/mklein-hans/publicat/conf/gbr5/kleinhans7.htm

Niemann, S.L, Fredsøe, J. and Jacobsen, N.G. (2010). Sand Dunes in Steady Flow at Low Froude Numbers: Dune Height Evolution and Flow Resistance. Journal of Hydraulic Engineering, 137: 5-14

Niemann, Sanne L. (2003). Modelling of sand dunes in steady and tidal flow, Phd-thesis, Coastal and River Engineering Section, Technical University of Denmark. http://www.skk.mek.dtu.dk/upload/institutter/mek/skk/pdf/phd_afhandlin-ger/2003/sanne%20niemann-phd.pdf

Novak and Björk (2002). Late Pleistocene Holocene fluvial faces and depositional processes in the Fehmarnbelt between Germany and Denmark, revealed by high-resolution seismic and litofacies analysis. Sedimentology 49, 451-465.

Oxford Dictionary of Earth Sciences. Oxford University Press. Edited by Michael Allaby (2008).

Swift, Stanley and Curray (1971). Relict sediments on continental shelves: a reconsideration. Journal of geology 79(3): 322-346.

Tjerry, Søren and Fredsøe, Jørgen (2005). Calculation of dune morphology, Journal of Geophysical Research, vol. 110, F04013.

Von Post (1929) Svea, Göta and Dana älvar. Ymer 49, 1-33.

Werner and Newton (1975). The pattern of large-scale bed forms in the Langeland Belt. Marine Geology 19, 29-59.

Wever, TF, Luhder, R, Voss, H, Knispel, U (2006). Potential environmental control of free shallow gas in the seafloor of Eckernforde Bay, Germany. Marine geology. 225(1-4): 1-4.

Wilcox, David C. (1993). Turbulence Modeling for CFD, DCW Industries, Inc., Second printing.

Wilcox, David C. (2006). Turbulence Modeling for CFD, DCW Industries, Inc., 3rd edition

Zyserman, J.A. and Fredsøe, J. (1994): Data analysis of bed concentration of suspended sediment. Journal of Hydr. Eng., ASCE, Vol. 120 (9), pp. 1021-1042

Table of figures

List of tables